HAL open science

A Mathematical Model of Phospholipid Biosynthesis

Mahsa Behzadi

To cite this version:

Mahsa Behzadi. A Mathematical Model of Phospholipid Biosynthesis. Bioinformatics [q-bio.QM]. Ecole Polytechnique X, 2011. English. NNT : . tel-00650399

HAL Id: tel-00650399

https://theses.hal.science/tel-00650399v1

Submitted on 10 Dec 2011

HAL is a multi-disciplinary open access archive for the deposit and dissemination of scientific research documents, whether they are published or not. The documents may come from teaching and research institutions in France or abroad, or from public or private research centers.

L'archive ouverte pluridisciplinaire **HAL**, est destinée au dépôt et à la diffusion de documents scientifiques de niveau recherche, publiés ou non, émanant des établissements d'enseignement et de recherche français ou étrangers, des laboratoires publics ou privés.

A Mathematical Model of Phospholipid Biosynthesis

Mahsa BEHZADI

Thèse de Doctorat
dirigée par Jean-Marc STEYAERT
effectuée au
Laboratoire d'Informatique de l'École Polytechnique

Soutenu le 12 juillet 2011

Jury

Mireille	RÉGNIER	Président
Gille	BERNOT	Rapporteurs
Jean-Pierre	MAZAT	
Joachim	SELBIG	
Peter	CLOTE	Examinateurs
Aicha	DEMIDEM	
Jean-Marc	STEYAERT	Directeur

Composed with LaTeX.

© Mahsa Behzadi. All rights reserved.

To my Family.

Remember that all models are wrong;
the practical question is how wrong do they have to be to not be useful.

George E. P. Box (statistician)

Acknowledgements

First and foremost I would like to express my deepest gratitude to my supervisor, Prof. Dr. Jean-Marc Steyaert, for his guidance, support, and encouragement throughout my studies. Without his kindness and willingness to give me a chance to pursue my goals, it would have been impossible for me to come this far. He is always willing to share his experience and I have learned innumerable lessons and insights on research and other academic issues from him.

My special thanks go to Dr. Aicha Demidem for her kind help with overcoming numerous obstacles when I started my Master and Ph.D. and for her numerous discussions and suggestions.

I feel especially indebted to Drs. Laurent Schwartz, Daniel Morvan, Mireille Regnier, Michel Rosso and Thahn-Tam Le for their help and guidance.

I am also indebted to my thesis reviewers: Drs. Gille Bernot, Jean-pierre Mazat and Joachim Selbig, for providing many valuable comments during my dissertation work.

Thanks to all my friends at Ecole Polytechnique for supplying many good hours.

I am deeply grateful that I can always count on my parents and my brother Behshad, who always provided me with vital encouragement and every support I could need.

Abstract

When measuring high-throughput data of cellular metabolism and its evolution, it is imperative to use appropriate models. These models allow the incorporation of these data into a coherent set. They also allow interpretation of the relevant metabolic variations and the key regulatory steps. Finally, they make contradictions apparent that question the basis on which the model itself is constructed.

I use the experimental data of the metabolism of tumor cells in response to an anti-cancer treatment obtained in the biological laboratory.

I focus on the modeling of a particular point: the metabolism of glycerophospholipids, which are good markers of cell proliferation. Phospholipids are essential parts of cell membranes and the study of their synthesis (especially mammalian cells) is therefore an important issue. In this work, our choice is to use a mathematical model by ordinary differential equations. This model relies essentially on hyperbolic equations (Michaelis-Menten) but also on kinetics, based on the law of mass action or on the diffusion. The model consists of 8 differential equations thus providing 8 substrates of interest. It has naturally some parameters which are unknown in vivo. Moreover some of them depend on the cellular conditions (cellular differentiation, pathologies).

The model is a collection of the structure of the metabolic network, the writing of the stoichiometry matrix, generating the rate equations and finally differential equations.

The chosen model is the mouse model (mouse / rat), because it is itself a model of human. To study the relationship between the synthesis of phospholipids and cancer, several conditions are successively considered for the identification of parameters: - The healthy liver of the rat - The B16 melanoma and 3LL carcinoma line in mice, respectively, without treatment, during treatment with chloroethyl-nitrosourea and after treatment - Finally, the B16 melanoma in mice under methionine deprivation stress.

In summary, my work provides a new interpretation of experimental data showing the essential role of PEMT enzyme and the superstable nature of

phospholipids metabolic network in carcinogenesis and cancer treatment. It shows the advantage of using a mathematical model in the interpretation of complex metabolic data.

Résumé

A l'heure de l'acquisition de données à haut débit concernant le métabolisme cellulaire et son évolution, il est absolument nécessaire de disposer de modèles permettant d'intégrer ces données en un ensemble cohérent, d'en interpréter les variations métaboliques révélatrice, les étapes clefs où peuvent s'exercer des régulations, voire même d'en révéler des contradictions apparentes mettant en cause les bases sur lesquelles le modèle lui-même est construit. C'est ce type de travail que j'ai entrepris à propos de données expérimentales obtenues dans le laboratoire biologique sur le métabolisme de cellules tumorales en réponse à un traitement anti-cancéreux. Je me suis attachée à la modélisation d'un point particulier de ce métabolisme. Il concerne le métabolisme des glycérophospholipides qui sont de bons marqueurs de la prolifération cellulaire. Les phospholipides constituent l'essentiel des membranes d'une cellule et l'étude de leur synthèse (en particulier chez les cellules de mammifères) est de ce fait un sujet important. Ici, nous avons pris le parti de mettre en place un modèle mathématique par équations différentielles ordinaires, qui est essentiellement basé sur des équations hyperboliques (Michaelis-Menten), mais aussi sur des cinétiques type loi d'action de masse et diffusion. Le modèle, composé de 8 équations différentielles, donc de 8 substrats d'intérêt, comporte naturellementdes paramètres inconnus in vivo, et certains dépendents des conditions cellulaires (différentiations de cellules, pathologies, . . .). Le modéle sépare la structure du réseau métabolique, l'écriture de la matrice de stoechiométrie, celles des équations de vitesse et enfin des équations différentielles. Le modèle choisi est le modèle murin (souris/rat), parce qu'il est lui-même un modèle de l'homme. Plusieurs conditions sont successivement considérées pour l'identification des paramètres, afin d'étudier les liens entre la synthèse de phospholipides et le cancer : - le foie sain du rat, - le mélanome B16 et le carcinome de la lignée 3LL chez la souris, respectivement sans traitement, en cours de traitement à la Chloroéthyl-nitrosourée et après traitement, - enfin le mélanome B16

chez la souris sous stress de privation de méthionine. En résumé, ce travail fourni une interprétation nouvelle des données exprimentales en montrant le rôle essentiel de la PEMT et la nature superstable de l'état stationnaire de fonctionnement du réseau métabolique des phospholipides lors de la cancérogénèse et du traitement des cancers. Il montre bien l'avantage de l'utilisation d'un modèle mathématique dans l'interprétation de données métaboliques complexes.

Contents

Acknowledgements 7

Abstract 9

Résumé 11

Chapter 1. Introduction 19
1.1. Computational biology 19
1.2. Systems biology 19
1.3. Modeling and Simulation 20
1.4. Kinetic modeling 21
1.5. Computational systems biology in cancer 22
1.6. The studied biological model 22
1.7. Manuscript Plan 23
1.8. Main results 24

Chapter 2. Cell metabolism and Phospholipid biosynthesis 27
Outline 27
2.1. Structure and processes in a cell 27
2.2. Metabolism 27
2.3. Phospholipids 29
2.4. Biochemistry of the phospholipid metabolism 31

Chapter 3. Mathematical modeling of phospholipid biosynthesis 37
Outline 37
3.1. An introduction to the mathematical modeling of metabolic networks 37
3.2. The mathematical translation of metabolic networks 39
3.3. Modeling process 39

Chapter 4. Parameter estimation, Simulation and Stability analysis 45
Outline 45
4.1. Where to get data from? 45
4.2. Parameter estimation 47
4.3. Simulation 49
4.4. Stability analysis 50

Chapter 5. Model's application to healthy rat's liver 55
Outline 55
5.1. Concentrations and Parameter estimation 55
5.2. Phase spaces 56
5.3. Stability analyses 59
5.4. Stability analyses results 63
5.5. Complexity study 64
5.6. Mathematical proof of stability (sketch) 64
5.7. Conclusion 65

Chapter 6. Model's application to B16 melanoma and 3LL carcinoma cells in response to CENU 67
Outline 67
6.1. Model application and Parameter estimation 67
6.2. Comparative analyses of parameters 69
6.3. Results 74
6.4. Conclusion 76

Chapter 7. Model's application to B16 melanoma cells in response to methionine deprivation 77
Outline 77
7.1. Mathematical model and parameter estimation 77
7.2. Comparative analyses of parameters 78
7.3. Sensitivity analysis 82
7.4. Conclusion and Discussion 84

Chapter 8. Conclusion 91
Outline 91
8.1. Summary and main results 91
8.2. Discussion and Future work 94

Appendix A. Chemical reactions and enzyme kinetics 97
Outline 97
A.1. Chemical Reactions 97
A.2. Reaction rate 99
A.3. System of chemical reactions 100
A.4. Enzyme kinetics 101

Appendix B. Parameter estimation methods 109
B.1. Forward or bottom-up modeling 109
B.2. Using steady-state data 109
B.3. Inverse or top-down modeling 110

Appendix C. Stability analysis in dynamic models 111
Outline 111
C.1. Stability Analysis of Dynamic Models 111

Appendix D. Experimental data of CENU 119
D.1. B16 melanoma and 3LL carcinoma cells in response to CENU 119

Appendix E. Experimental data of MDS 121
E.1. B16 melanoma cells and response to methionine deprivation (MDS) 121
E.2. Biological global effect of MDS 123

Appendix F. Basis for a new software for biological networks modeling 127
Outline 127
F.1. Introduction 127
F.2. Goal 127
F.3. Data and Methods 128
F.4. Development tools 129
F.5. Graph construction 130
F.6. Analyses 130
F.7. Rate laws to construct the equations 130
F.8. Inhibitors 132

Bibliography 135
Bibliography 135
List of Figures 141
List of Tables 147
Index 149

CHAPTER 1

Introduction

1.1. Computational biology

Biological systems are groups of organs that interact and work together to perform certain functions in living organisms. The complexity of biological systems and also the fact that biological sciences become more quantitative, lead to the increasing use of computer in biology and make multidisciplinary involvement essential: this scientific activity can take the form of data anallysis, molecular modeling and prediction and simulation, etc.

Computational biology is a fast growing and cutting edge field that develops a blend of computer science, applied mathematics, statistic and engineering to shed light on biological problems. The term *computational biology* describes the development of computer-based techniques for the collection and manipulation of biological data, and the use of these data to make biological predictions. In 1919 one of the first mathematical models of a living system was proposed by August Krogh and Agner Erlang [**1**]. This model which is still in use today had the aim to predict the oxygen distribution around a capillary based on a system of differential equations. This example can show the oldness of the practice of computational biology [**2**, **3**, **4**]. However now we have a computational power unimaginable to the earlier researchers, and simultaneously a tremendous increase in available data. This makes modeling and analysis of complex biological systems, our challenges.

1.2. Systems biology

Living biological systems are complex collections of interacting parts, that cannot be understood completely by studying just individual parts: experiments are too complex of not imposible to allow a precise understnading of the globality of the interactions and we need a computational approach for this aim. *Systems biology* is a new emergent field that attempts to study the organisms via integrated and interacting networks. These networks can include genes, proteins, and biochemical reactions. Systems biologists are

focussed on the behaviour of the different components of an organism and on the interactions among them. Thus computational biology is an important domain of systems biology which plays different roles including data analyses, formulating, fixing or improving hypotheses and optimal experiments design [4].

Computational systems biology includes two branche. The first branch is *knowledge discovery*, that describes the process of automatically searching large quantities of experimental data for patterns that can be considered as knowledge about the data, and that are difficult to identify without computational tools. The second branch is simulation based methods, that use computational modeling methods to represent the characteristics and predict the behaviour of biological systems. Once computer models have been validated, they can be used to make predictions about the behaviour of biological systems.

1.3. Modeling and Simulation

In systems biology, the term *model* is an artificial construct that reproduces the particularly desired behaviors and properties of a biological system. Models can have different forms, such as physical, logical, or mathematical models. In this dissertation our study is focused on a mathematical model based on mathematical equations with the aim of capturing the important properties of certain biological systems. After performing experiments on the model, we then check the results of the model simulations against equivalent experiments in the biological system.
Computer *simulation* as a useful part of mathematical modeling is a method for studying the evolution of model behaviors over time. We can use computer simulations to explore and find new insights into new technology, and to estimate the performance of systems. Although simulation has a heavily developed theory within the field of computer science, the practice of modeling and simulation is still more of an art than a science.

Computer simulations vary from small computer programs that run a few minutes, to network-based groups of computers running for hours or even for days. The importance of mathematical modeling, and the simulation of complex biochemical processes increased because of the advances in information technology in combination with more comprehensive databases and less expensive computing power [5]. Many modeling and simulation experts have published guides based on specific past experiences. We can employ

computer modeling and mathematical simulation to test the hypotheses of biologists about a biochemical reaction network. However testing the actual physical system is either expensive or dangerous, the cost of building a mathematical model and performing theoretical experiments on that model almost always is much less than the cost of laboratory experimentations. Since the decisions that biologists make as a result of modeling and experimentation have significant consequences, it is crucial that the models are credible and reliable, and that biologists understand the limitations of their modeling efforts [6].

1.4. Kinetic modeling

1.4.1. Kinetic modeling and data. The field of *kinetic modeling* is an important approach in systems biology that comprises the use of mathematical models to examine the metabolic networks. These kinetic models represent the structure and the dynamics of a system in order to predict its behaviour under different conditions. To make numeric simulations we need experimental kinetic data.

1.4.1.1. *The incompleteness of kinetic data:* The connection between iterative experimental testing and mathematical modeling of the interactions of cellular components is one definition of Systems Biology [7]. The modeling process comprises 3 steps; firstly developing a model using experimental data, secondly using the developped model for a prediction of its behaviour, and thirdly the validation of model's predictions.

The computational modeler needs a large amount of experimental data in order to produce models that are close to real nature. Since on the one hand it is difficult to collect all the experimental knowledge in metabolism field and on the other hand there are always a number of parameters which are not experimentally measurable, we will meet the problem of incompleteness of kinetic data in a biochemical network.

1.4.1.2. *The importance of kinetic data:* Growing knowledge about biochemical reactions, pathways and networks, makes scientists capable of better understanding biological phenomens. Although this fact is very global and can have a significant impact on life, it is the outcome of many small things. The bottom-up modeling approach proposes the understanding of a biological system by finding pathways and networks. The details about pathways and networks are based on our knowledge of the underlying reactions. We describe reactions by their kinetic parameters: equilibrium constants,

rate constants, Michaelis constants, velocity constants, etc. The more we know about these parameters, the better we can build up our knowledge about the reactants and their corresponding interactions.

1.5. Computational systems biology in cancer

Cancer is a serious disease that results in a disruption of cellular communication, coupled with the absence of cell death, causing the development of clusters of cancer cells (called tumors) that are beyond the rules of the body. Carcinogenesis is a complex process at the molecular and cellular levels. Understanding different phases of cancer (origin, growth and spread), requires an integrated or system-wide approach. Computational systems biology studies the large pool of experimental data of different ranges (genomic, proteomic and metabolomic) to build computer simulations. Several useful descriptive and predictive models of different kinds of cancers have been developed in order to better understand the origin of the disease and possible therapeutic treatments. Systems biology in cancer aims to give researchers a knowledge of some unobvious characteristics of the simulated process of cancer to researchers. Now a question to answer is: how computational systems biology in cancer can lead to novel insights into the understanding of disease's origin and determining new targets for anticancer therapy?[**8**]

1.6. The studied biological model

We study, in this dissertation, a model of the phospholipids which are the core of the system of the Glycerophospholipid metabolism. The development of methods for pathway-specific analyses of the phospholipid biosynthesis in intact tissue can help in our understanding of numerous cellular processes, and may be important for cancer studies. This is why the Phospholipid metabolism has attracted the attention in cancer research. It is of interest to biologists to be able to follow the phospholipid metabolism in circumstances in which cell survival and cell proliferation are of concern, *e.g.* neurological disorders and cancer [**9, 10**]. Thus there is a need to develop a model for their biosynthesis and turnover: this is why we tried to describe this system. Our goal is to build a model with which one could simulate the behavior of phospholipids interactions taking into account the impact of the environment. Due to the complexity of this system, we use mathematical modeling and numerical simulation to enable a compact representation of the current knowledge and to make meaningful quantitative predictions guiding future experimental studies.

Several formalisms have been proposed in the recent years for kinetic modeling of biochemical processes, either qualitatively, or quantitatively which provide a graphical user interface and a simulator [**11, 12, 13**]. Yet few formal tools are available for reasoning about these processes and proving properties about them. In this dissertation, we propose a kinetic model by directly translating the biochemical reactions of phospholipid biosynthesis into ordinary differential equation (ODEs), following the Michaelis-Menten chemical paradigm. Other authors have used probabilistic models or computer science models based on the π-calculus; under very reasonable assumptions all these models yield ODEs as stated by L. Cardelli in his series on Artificial Biochemistry [**14**].

1.7. Manuscript Plan

The central topic of this study is the mathematical modeling of the phospholipid biosynthesis. A dynamic, continuous and deterministic modeling approach is chosen to represent the behavior of the phospholipid metabolic pathway; the temporal changes of metabolites are formulated as a generic set of ODEs. Next we apply this model to different experimental datasets in healthy and tumoral cells; each of these applications consists of a parameter estimation process, followed by the mathematical simulation of the model and finally a set of analyses such as stability analysis or sensitivity analysis. We end this thesis by describing introduce the basis for a new software for biological networks modeling in **Appendix F**.

In **Chapter 2** cell metabolism and phospholipid biosynthesis are described. **Chapter 3** presents the modeling process that we chose in order to describe phospholipid biosynthesis and states the model as a set of ODEs. **Chapter 4** then presents the parameter estimation process and the mathematical simulation of the proposed model. Next three Chapters present the application of this model on experimental data; in **Chapter 5** the model is applied to the healthy rat's liver and in **Chapters 6 and 7** the model is applied to B16 melanoma and 3LL carcinoma, in response to CENU treatment and methionine depriviation respectively. Chapter 8 points out essential aspects of this work. Moreover, **Appendix A** introduces basic knowledge of chemical reactions and enzyme kinetics which are used as base of kinetic modeling. **Appendix B** gives a general view of three main methods of parameter estimation. **Appendix C** gives an introduction to stability analysis in dynamic models with an application of this analysis. **Appendices D and**

E give details on experiments by biologists and results of CENU and MDS treatments respectively. Finally **Appendix F** presents the basis for a new software for biological networks modeling.

1.8. Main results

We study, in this dissertation, a model for the core of the system of the Glycerophospholipid metabolism. As we describe in Chapter 2 this model comprises 24 simple and enzymatic reactions making explicit the intertwined cycles of PhosphatidylEthanolamine (PtdEth) and PhosphatidylCholine (PtdCho). The model's general structure is taken from a number of books and articles. We translate this model (in the mathematical framework) into a set of ordinary differential equations (ODEs), to propose a quantitative explanation of the experimental experiences and the observed results. In order to make it usable as a basis for simulations and mathematical analysis we need to make precise the various constants present in the equations but which are usually not directly accessible in the literature.

In the first application of the model we consider experimental data of rat's liver cells; given the values of metabolite concentrations we find appropriate parameter values which allow us to describe the system with ODEs. We have then performed several analyses using the developed model such as stability analysis and the time necessary to reach the steady state point. A first interesting result is the global stability of the system which was observed by simulation and then proved by mathematical arguments. A second important result is that we observe on the diagrams that the steady state for healthy cells is precisely a very special point of equilibrium which is a singular point of order two, whereas tumoral cells present different characteristics; this fact has been proved for PhosphatidylEthanolamine N-Methyl transferase (PEMT), an enzyme which seems to be identified for the first time as a crucial element in the tumoral process. Our results provide that all the evolutions of this metabolic network are stable in the Michaelis-Menten formalism, and that the healthy cell behaviour corresponds to a "super-stable" steady state.

As a second application of the model, we apply our proposed ODE-based model for phospholipids to experimental data of proton HRMAS NMR spectroscopy for solid B16 melanoma and Lewis lung (3LL) 3LL carcinoma cells

treated by Chloroethyl Nitrosourea (CENU). Once the estimation of unknown parameters is done we perform a complete comparative analysis of parameters in order to learn the predictive statements to explain increases and decreases which one can observe in concentrations. We checked our model against a series of biological experiments and give evidence for the crucial role of PhosphatidylEthanolamine N-Methyl transferase (PEMT) in tumor cells under CENU treatment. Our results show that the model fits "in vivo" observations and experiments with CENU tumor inhibitor, and provide new hypotheses on the metabolic pathway activity from the metabolite profiling of the phospholipid derivatives.

In the third application of the model, our study is devoted to the understanding of the Methionine deprivation stress (MDS) and of its interactions with chemotherapy, a standard treatment of advanced stage cancers. At present, little is known on the metabolic impact of the interaction between MDS and chemotherapy. This study has a twofold approach to the modeling of the phenomena happening in the treatment. Firstly the biologists use a metabolomics approach using ^{1}H-NMR spectroscopy to get novel insights into the mechanism of the action of the MDS. To this aim they investigated, in vitro, the growth and metabolic response of B16 melanoma cells to MDS. They showed that MDS provoked a cell growth delay and induced disorders of phospholipid metabolism such as a increase in Glycerophosphocholine (GPC), Phosphocholine (PC) and Phosphoethanolamine (PE) levels and an activation of the phosphatidylethanolamine-N-methyltransferase (PEMT) involved in phosphatidylcholine synthesis. After the cessation of MDS, tumor cells metabolism exhibited persistent alterations such as increased PEMT activity. These metabolic events probably explained the increased growth delay induced by the MDS. Secondly from the data we are able to propose a mathematical model which fits these biological experiments and "explains" the respective roles of PEMT. This model is very stable and is robust w.r.t. reasonable variations that can be induced by experimental errors and individual characteristics. We have performed several analyses using the developed model such as comparative analysis and sensitivity analysis. These analyses designated a set of kinetic parameters as essential parameters to give evidence for the effect of MDS on PEMT enzyme activity. From a methodological point of view, we also demonstrate that metabolomics may help understanding tumor response to nutritional

therapeutics and discovering new targets for anticancer therapy. In conclusion, this work showed that MDS induces Phospholipids metabolite disorders including Glycerophosphocholine (GPC), Phosphocholine (PC) and Phosphoethanolamine (PE) from phospholipid metabolism and transmethylation reactions. The MDS treatment allowed us to demonstrate that there is a tumor metabolism reprogramming at the level of Met metabolism. These findings shed new lights about the understanding of the metabolic interference of MDS. Using an ODEs-based mathematical model, we presented comparative and sensitivity analysis, which designated a set of kinetic parameters as essential parameters to understand the effect of MDS treatment on B16-cells. Our analyses also give evidence for the effect of MDS on PEMT enzyme activity which has a crucial role in tumor cells and propose the activated pathway which witnesses for a metabolomic reprogramming of the B16-cells allowing then to escape cell death during the MDS period. Therefore these pathways represent putative candidate targets for therapies combined with MDS.

CHAPTER 2

Cell metabolism and Phospholipid biosynthesis

Outline

This Chapter is mainly focused on the cell metabolism as a vital cellular process and on the phospholipids which are the major component of biological membranes. We next present a graph implementation for the core of Glycerophospholipid metabolism in which the pathways are supplied from bibliographical references and some online databases. [**15**, **16**, **17**, **18**, **19**, **20**]

2.1. Structure and processes in a cell

The cell surrounded by a lipid membrane is the smallest functional basic unit of life. A cell contains all the components required for its replication and this is the reason to be distinguished from smaller biological units. There are two types of cells: eukaryotic (with nucleus) and prokaryotic (without nucleus). Prokaryotic cells are relatively small in size and independent, while eukaryotic cells, which are typically larger than prokaryotic cells, are usually found in multicellular organisms. Diverse biological processes such as growth, metabolism and replication are carried out by prokaryotic and eukaryotic. All cells, whether prokaryotic or eukaryotic, have a membrane that envelops the cell, separates its interior from its environment, regulates what moves in and out, and maintains the electric potential of the cell.

2.2. Metabolism

Metabolism is a vital cellular process that consists of the set of chemical reactions that happen in living organisms to maintain life. Since the malfunction in metabolism is a major reason of human disease, it is important to construct and study metabolic networks. That is to say, the sets of coherent processes that organize metabolic networks are complex and highly interconnected, therefore there is a need to the computational approaches (see Chapter 1). The reconstruction of the metabolic networks and kinetic modeling is the core of systems biology. [**21**, **22**]. One can use the metabolic

network to suggest potential alternatives to drug targets or study the effects and causes of diseases like cancer and copnsequently hints for tentative therapies. Next we formulate the metabolic network into a mathematical model based on rate laws for enzymatic or non enzymatic reactions. This kinetic model can become quite complex with a large quantity of parameters.

Metabolism is defined as the totality of the chemical reactions catalyzed by enzymes that are carried out in an organism. The changes in metabolites are called biotransformations and a metabolic pathway is a sequence of biotransformations [**23**] as illustrated in figure 2.1.

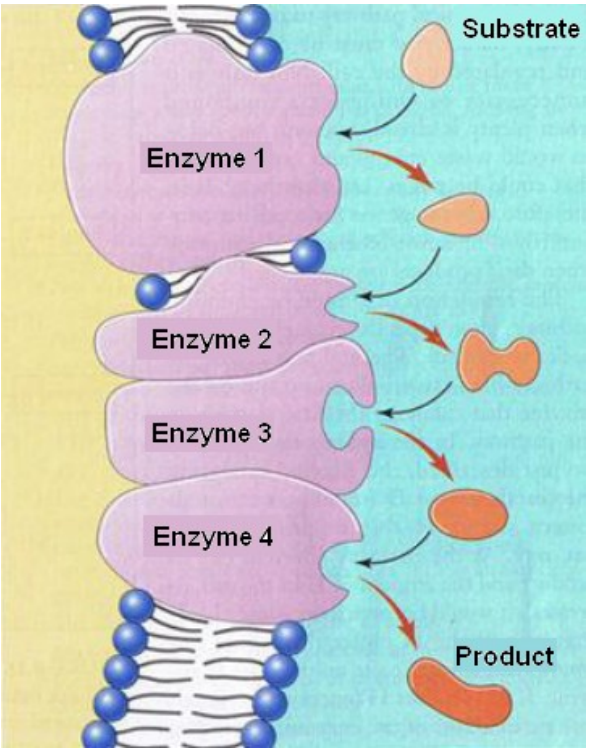

FIGURE 2.1. **Multi-enzyme reaction**: metabolic pathway where multiple biotransformations take place. The substrate of each reaction is the product of the previous reaction.(See [**23**])

In a metabolic pathway the input metabolites are called *substrates* and output metabolites are called *products*. Metabolites can originate from food, but can also be products of other metabolic pathways in the cell. The

phenotype of the cell is determined by its metabolism. One can improve the cellular properties by changing the regulation of metabolic pathways through changes in enzyme and metabolite concentrations. Enzymes, metabolites, their respective interactions and the reactions involved in these pathways have been studied by many researchers and are stored in different databases, e.g.:

- Kyoto Encyclopedia of Genes and Genomes (KEGG) Pathway database. (http://www.genome.ad.jp.kegg/pathway.html)
- BRENDA. (http://www.brenda-enzymes.info/)
- a Biochemical Genetic and Genomic knowledgebase of large scale metabolic reconstruction (BiGG). (http://www.bigg.ucsd.edu)

KEGG is a collection of online databases dealing with genomes, enzymatic pathways and biological chemicals. The pathway database of KEGG records networks of molecular interactions in the cells and variants of them specific to particular organisms. The KEGG database can be used for modeling and simulation, browsing and retrieval of data. Such data bases are essential in the systems biology approach.

2.3. Phospholipids

Phospholipids are a major component of biological membranes.(Fig. 2.2) They are a class of lipids formed from four components: fatty acids, a negatively-charged phosphate group, alcoholamine and a backbone. PhosphatidylCholine (PtdCho) and PhosphatidylEthanolamine (PtdEth) are two of the most abundant phospholipids. Biosynthesis and metabolism of these and other phospholipids are important for proliferation of membrane-bound organelles, lipoprotein synthesis, and signal transduction affecting processes of cell proliferation, differentiation and apoptosis. Yet our understanding of this metabolism and its regulation is far from complete.
It has long been recognized that different cell types and tissus display unique and stable profiles of PtdCho and other phospholipid species. Perturbation of PtdCho homeostasis in mamalian cells leads to cell death. In the early 1970s Sundler et al. [**24, 25**] examined the rates of synthesis for liver PtdCho and PtdEth using radioisotope methods. Their data could not be described by a simple precursor-product relationship and raise questions about the compartment of metabolite pools and/or channeling of metabolic pathways which are yet to be fully answered. Additionally, many questions about the metabolic pathways themselves remain unanswered.

In most eukaryotic cells, PtdCho is synthesized through two different pathways [26]; in the cytidine diphosphate-choline (CDP-choline) pathway (also known as the Kennedy pathway) and via the transmethylation of PtdEth catalysed by PE-N-methyltransferase (PEMT). Choline, supplied by food, is principally in the form of PtdCho but also exists as free Choline [27, 28]. Choline is an essential nutrient for all cells because it plays a role in the synthesis of the phospholipid components of the cell membranes, as a methyl-group donor in methionine metabolism. Quantitatively, PtdCho is the most important metabolite of Choline and accounts for approximately one half of the total membrane lipid content.

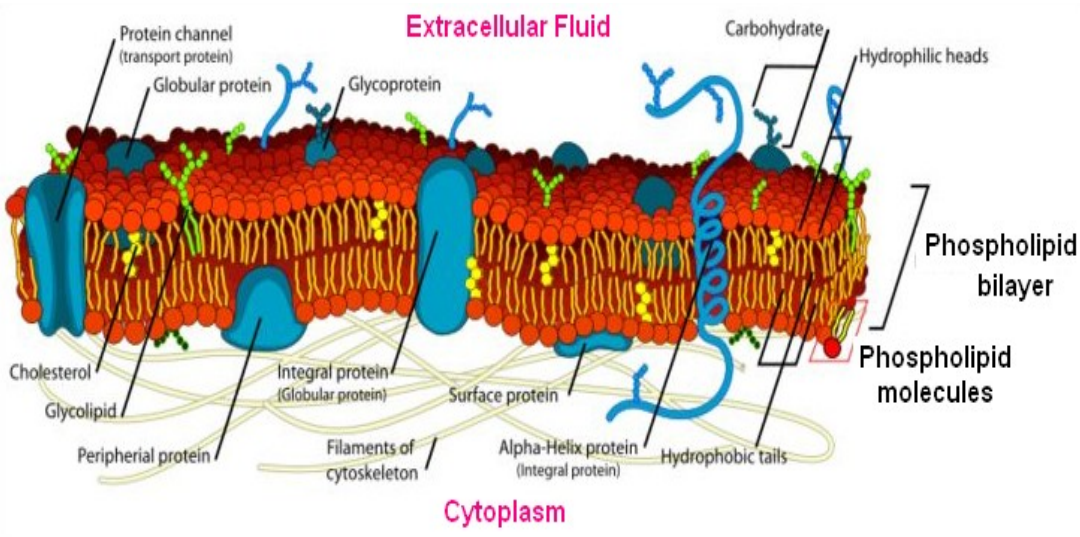

FIGURE 2.2. **Cell membrane structure:** proteins and phospholipids are major components of biological membranes. (Image source: http://commons.wikimedia.org/wiki/File:Cell membrane detailed diagram

The Kennedy pathway for producing PtdCho, involves the activation of Choline (Cho) to CDP-choline through an intermediate product, Phospho-Choline (P-Cho). The second pathway to produce PtdCho consists of three sequential methylations of phosphatidylethanolamine. Cho derived from the turnover of PtdCho produced by the methylation pathway is used for PtdCho synthesis through the Kennedy pathway. Therefore the activity of the Kennedy pathway does not reduce even in the absence of Cho in the growth medium [29].

In 1975, Sundler *et al.* used radioisotope methods to examine the rates of

synthesis for PtdCho and PtdEt of liver [**30**, **31**]. In their study, there are still questions about compartmentation of metabolite pools and channeling of metabolic pathways to be answered. However evidence of the two different pathways of PtdCho synthesis and the relative activities of these pathways was provided by Vance et al. [**32**, **33**]. The Nuclear Magnetic Resonance (NMR) spectroscopy method has been used to study the biosynthesis of PtdCho and PtdEth [**34**, **35**]. The NMR technique can also provide a detailed examination of the specific metabolic pathways. Reo *et al.* performed kinetic analyses of liver PtdCh and PtdEth biosynthesis using ^{13}C NMR spectroscopy [**36**].
The development of methods for pathway-specific analyses of phospholipid biosynthesis in intact tissue can help in our understanding of numerous cellular processes, and may be important for cancer studies. This is why the Phospholipid metabolism has attracted the attention in cancer research. It is of interest to biologists to be able to follow the phospholipid metabolism in circumstances in which cell survival and cell proliferation are of concern, *e.g.* neurological disorders and cancer [**37**, **38**]. Thus there is a need to develop a model for their biosynthesis and turnover. This is why we tried to find a model for the core of GlyceroPhospholilid metabolism. Our goal is to build a model with which one could simulate the behavior of phospholipid interactions taking into account the impact of the environment. Due to the complexity of this system, mathematical modeling and numerical simulation are necessary to enable a compact representation of the current knowledge and to make meaningful quantitative predictions guiding future experimental studies.(See section 3).

2.4. Biochemistry of the phospholipid metabolism

Figure 2.3 illustrates the model of Glycerophospholipid metabolism. The model of phospholipid metabolism that we describe here is the core of Glycerophospholipid metabolism which is supplied from bibliographical references(e.g. M.Israel and L.Schwartz [**15**, **16**, **17**, **18**, **19**, **20**]).

Our analysis concerns twenty-four biochemical reactions, as illustrated in Fig.2.4. In this system there are two main sub-systems, which have almost the same reaction structures; the first one is the Choline (Cho) cycle and the second one is the Ethanolamine (Eth) cycle. In order to have a more complete model several reactions involving external reactants are also

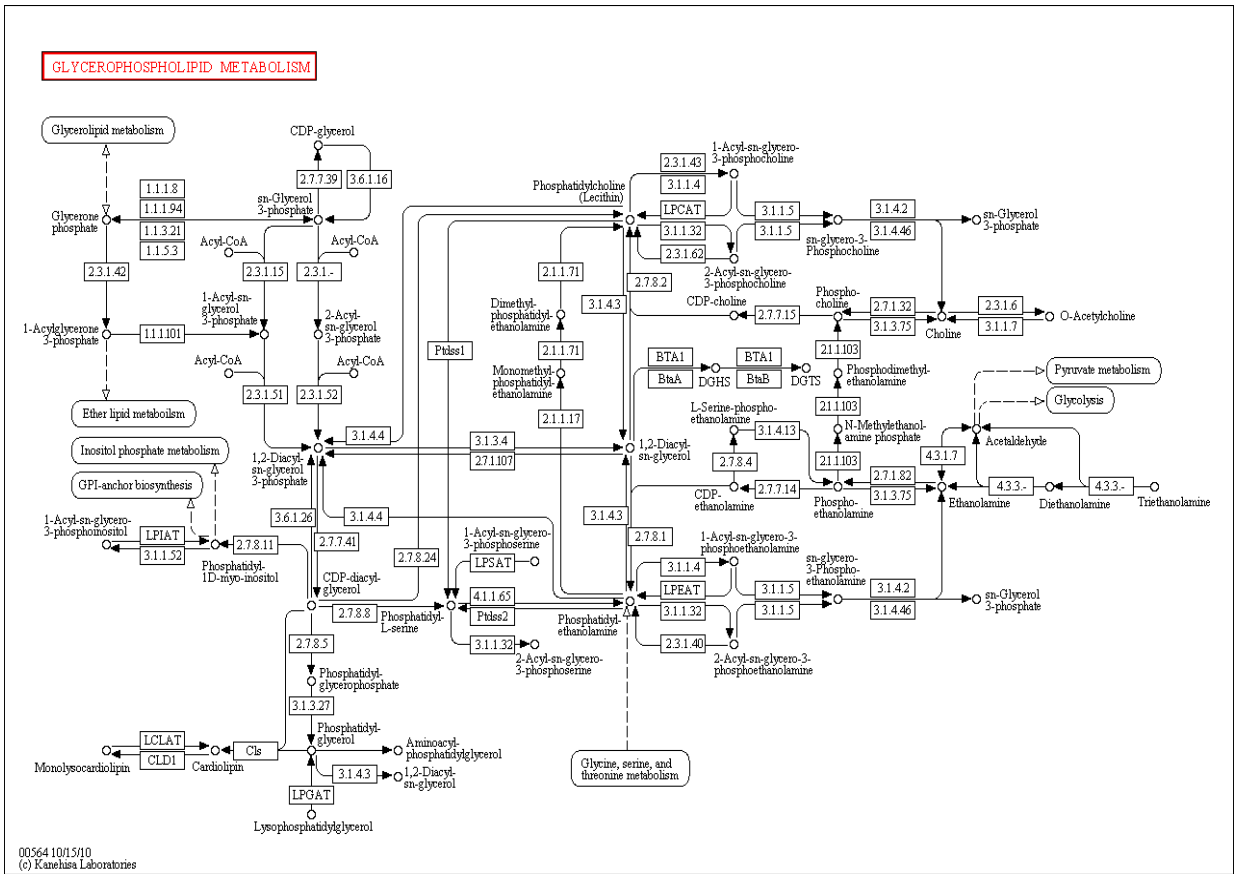

FIGURE 2.3. Glycerophospholipid metabolism ; supplied from KEGG database.

considered and studied in the model; In figure 2.4 blue and green arrows represent Choline cycle and Ethanolamine cycle respectively and Pink arrows correspond to reactions which connect these two sub-cycles. The chemical structures of metabolites are shown in figure 2.5.

2.4.1. Choline cycle. Cho is phosphorylated in an enzymatic reaction catalyzed by Choline-Kinase (CK), resulting in the formation of Phospho-Choline (PC)[**16**]. PC is converted to PhosphatidyleCholine (PtdCho) in a two step reaction, first catalyzed by regulatory enzyme PhosphoCholine-Cytidyl-transferase (CCT), then by PC-transferase (CTP)[**16, 17**]. PtdCh is converted to Glycero-PhosphoCholine (GPC) in the reaction catalyzed by Phospholipase A2 (PlpA2)[**17**]. In addition, PC and Cho can be synthesized from hydrolysis of PtdCho through the reactions catalyzed by Phospholipase

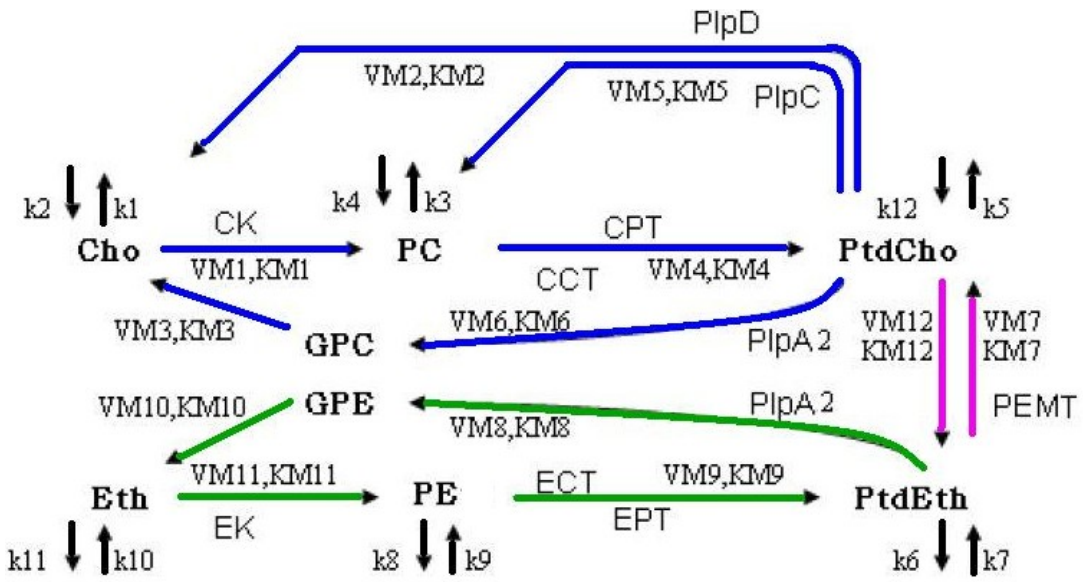

FIGURE 2.4. **Schematic representation of the model.** Arrows with VM_i and KM_i parameters refer to enzymatic reactions while the others represent simple reactions. Blue and green arrows represent Choline cycle and Ethanolamine cycle repectively and Pink arrows correspond to reactions which connect these two sub-cycles. **Reactants:** Cho (Choline), PC (Phospho-Choline), PtdCho (Phosphatidyle-Choline), GPC (Glycero-PhosphoCholine), Eth (Ethanolamine), PE (Phospho-Ethanolamine), PtdEth (Phosphatidyle-Ethanolamine), GPE (Glycero-PhosphoEthanolamine). **Enzymes:** CK (Choline-Kinase), EK (Ethanolamine-Kinase), CCT/CPT (PhosphoCholine-Cytidyl-Transferase), ECT/EPT (PhosphoEthanolamine-Cytidyl-Transferase), PEMT (PhosphatidyleEthanolamine-N-methyl-Transferase), PlpA2 (PhosphoLipase A2), PlpC (PhosphoLipase C), PlpD (PhosphoLipase D). **Parameters:** VM (Michaelis maximum reaction rate), KM (Michaelis concentration constant), k_i(Rate constants for external reactions).

C (PlpC) and Phospholipase D(PlpD) respectively[17, 18]. Cho can be also synthesized from GPC[18].

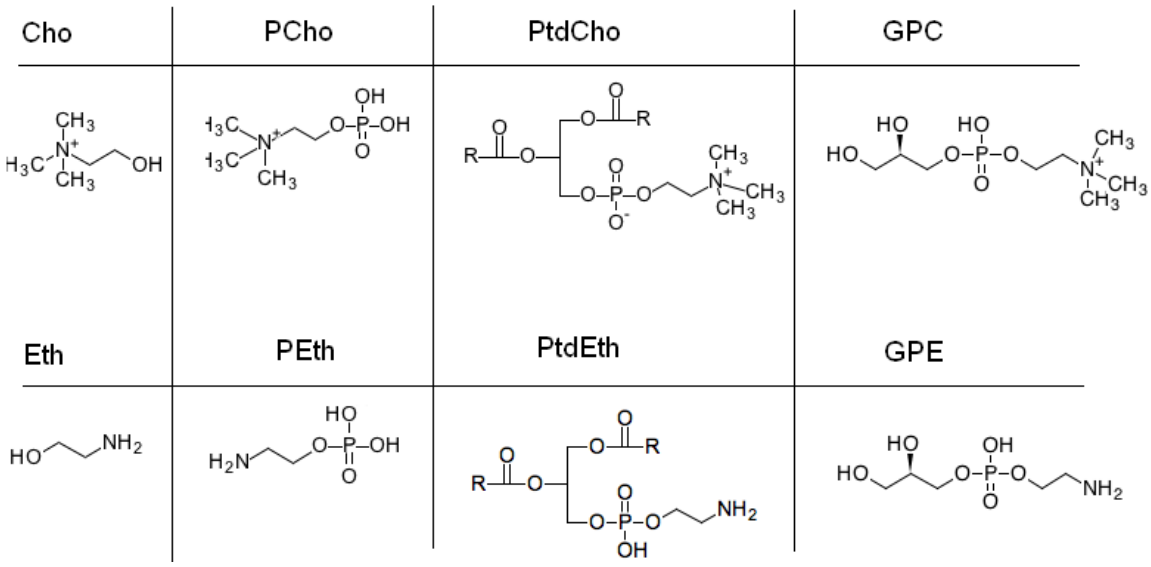

FIGURE 2.5. **Chemical structures of metabolites.**

2.4.2. Ethanolamine cycle. Eth is phosphorylated in an enzymatic reaction catalyzed by Ethanolamine-Kinase (EK), resulting in the formation of PhosphoEthanolamine (PE)[19]. PE is converted to Phosphatidyle-Ethanolamine (PtdEth) in a two step reaction, first catalyzed by the regulatory enzyme PhosphoEthanolamine-Cytidyl-transferase (ECT), then by PE-transferase (EPT)[19, 20]. PtdEth is converted to Glycero-PhosphoEthanolamine (GPE) in the reaction catalyzed by Phospholipase A2 (PlpA2)[33, 17]. Eth is synthesized from GPE[18].

The above two sub-systems are related through the reaction between PtdEth and PtdCho where PhosphatidylEthanolamine N-Methyl Transferase (PEMT) plays the role of catalyst[29, 32, 33]. This reaction seems to be an important reaction in this system, and is the basis of the main analysis in our study, since the homeostasis of PtdCho is essential to maintain cell survival.

2.4.3. External reactions. In addition to the reactions described so far, most of the reactants in phospholipid metabolism models have external reactions. For example there is a reversible reaction in which Phosphatidyle-Serine (PtdSer) releases CO_2 and PtdEth as products [39]. In the same way there are several external reactions in which Cho, Eth, PC, PE, PtdCho and

PtdEth have the role of substrate or product. We present these external reactions by input or output arrows in the model(Fig.2.4)[**34, 39, 16**].

CHAPTER 3

Mathematical modeling of phospholipid biosynthesis

Outline

This Chapter is conserned with the construction of a mathematical model for the reaction network of phospholipids which is illustrated in figure 2.4 with a graph implementation. For this aim, we first explain the reason of choosing the ODE-based enzyme-kinetic modeling. Then we describe the modeling process as a means by which we formalize a natural system to produce a mathematical system and as the means by which we interpret this mathematical system to derive information about a natural system. The basic biochemical definitions and the basic building blocks from which we construct the mathematical model are intorduced in Appendix A. This ODE-based model will be used later in the next Chapters to apply on experimental data and to perform stability analyses.

3.1. An introduction to the mathematical modeling of metabolic networks

Since the metabolic networks and their regulation are complex, an intuitive analysis of the biological systems is a difficult task. Different mathematical modeling methods help to deal with this complexity. The question thus is to determine the most useful mathematical tools and frameworks for this aim. The biological systems are complex and this may lead to the temptation that one should include every detail in the mathematical model. However, it is impossible to be complete and we have to do some simplifications and approximations. Furthermore the aim of modeling is not just finding a valid description of the given system, but also performing analysis and simulation. Therefore, the decisions on simplifications and approximations should be based on several factors, such as the validity of the system description, the mathematical convenience, and the goals of modeling.

Different methods have been developed, ranging from basic stoichiometric models up to fine-grained kinetic models. Kinetic modeling which constitutes an important branch in the growing field of systems biology, is the most complex mathematical description of a metabolic network. We consider several properties in order to decide what kind of model is suitable for the experimental data and for the aim of modeling [40]:

(i) Dynamic or static
(ii) Discrete or continuous
(iii) Stochastic or deterministic
(iv) Spatial or homogeneous

Since in the metabolic pathway modeling, we usually study the dynamic and continuous changes of metabolites, a dynamic and continuous model is a better choice than static and discrete method. Furthermore, since we are interested in average model responses rather than unlikely cases, a deterministic model is preferred to the stochastic methods. Another reason to choose a deterministic model is the limit that exists for the number of molecules in the stochastic methods such as process algebra (Pi-calculus)[14]. Finally since all the reactions take place in the cytoplasm we ignore the spatial aspects, and assume the environment is homogenous.

Once a dynamic, continuous, deterministic, and homogenous model is chosen, the changes of metabolites can be formulated as a generic set of ordinary differential equation (ODE) of the form:

$$X_i = V_i^+ - V_i^- = V_i^+(X_1, ..., X_n) - V_i^-(X_1, ..., X_n), \quad i = 1, ..., n \qquad (1)$$

where X_i denotes the concentration of a metabolite or metabolite pool and n is the number of metabolites in the system. The functions V_i^+ and V_i^- represent the reaction rates or fluxes coming in and going out of the metabolite pool X_i. This general framework has numerous alternatives and applications in metabolic pathway modeling depending on the functions used to describe V_i^+ and V_i^-.

After we choose the mathematical model framework, a symbolic model which is described as a set of ordinary equations can be derived. The next step is to assign numerical values to the parameters of the model. There exist different ways for the parameter estimation. Chapter 4 will introduce different methods which are developed for parameter estimation.

3.2. The mathematical translation of metabolic networks

We can translate a metabolic network into mathematical terms by easy means: The concentration of a metabolite is described by a variable C_i. The change of concentration over time $\frac{\partial C_i}{\partial t}$ is given by the sum of the rates of the enzymes synthesizing the metabolite minus the sum of the rates of the enzymes consuming the metabolite (result of mass balances). The rate of an enzymatic reaction is described by enzyme kinetic rate laws, such as the Michaelis-Menten equation. This equation is a function which depends on the concentration of metabolites and various parameters such as the maximal velocity of a reaction (V_{max}), or binding constants. This process yields a system of ordinary differential equations (ODEs) in which $\frac{\partial C_i}{\partial t}$ is on one side and the metabolite-dependent rate laws are on the other side of the equations (see evolution equations for reaction 23 in Appendix A). With this system of differential equations, the metabolic network can be simulated. Furthermore by solving the system of ODEs the steady state can be computed.

3.3. Modeling process

The modeling process in general is summarized in 4 steps:

(i) Network structure
(ii) Stoichiometric matrix
(iii) Rate laws
(iv) Differential equations

The first step is to obtain chemical information about the network structure, in order to derive the stoichiometric relations. In some modeling approaches the inclusion of a large number of reactions and metabolites in the model would make the processing very complex and computationally inefficient. But in deterministic ODE-based models normally we do not have a limitation on the number of reactions. The 24 reactions of our example model for phospholipids are shown in table 1.

In table 1 we observe three type of reactions; R1-R6 show that reactants are imported into the modeled system by these reactions, R13-R24 concern the reactants which are converted to other products, and finally R7-R12 concern the reactants which are taken out of the system.
The stoichiometric matrix N of the reaction system is the following:

Table 1. List of the reactions of the phospholipids system

Reactanions:
R1: → Cho
R2: → PC
R3: → Eth
R4: → PtdCho
R5: → PE
R6: → PtdEth
R7: Cho →
R8: PC →
R9: PtdCho →
R10: Eth →
R11: PE →
R12: PtdEth →
R13: Cho → PC
R14: GPE → Eth
R15: Eth → PE
R16: PtdCho → PtdEth
R17: PtdCho → Cho
R18: GPC → Cho
R19: PC → PtdCho
R20: PtdCho → PC
R21: PtdCho → GPC
R22: PtdEth → PtdCho
R23: PtdEth → GPE
R24: PE → PtdEth

$$N = \begin{array}{c} \\ R1: \\ R2: \\ R3: \\ R4: \\ R5: \\ R6: \\ R7: \\ R8: \\ R9: \\ R10: \\ R11: \\ R12: \\ R13: \\ R14: \\ R15: \\ R16: \\ R17: \\ R18: \\ R19: \\ R20: \\ R21: \\ R22: \\ R23: \\ R24: \end{array} \begin{array}{c} \begin{array}{cccccccc} Cho & Eth & PC & PE & PtdCho & PtdEth & GPC & GPE \end{array} \\ \begin{pmatrix} 1 & 0 & 0 & 0 & 0 & 0 & 0 & 0 \\ 0 & 0 & 1 & 0 & 0 & 0 & 0 & 0 \\ 0 & 1 & 0 & 0 & 0 & 0 & 0 & 0 \\ 0 & 0 & 0 & 0 & 1 & 0 & 0 & 0 \\ 0 & 0 & 0 & 1 & 0 & 0 & 0 & 0 \\ 0 & 0 & 0 & 0 & 0 & 1 & 0 & 0 \\ -1 & 0 & 0 & 0 & 0 & 0 & 0 & 0 \\ 0 & 0 & -1 & 0 & 0 & 0 & 0 & 0 \\ 0 & 0 & 0 & 0 & -1 & 0 & 0 & 0 \\ 0 & -1 & 0 & 0 & 0 & 0 & 0 & 0 \\ 0 & 0 & 0 & -1 & 0 & 0 & 0 & 0 \\ 0 & 0 & 0 & 0 & 0 & -1 & 0 & 0 \\ -1 & 0 & 1 & 0 & 0 & 0 & 0 & 0 \\ 0 & 1 & 0 & 0 & 0 & 0 & 0 & -1 \\ 0 & -1 & 0 & 1 & 0 & 0 & 0 & 0 \\ 0 & 0 & 0 & 0 & -1 & 0 & 0 & 0 \\ 1 & 0 & 0 & 0 & -1 & 0 & 0 & 0 \\ 1 & 0 & 0 & 0 & 0 & 0 & -1 & 0 \\ 0 & 0 & -1 & 0 & 1 & 0 & 0 & 0 \\ 0 & 0 & 1 & 0 & -1 & 0 & 0 & 0 \\ 0 & 0 & 0 & 0 & -1 & 0 & 1 & 0 \\ 0 & 0 & 0 & 0 & 1 & -1 & 0 & 0 \\ 0 & 0 & 0 & 0 & 0 & -1 & 0 & 1 \\ 0 & 0 & 0 & -1 & 0 & 1 & 0 & 0 \end{pmatrix} \end{array}$$

With the stoichiometric data and the derived stoichiometric matrix, structural problems like inactive reactions or nonbalanced metabolites can be identified [41]. In the system of phospholipids, we have a single elementary flux model and there are no structural problems such as deadlocks. The next step is the detailed description of the reactions of the model based on *rate laws*. There are different levels of model accuracy. In a simple model one can keep the simple mass action law for all the rate laws. In order to make a more realistic model, our model contains details about enzyme saturation and inhibition, which is included using *Michaelis-Menten* kinetics. We also propose an *exponential formula* for the reactions which import reactants to our model and follow a *diffusion phenomena*. Table 2 illustrates an example of each of these three different rate laws which we use in our modeling approach.

TABLE 2. An example of the different rate laws used in the model of the phospholipids

Reactanion:	followed rate law	Rate law
R1: → Cho	*Diffusion phenomena*	$v_1 = k_2.e^{-[Cho]}$
R9: PtdCho →	*Mass action*	$v_9 = k_5.[PtdCho]$
R15: Eth → PE	*Michaelis-Menten*	$v_{15} = \frac{VM_{11}.[Eth]}{KM_{11}+[Eth]}$

In table 2, v_i specifies the flux throught the ith reaction, k_i, KM_i and VM_i are parameters indicating the velocities of the reactions, and *[X]*s are the concentrations of metabolites. *R1* follows diffusion phenomena, while *R9* and *R15* follow mass action and michaelis-menten kinetics in order. Using the rate laws and the stoichiometric matrix, the time-dependent differential equations for the metabolites can be established:

$$\begin{aligned}\frac{\partial}{\partial t}[Cho] = k_2.e^{-[Cho]} &+ \frac{VM_2.[PtdCho]}{KM_2 + [PtdCho]} \\ &+ \frac{VM_3.[GPC]}{KM_3 + [GPC]} - \frac{VM_1.[Cho]}{KM_1 + [Cho]} \\ &- k_1.[Cho] \end{aligned} \tag{2}$$

$$\frac{\partial}{\partial t}[Eth] = k_{10}.e^{-[Eth]} + \frac{VM_{10}.[GPE]}{KM_{10} + [GPE]} - \frac{VM_{11}.[Eth]}{KM_{11} + [Eth]} - k_{11}.[Eth] \tag{3}$$

$$\frac{\partial}{\partial t}[PC] = k_4.e^{-[PC]} + \frac{VM_1.[Cho]}{KM_1 + [Cho]} + \frac{VM_5.[PtdCho]}{KM_5 + [PtdCho]} - \frac{VM_4.[PC]}{KM_4 + [PC]} - k_3.[PC] \tag{4}$$

$$\frac{\partial}{\partial t}[PE] = k_9.e^{-[PE]} + \frac{VM_{11}.[Eth]}{KM_{11} + [Eth]} - \frac{VM_9.[PE]}{KM_9 + [PE]} - k_8.[PE] \tag{5}$$

$$\frac{\partial}{\partial t}[PtdCho] = k_{12}.e^{-[PtdCho]} + \frac{VM_4.[PC]}{KM_4 + [PC]} + \frac{VM_7.[PtdEth]}{KM_7 + [PtdEth]} - \frac{VM_6.[PtdCho]}{KM_6 + [PtdCho]} - \frac{VM_5.[PtdCho]}{KM_5 + [PtdCho]} - \frac{VM_2.[PtdCho]}{KM_2 + [PtdCho]} - \frac{VM_{12}.[PtdCho]}{KM_{12} + [PtdCho]} - k_5.[PtdCho] \tag{6}$$

$$\frac{\partial}{\partial t}[PtdEth] = k_7.e^{-[PtdEth]} + \frac{VM_{12}.[PtdCho]}{KM_{12} + [PtdCho]} + \frac{VM_9.[PE]}{KM_9 + [PE]} - \frac{VM_8.[PtdEth]}{KM_8 + [PtdEth]} - \frac{VM_7.[PtdEth]}{KM_7 + [PtdEth]} - k_6.[PtdEth] \tag{7}$$

$$\frac{\partial}{\partial t}[GPC] = \frac{VM_6.[PtdCho]}{KM_6 + [PtdCho]} - \frac{VM_3.[GPC]}{KM_3 + [GPC]} \tag{8}$$

$$\frac{\partial}{\partial t}[GPE] = \frac{VM_8.[PtdEth]}{KM_8 + [PtdEth]} - \frac{VM_{10}.[GPE]}{KM_{10} + [GPE]} \tag{9}$$

In this model, each of these differential equations expresses the rate of change of one reactant as a sum of fractional terms for enzymatic reactions and non-fractional terms for simple reactions. Furthermore, we proposed an exponential formula with concentrations of studied reactants in our system as variables, to explain the kinetics of reactions with reactants from the external environment. Diffusion phenomena are the reason for this exponential form. Molecular diffusion, often called simply diffusion, is a net transport of molecules from a region of higher concentration to one of lower concentration by random molecular motion: hence this standard representaion.

In the next Chapters, we will use this mathematical model in several applications for two aims; firstly we try to use an estimation method in order to find the different required parameters in the system of equations, such as the rate constants for each reaction, using the experimental values of the concentrations in steady state points (see Chapter 4), then we try to perform different analyses such as stability analysis and sensitivity analysis, using the parameters obtained for each of the applications of the model. (see Chapters 5, 6 and 7).

CHAPTER 4

Parameter estimation, Simulation and Stability analysis

Outline

There has been a lot of research on kinetic modeling as a major method in systems biology. Every modeling effort depends on (a) information about the underlying metabolic pathways and (b) the kinetic data derived by experiments. The kinetic data for a model, available from web resources, is incomplete, difficult to accumulate, or not available at all. One of the difficulties is to determine the rate of each reaction of a metabolic network using Michaelis-Menten equations. The rate itself is not the problem but the values of the constant parameters K_m and V_{max} that are present in Michaelis-Menten equation. Only few of these values are already found and mentioned in the literature. Therefore in order to design accurate kinetic models, we need to guess reasonable values for each parameter. This Chapter will focus on estimating the parameters K_m and V_{max}, that are used in the kinetic model that we proposed in Chapter 3. This will be implemented by minimizing the value of a function which represents the sum of the squares of the right hand side equations of the ODE system, using the KKT conditions. For this proposed optimization method, the minimization is carried out with Matlab.

4.1. Where to get data from?

In a detailed kinetic model, there is a need to get access to different data sources to obtain detailed information. The stoichiometry of a reaction can be usually taken from standard biochemistry textbooks or from online databases (e.g. KEGG or BiGG). In the case of phospholipids metabolism, we supplied our model from bibliographical refrences (e.g. M. Israel and L. Schwartz [**15**, **16**, **17**, **18**, **19**, **20**]) and the KEGG online database.

The structure of the rate law depends on the stoichiometry of the reaction and on the enzyme's mechanism and may be derived from enzyme kinetics textbooks [**42**].

In the model of phospholopids, as explained in section 3.3, we describe the rate of enzymatic reactions by the fractional term of Michaelis-Menten law and the simple reaction rate by the non-fractional term of the mass action law. Furthermore, we proposed an exponential formula with concentrations of reactants in our system as variables, to explain the rate of reactions with reactants from the external environment: diffusion phenomena are the reason of this exponential form. Molecular diffusion, often called simply diffusion, is a net transport of molecules from a region of higher concentration to one of lower concentration by random molecular motion.

The metabolite concentrations can be measured for a system, usually at (quasi) steady state points, but sometimes also as time course. We applied the model of phospholipids on different data sets of concentrations which are derived experimentally by means of 1D or 2D spectra measurements. (See Chapters 5, 6 and 7).

The maximal velocity of the reaction (V_{max}) is dependent on the concentration of the enzyme in the cell or the extract; Since this concentration is rather a result of regulated gene expression, thus it has to be measured for each situation again and again. We note here that the V_{max} used in kinetic models is not the specific activity that is measured with the purified enzyme. Thus, V_{max} is dependent on the enzymes concentrations and normally needs to be measured *in vivo* or *in vitro* when not possible. For reversible reactions the V_{max} is different for the forward and reverse reactions, respectively.
The binding constant (or K_M) results from the structure of the enzyme, and thus is independent of the enzymes concentration. We therefore argue that in many cases it is a legitimate simplification to take the K_M values from the literature, even from related species if required by the lack of human data.

In the deterministic ODE-based modeling approach, if enough values of concentrations of the model are known, it is theoretically possible to estimate the missing parameters. For this aim one has to fit the system variables (metabolite concentrations) to data sets from measurements.

4.2. Parameter estimation

Since now different methods are developed for parameter estimation. The nature of suitable data for each type of estimation is different, and so are the methods of analysis. These approaches complement each other and maybe in the future, a combined method will be choosed as the standard. The major methods of parameter estimation are (see Appendix B):

(1) Forward or bottom-up modeling
(2) Using steady-state data
(3) Inverse or top-down modeling

4.2.1. Parameters estimation in the phospholipids' model applications. The described kinetic equations for phospholipids metabolism require a number of parameters, such as the rate constants for each reaction. The parameter values have an important effect on the precision of the model which is representing this biological system. However these values, k_i, VM_i and KM_i, are difficult to estimate experimentally and many are unknown; that is why we estimate them by means of a numerical method.

In all applications of the model of phospholipids (see Chapters 5, 6 and 7) our experimental data associates to the local and global steady states values of concentrations. Thus we choose the method of using steady state data to estimate parameters. Since at steady state points the concentrations do not change, we treat our system of ODEs as a nonlinear algebraic problem (all the derivatives are zero). Mathematically we have a set of possible solutions of this system. Furthermore we know that the vector of these rate constants needs to insure the behavior of the model in such a way that the cell is viable. Once we take into account all these biological constraints, the possible rate constant vectors fall into a subset of the parameter space. Characterizing this subset would be a prediction of the model, and so would be characterizing the set of all the dynamics of the model consistent with the parameter vectors in this subset. Although mathematically correct this answer is not satisfactory. We need to put a better and more understandable description of this space of solutions. We thus aim to find a representative value of this space and which has the property of achieving a minimum for a certain function of the rate parameters. For this purpose we:

(1) Define the sum of squares of rate equations as function 'F'. In other words, instead of solving a system of nonlinear equations which vanish

at steady state points, we propose to minimize the function 'F' which is the sum of subexpressions which are positive or equal to zero.

(2) Find a solution vector which minimizes the value of the function 'F', in the given range of each parameter. We perform this step by using the "**fmincon**" function which is developed in the *Matlab* software as an optimization tool in order to find the minimum of a constrained nonlinear multivariable function.

The **fmincon** function attempts to find a constrained minimum of a scalar function of several variables starting at an initial estimate. This is generally referred to as *constrained nonlinear optimization* or *nonlinear programming*. In more details, **fmincon** is using an *"interior point method"* (IP) to solve nonlinear convex optimization problems. In the case of our model, since we have inequality constraints, **fmincon** respects the Karuch-Kuhn-Tucker (KKT) theorem [**43, 44**] (see the application of this method in Chapter 5, 6 and 7). This theorem gives the conditions which are necessary for a solution of a nonlinear programming problem to be optimal, provided that some regularity conditions are satisfied. Allowing inequality constraints, this approach is a generalization of the method of Lagrange multipliers which allows only equality constraints [**43**].

Although we proposed to use this method in the field of kinetic modeling, it was already used in other fields; For example applying IP methods to power system optimisation problems began early in 1990s. They were applied by Clements et al. in 1991, to power systems [**45**]. The objective of this research was to apply a non-linear programming IP technique to solve the state estimation problems in power systems. As another application, we can name the central role of constrained optimization in economics. For example, the choice problem for a consumer is represented as one of maximizing a utility function subject to a budget constraint. The Lagrange multiplier has an economic interpretation as the shadow price associated with the constraint, in this example the marginal utility of income [**46**]. KKT conditions is also already used in a large number of optimization problems such as Knapsack maximization, Fisher's Exchange market, etc [**47**]. The problem of resource allocation among different activities, such as allocating a marketing budget among sales territories is analyzed by Luss and Gupta [**48**]. They assume that the return function for each territory uses different parameters, and derive single-pass algorithms for different concave payoff

functions (based on the KKT conditions) in order to maximize total returns for a given amount of effort.

4.2.2. Comparison of applied estimation method to the other methods. The method explained in section 4.2.1 is a refinement of "Using steady state data" method. We apply parameter estimation on each experimental data set which is associated to a steady state of system.

In a bottom-up modeling, the strategy consists of setting up a symbolic model, estimating local parameters, studying the integration of all individual rate laws into a comprehensive model, testing the model, and making refinements to some of the model structure and the parameter values. But we did not choose this method because of the disadvantages of this approach: in particular the need of a considerable amount of local kinetic informations which should in a unique experiment. The reason for which we did not choose a top-down modeling, is that in this method one needs measurements for all metabolites at sequential points in time (time series data), while our experimental data is local data at the steady states.

4.3. Simulation

Once the stoichiometry, the rate laws, and all parameters are collected, the system of equations of the kinetic model is fully specified. Using Scilab or Matlab software, we write a code with which the model can thus be deterministically simulated in a stepwise manner:

(i) Start from a given point.
(ii) Solve the differential equations to obtain the expected changes in metabolite concentrations over a short time period.
(iii) The concentrations are then updated with these changes.
(iv) Repeat the process.

While we simulate a model, depending on the equations and their parameters, different behaviors may be observed; even sometimes a same model can be characterized by different sets of parameters that result in different behaviors. It is possible that the system converges toward a steady state, which is the case for most biological systems if they are kept under constant conditions. At the steady state, all fluxes in this linear pathway are the same, so that the concentrations of the metabolites do not vary. Another possibilty is a divergent behavior which means that the metabolite concentration is constantly increasing. There is also a possibility of observing an

oscillatory behavior of the system. It has been shown that the probability of a model to exhibit oscillatory behavior or other instability actually increases with its size [**49**]. (see Chapter 5).

4.4. Stability analysis

The stability analysis of the steady state is an important aspect for the further interpretation of dynamic models. Only if the model has a stable steady state can a sensitivity analysis of its variables be performed. In Appendix C we give an introduction to the stability analysis of dynamic models. In this section we explain the application and advantage of this analysis by considering an example of cell cycle division. Furthermore this analysis will be used in applications of our proposed model for phospholipids in the next Chapters.

As explained in Appendix C, the stability of the system depends only on the eigenvalues of the Jacobian matrix. If one or more of the eigenvalues have a positive real part the associated solutions will grow exponentially. The stability criterion can therefore be formulated as:

THEOREM 4.1 (Stability criterion). *A steady state is stable if, and only if, the eigenvalues of the associated Jacobian matrix all have negative real parts.*

Thus, the stability is evaluated by calculating the eigenvalues of the Jacobian of the system of ODEs. The issue of stability of mathematical models is common in all engineering disciplines and the theorem above is well known.

4.4.1. Application of stability analysis to the cell division cycle model. In this section we refere to cdc2 and cyclin interactions in the model of the cell division cycle proposed by J. Tyson in [**50**], to apply stability analysis on two of the parameters of this model. A simplified model of cdc2-cyclin interactions is summarized in figure 4.1. This model is translated into the precise mathematical equations. The solution of the following equations depends on the values assumed by the 10 parameters in the model(Table. 1).

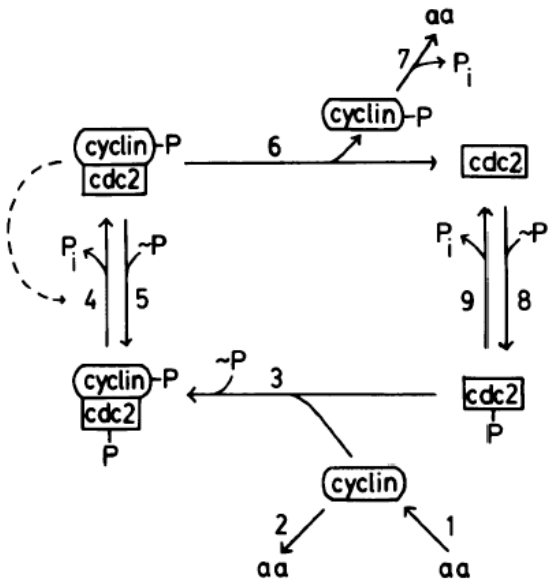

FIGURE 4.1. The relationship between cyclin and cdc2 in the cell cycle (proposed by J. Tyson in [50]).

$$\begin{cases} \frac{\partial C2}{\partial t} = k_6[M] - k_8[\sim P][C2] + k_9[CP] \\ \frac{\partial CP}{\partial t} = -k_3[CP][Y] + k_8[\sim P][C2] - k_9[CP] \\ \frac{\partial pM}{\partial t} = k_3[CP][Y] - [pM]F([M]) + k_5[\sim P][M] \\ \frac{\partial M}{\partial t} = [pM]F([M]) - k_5[\sim P][M] - k_6[M] \\ \frac{\partial Y}{\partial t} = k_1[aa] - k_2[Y] - k_3[CP][Y] \\ \frac{\partial YP}{\partial t} = k_6[M] - k_7[YP] \end{cases}$$

TABLE 1. Parameter values used in the numerical solution of the model equations (proposed by J. Tyson in [50]).

Parameter	Value
k_1[aa]/[CT]	0.015 min^{-1}
k_2	0
$k_3[CT]$	200 min^{-1}
k_4	10-1000 min^{-1} (abjustable)
$k_4\prime$	0.018 min^{-1}
$k_5[\sim P]$	0
k_6	0.1-10 min^{-1} (abjustable)
k_7	0.6 min^{-1}
$k_8[\sim P]$	$\gg k_9$
k_9	$\gg k_6$

Using this system of equations and the given parameter values, we apply the stability analysis to this model, focusing on two parameters k_4 and k_6. We performed this analysis in these steps:

(i) Find a fixed point: we try to find a fixed point using the given parameter values, such as it would be the closest fixed point to steady state concentrations.
(ii) System's linearization: which refers to finding the linear approximation of the model's equations at this fixed point.
(iii) Jacobian matrix: Determine the matrix of coefficients of all concentrations in the linearized system of equations.
(iv) Eigenvalues: Find the eigenvalues of this Jacobian matrix, for different values of the choosen parameters. ($0 < k_4 < 500$ and $0 < k_6 < 5$)
(v) Stability criterion: Verify for each set of eigenvalues, whether they all have negative real parts.

Figure 4.2 illustrates the result of the above stability analysis. In this figure regions which are shown by black color correspond to stable steady state behaviour of the model (all of the eigenvalues have negative real parts).

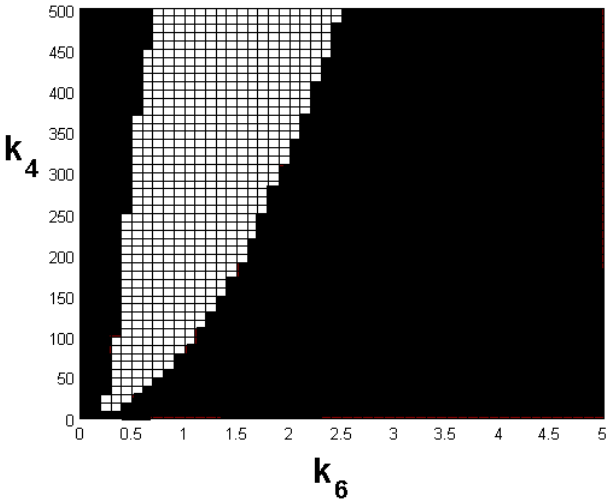

FIGURE 4.2. result of stability analysis for steady state point associated to values correspond to $0 < k_4 < 500$ and $0 < k_6 < 5$. Black color shows the stable regions.

This result is in a good agreement with the results of J. Tyson in [**50**]; in which the boundaries of stable regions were determined by integrating the

differential equations of the model, for the given parameter values, using Gear's algorthm for solving stiff ordinary differential equations [**51**].

In Chapter 5 we will show the application of stability analysis to a model for phospholipids. We will first show the stability by numerical simulation, and then present a proof of stability using the stability criterion theorem for the experimental data of healthy rat's liver.

CHAPTER 5

Model's application to healthy rat's liver

Outline

In this Chapter, we apply the mathematical model described in Chapter 3 to experimental data of rat's liver cells (obtained by NMR spectroscopy), in two steps: firstly we try to determine the various parameters required in the system of equations, such as the rate constants for each reaction, using the experimental values of the concentrations in healthy rat liver metabolism. For this aim we use the parameter estimation method that we explained in Chapter 4. The second step is to study the phase spaces diagrams and also to perform the different stability analyses using the parameters obtained for healthy liver cells. A first interesting result is the global stability of the system which was observed by simulation and then proved by mathematical arguments. A second important result is that we observe on the diagrams that the steady state for normal cells is precisely a singular point of order two, whereas tumoral cells present different characteristics; this fact has been proved, in particular, for PhosphatidylEthanolamine N-Methyl transferase (PEMT), an enzyme which seems to be identified as a crucial element in the tumoral process.

5.1. Concentrations and Parameter estimation

The kinetic equations of Chapter 3 are satisfied by various parameters, such as the rate constants for each reaction. In the first application of the mathematical model, the experimental values that we use are derived from the concentrations of rat's liver metabolism measured at several instants during the perfusion with Choline and Ethanolamine [**36**]. The concentration of [PtdCho] and [PtdEth] were measured from the ^{31}P NMR spectra of the lipide extracts [**36**]. A description of these experimental analyses is given in [**52, 53**].

The parameter values have a priori an important effect on the precision of the model which is representing this biological system. However these values, k_i, VM_i and KM_i, are difficult to estimate experimentally and many

are unknown; that is why we estimate them by means of the numerical method that we described in section 4.2

As it is explained in section 4 we know that the vector of the rate constants needs to ensure the behavior of the model in such a way that the cell is viable. For example there exist specific limited ranges of the concentrations, for some metabolites, in which the cell can stay alive. These ranges can give upper and lower bounds for the parameters.[**54**]. We assume that there are no singular points in the domain of study; hence all the parameters vary continuously and do not go to infinity. Once we have taken into account all these biological constraints, the possible rate constant vectors fall into a subset of the parameter space. Characterizing this subset would be a prediction of the model, and so would be characterizing the set of all the dynamics of the model consistent with the parameter vectors in this subset. The vector of parameters which are shown in Table 2 is one of these possible solutions. To obtain this we used the algorithm which is described in Chapter 4.

Table 1 shows the averages of the concentrations which are measured experimentally, for 8 reactants of our system. We first try to use the average values presented in Table 1, to obtain a possible vector of the constants of reactions k_i, the maximum velocities and kinetic constants of the Michaelis-Menten model VM_i and KM_i (Table 2). We also try to find a possible vector of the constants, for each set of concentrations measured in each of 6 time points [**36**]. Comparing the vectors obtained in each of these two cases, we do observe only small variations in the parameters, which means that this is a robust solution. The results and variations are shown in Table 2. We also observe similar results for 100 other vectors in the subset of parameter space, corresponding to different concentrations.

5.2. Phase spaces

In this section we compute and study the phase spaces diagrams using the parameters obtained by our estimation method. The goal is to obtain the behaviour of the system with respect to time. The simulation results show that for these parameter values there exists only one steady state point in the neighborhood of the studied initial concentration values. When we

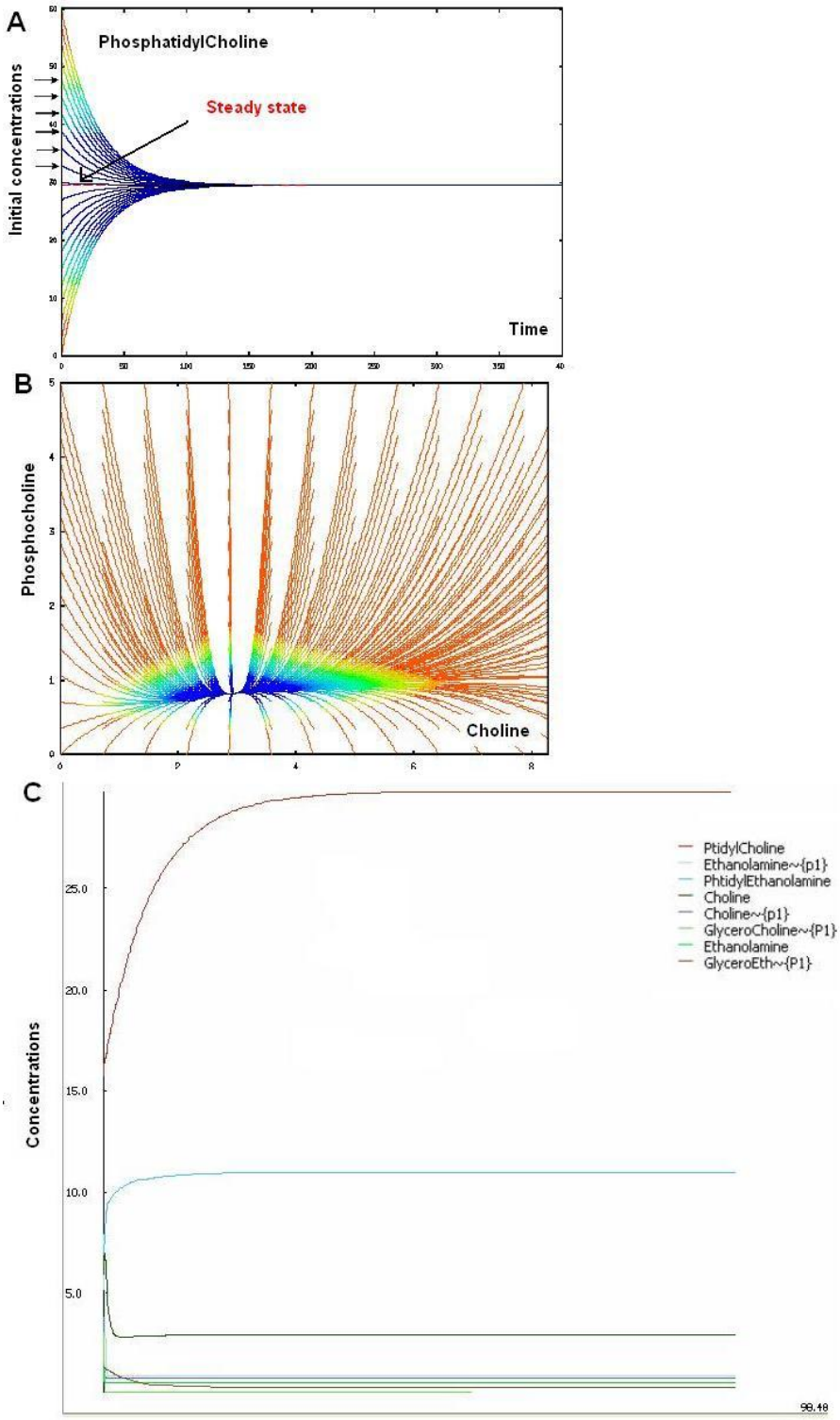

FIGURE 5.1. **Changes in initial concentrations** [**A**] Changes of initial concentration of PhosphatidylCholine. [**B**] Phase space for Choline and PhosphoCholine. [**C**] An Example of different initial concentrations evoluing into steady state. In **A** and **B** the color change from red to blue refers to approaching the steady-state. In **C** each color associates to the concentration of one of the reactants. Concentrations values are given in $\mu mol.g^{-1}$.

TABLE 1. **Concentrations of rat's liver metabolites**

Reactant	Initial concentration
Choline	0.51±0.11
Ethanolamine	0.11±0.01
PhosphoCholine	0.88±0.18
PhosphoEthanolamine	1.02±0.15
PhosphatidylCholine	29.57±2.76
PhosphatidylEthanolamine	9.85±1.15
GlyceroPhosphoCholine	0.41±0.09
GlyceroPhosphoEthanolamine	0.35±0.05

Values are given in $\mu mol.g^{-1}$ liver, measured by P-NMR.

doi:10.1016/S1388-1981(01)00202-5

TABLE 2. **Estimated parameter values for rat's liver metabolites**

Param	Value	Param	Value	Param	Value
k_1	1.465±0.091	VM_1	2.289±0.105	KM_1	0.567±0.015
k_2	1.882±0.110	VM_2	0.624±0.076	KM_2	29.707±0.195
k_3	0.281±0.013	VM_3	0.814±0.040	KM_3	0.549±0.033
k_4	2.981±0.118	VM_4	4.898±0.122	KM_4	0.950±0.010
k_5	0.064±0.007	VM_5	0.575±0.032	KM_5	29.812±0.252
k_6	0.054±0.003	VM_6	0.696±0.009	KM_6	29.634±0.310
k_7	1.001±0.081	VM_7	10.451±0.094	KM_7	4.845±0.046
k_8	0.786±0.041	VM_8	0.505±0.008	KM_8	10.060±0.096
k_9	2.206±0.109	VM_9	3.629±0.086	KM_9	1.888±0.015
k_{10}	1.238±0.074	VM_{10}	0.577±0.002	KM_{10}	0.457±0.002
k_{11}	0.980±0.079	VM_{11}	2.825±0.075	KM_{11}	0.121±0.011
k_{12}	1.000±0.042	VM_{12}	1.657±0.009	KM_{12}	29.844±0.155

Values are given in $\mu mol.g^{-1}$ liver for KM_i and in $\mu mol.g^{-1}.s^{-1}$ for VM_i and s^{-1} for k_i.

try to change one or several initial concentrations at time t_0, we see that after passing a period of time the concentrations of all the reactants converge finally toward the concentrations of the steady state point. Therefore one can conclude that the change in the initial concentration of each of the reactants does not modify the behaviour of the system at infinity ($+\infty$). (Fig.5.1).

5.3. Stability analyses

5.3.1. Steady State Concentration vs. Enzyme Concentration. As a first set of stability analyses we study the changes in steady states by modifying the concentrations of enzymes in enzimatic reactions. To determine the maximum rate of an enzymatic reaction (like most of the reactions in our model) we use the Michaelis-Menten model. In this model, the maximum initial velocity (a kinetic constant of the enzymatic reactions) reflects the activity of an enzyme and is proportional to its concentration. Therefore, in our simulation and in order to represent changes in enzyme concentrations, we simply modified the value of the maximum initial velocities of the reactions (VM_i). For example in the case of the reaction between PtdEth and GPE, the diagrams of changes of steady state resulting from the change of maximum velocity are shown in figure 5.2(a). On each of these diagrams, each point (VM, $\tilde{X}i$) corresponds to a concentration of the reactant X_i at the steady state.

The simulation diagrams are as expected. When the velocity of the reaction from PtdEth to GPE increases, the concentrations of GPE, PE and Eth increase and the concentrations of PtdEth, Cho, PtdCho, PC and GPC decrease.
Here it is worth recalling the special role of PtdEth N-methyltransferase enzyme(PEMT) in phospholipid biosynthesis. The PEMT pathway is especially functional in the liver. It is a minor pathway for phosphatidylcholine synthesis from phosphatidylethanolamine, the major pathway being the Kennedy pathway which involves the metabolism of Choline taken from the blood. The PEMT pathway is implicated in the biosynthesis of lipoproteins in the liver. In contrast, its role is poorly known in tumors, excepted in hepatocarcinoma [**55**]. It was recently shown that some tumor cell types could compensate for the deficiency of the Kennedy pathway by upregulating the PEMT pathway, thus surviving. Therefore a complementary aim for our modelling was to get further insight into the possible role of the PEMT pathway in the regulation of tumoral phospholipid metabolism. To our knowledge, the implication of PEMT in response to an anticancer agent, in melanoma and 3LL carcinoma has never been investigated. Now we get back to our model and take the reaction of first order, related to PtdEth and PtdCho for which PtdEth N-methyltransferase (PEMT) plays the role of enzyme. Figure 5.2(b) represents the changes of the steady state point associated to different reactants. On each of its diagrams, each point ([PEMT], $\tilde{X}i$) corresponds to a concentration of reactant X_i at steady state. So if we

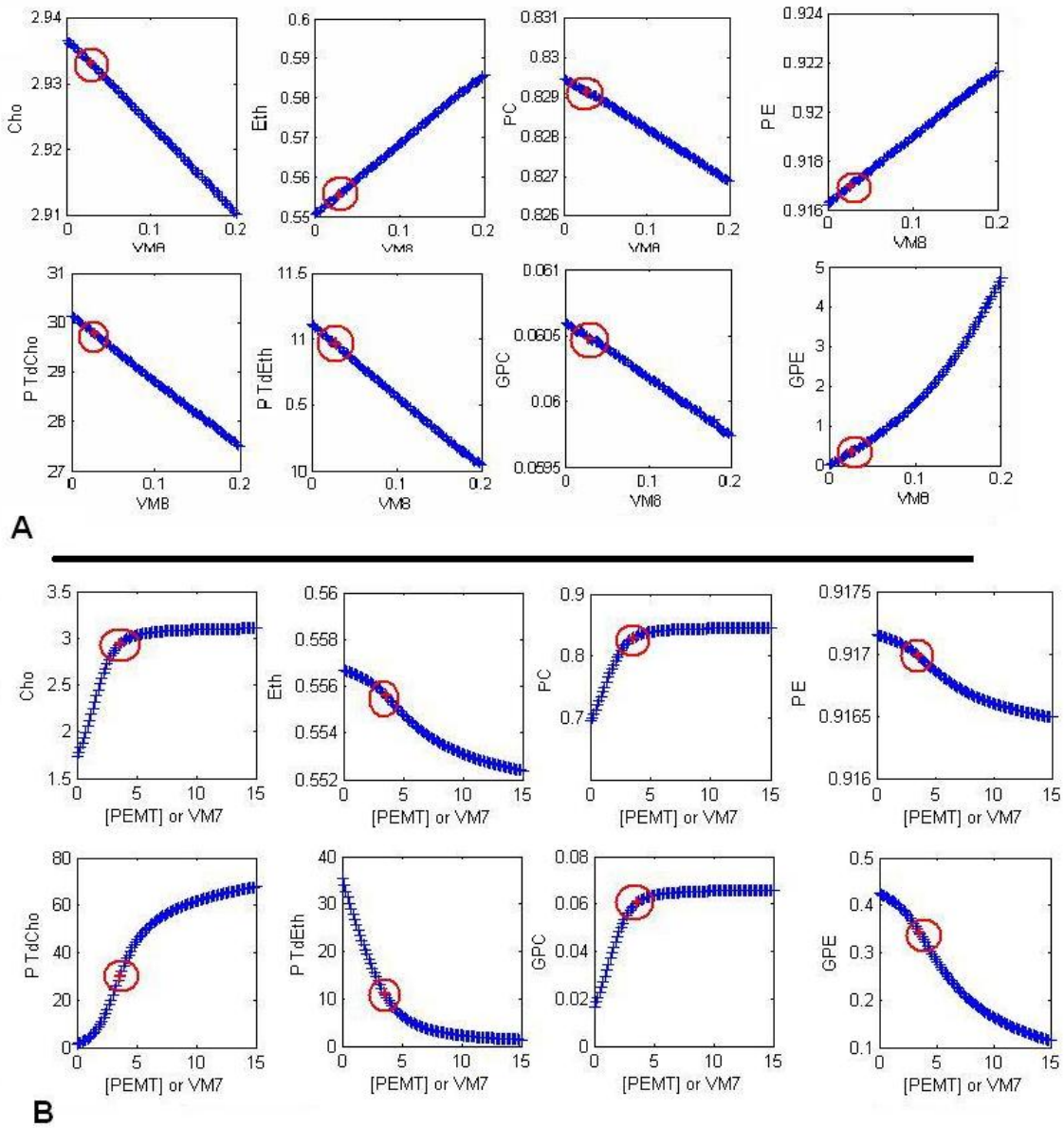

FIGURE 5.2. **Steady State Concentration vs. Enzyme Concentration** [**A**] Change of steady state point for the reaction of PtdEth and GPE. On each of these diagrams, each point (VM, $\tilde{X}i$) corresponds to a concentration of the reactant X_i at the steady state. [**B**] Change of steady state point for the reaction of PtdEth and PtdCho. The red point in each of these diagrams is associated to the concentration at the steady state of the experimental values. Concentration values are given in $\mu mol.g^{-1}$.

change the enzyme concentration, for an arbitrary value of the initial concentration like X_{i0} the concentration $[X_i]$ will tend towards its steady state concentration value. In figure 5.2(b), the red point (also shown by a circle) in each of the diagrams is associated to the concentration of the steady state among the experimental values.

5.3.2. Rate vs. Concentration. In the second set of stability analysis, we studied the effects of the changes in reaction rates on concentrations and their relation to the steady state. For this aim, we performed several different simulations for each reaction. In the diagrams presented in the example of figure 5.3(a), each colour is associated to one of the simulations. Each of these diagrams represents the changes of concentrations of the reactants vs. the reaction rate for that reactant.

Let us recall that the point where the rate of reaction reaches zero, is called the steady state point for a given reactant. To make it clearer, let us explain the corresponding diagram for PtdEth. This is also shown in figure 5.3(b) with a better resolution. The steady state is obtained when the concentration is around 11 $\mu mol.g^{-1}$. This is obtained by taking some random concentrations and measuring the reaction rates for each of them. Then we connect the resulting points to see when the zero rate is obtained. For all the other points in this diagram, which are not the steady state, concentration tends towards the steady state concentration. In other words the normal cell behaviour corresponds to a "superstable" steady state. As shown in figures 5.3(a) and 5.3(b), for all the reactants, these diagrams have proved to be linear and all the simulations coincide for all the reactants.

5.3.3. Speed analysis. In the third set of stability analyses on the concentrations of rat liver metabolism, we tried to study the speed to reach the steady state point. In figure 5.3(b) for the points whose concentrations are far from the steady state point (which is shown by an arrow), the absolute value of this rate is bigger than for the points whose concentrations are close to the steady state. This means that the speed to reach the steady state point increases when we try to change the concentration of reactants. One of the parameters which could influence this speed is the concentration of the enzyme. To study the effect of the change of concentration or activity of an enzyme on this speed, as it is shown in figure 5.3(b), we consider the slopes of the diagrams as an indicating coefficient for the reaction speed. Let us call this slope the *rate coefficient (k)*. If the concentration of one of the enzymes changes, the rate coefficient does so. When the rate coefficient

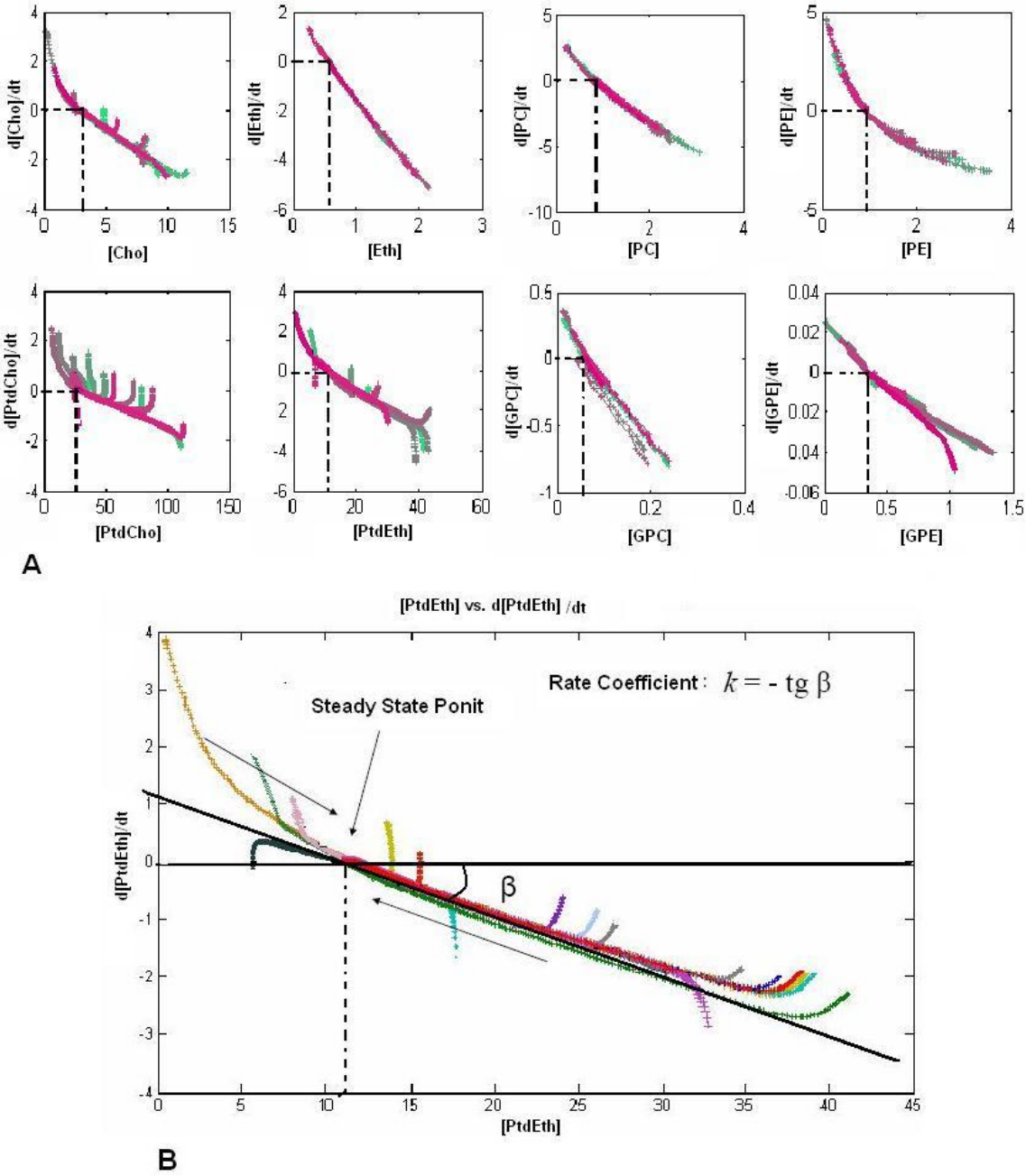

FIGURE 5.3. Rate vs. Concentration A: Rate vs. Concentration for PhtdEth: Each experiment is shown by a different colour in this diagram. The steady state is obtained when the concentration of PtdEth is around 11 $\mu mol.g^{-1}$. B: Rate vs. Concentration: Each diagram corresponds to the change in concentration of one reactant vs. its reaction rate. We define the slope (k) as 'rate coefficient' which is used as a parameter in analysis concerning the speed of reaching the steady state. Values are given in $\mu mol.g^{-1}$ for Concentrations and in $\mu mol.g^{-1}.s^{-1}$ for Rates .

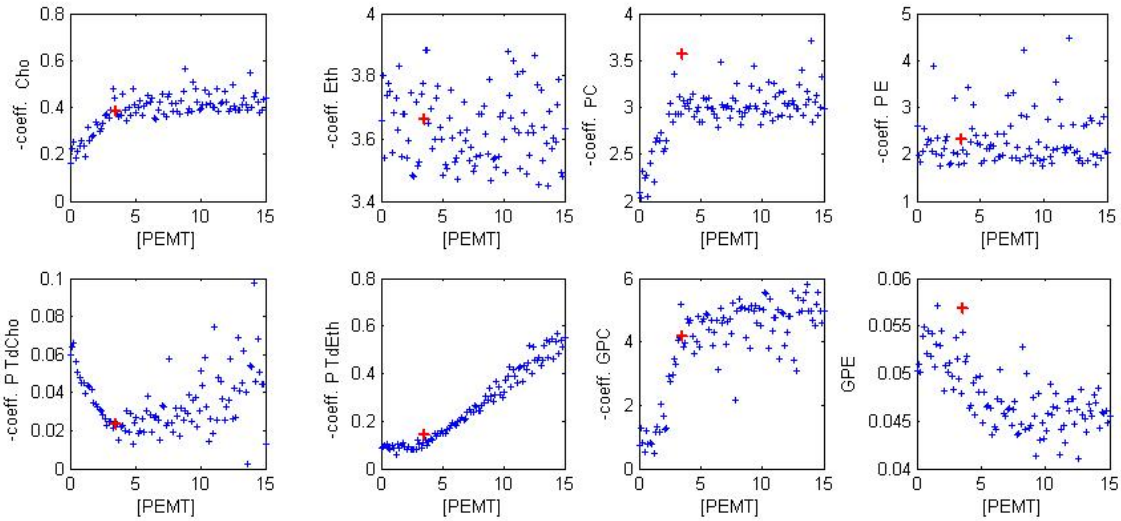

FIGURE 5.4. **Speed Analysis** -k (Rate Coefficients) vs. Concentration of enzyme PEMT(real values). The red point on each diagram is associated to rate coefficient at the steady state of the experimental values. Concentrations values are given in $\mu mol.g^{-1}$.

is small, the rate changes more slowly than when the rate coefficient is large. The diagrams of rate coefficients vs. concentration of enzyme PEMT are shown in figure 5.4.

In the next sections we will firstly study some interesting results obtained from the stability analyses of section 5.3 We will also discuss the complexity of the algorithm applied to Rate vs. Concentration stability analysis. Then in the next step we give a mathematical proof for the stability of this model of equations.

5.4. Stability analyses results

The analysis of reactant concentrations vs. enzyme concentrations in section 5.3 shows that:

- The PEMT Enzyme is found to provoke a reciprocal trend between PE and PC. This means that there is a balance between the change of concentration of PE and the change of concentration of PC.

- One can note from figure 5.2(b) that when the concentration of PEMT increases the concentrations of Cho and PC saturate after

a certain value of [PEMT], while the concentration of PtdCh still increases. This fits with the fact that the methylation of phosphatidylethanolamine may relay phosphatidylcholine biosynthesis when the choline pathway is saturated or blocked[**32, 33, 55**].

- The interesting result about the red points (also shown by a circle) in figure 5.2(b), is that these positions are the places where the behaviour of diagrams changes (either inflexion point in mathematical term which means where the second derivative is zero or in some situations it is the third derivative which vanishes).

5.5. Complexity study

In the stability analyses of Rate vs. Concentration in 5.3, given the values of concentrations $[C_i]$ which were observed experimentally, we managed to find appropriate parameter values $\{P_i\}$. With these parameter values, the ODEs system has a stable solution, and the resulting concentration values are equal to the initial ones ($[C_i]$). However, one could ask whether a change in parameter values could give an unstable or oscillating solution. For that purpose we studied the eigenvalues of the Jabobian matrix in a number of points close to $[C_i]$. As we had 41 parameters we just could not try all variations of them at the same time. For instance, even to try 10 values for each parameter would take $O(10^{41})$ operations. So we used random sampling to change all parameter values simultaneously. In each of the 10 000 experiments we made, each parameter took a value, where rand factor was a uniformly distributed random value in a range from 0 to 20. In all the experiments we observed the stability of the system.

5.6. Mathematical proof of stability (sketch)

We tried to find a fixed point for the proposed ODEs system using the parameter values that we found in section 5.1, such as it would be the closest fixed point to the steady state associated to experimental values of concentration. The eigenvalues for Jacobian matrix of the system in such fixed points are always real and negative.(See Appendix C). This indicates that the solution is always stable and without oscillations regardless of the parameter values of the system.

More generally if we study the system of ODE where most of the equations have the general form of Michaelis-Menten, we can prove that all the

solutions for this system are stable. The proof is that we have a diagonally dominant Jacobian matrix. This means that, in every row of this matrix, the magnitude of the diagonal entry in the row is larger than the sum of the magnitudes of all the other (non-diagonal) entries in that row. More precisely, the matrix A is diagonally dominant if

$$|a_{ii}| \ > \ \sum_{j \neq i} |a_{ij}| \ \ for\ all\ i \tag{10}$$

where a_{ij} denotes the entry in the ith row and j_{th} column. The Jacobi method for solving a linear system converges if the matrix is diagonally dominant. The eigenvalues for the Jacobian matrix in such systems are always real and negative . This indicates that the solution is always stable and without oscillations regardless the particular parameters of the system. In other words all the evolutions of the cell metabolism are stable in the proposed mathematical model which is based on Michaelis-Menten kinetics (See Appendix C).

5.7. Conclusion

Understanding cell metabolism evolution and changes is for many scientists more than a challenge; it is the key to a thorough understanding of cell dysfunction and very likely a step toward the elucidation of carcinogenesis along the lines of Warburg's seminal papers. In this Chapter we presented a mathematical analysis of the metabolic pathways which control and command the production of Glycerophospholipids through the enzymatic reactions of PhosphatidylEthanolamine and PhosphatidylCholine. The analysis shows that the healty cell stands at very special points of equilibrium. We also checked our model against a series of experiments and gave evidence for the crucial role of PhosphatidylEthanolamine N-Methyl transferase (PEMT). About the general beaviour of such systems we show that:

- All the evolutions of the cell metabolism are stable in the Michaelis-Menten formula.
- The normal cell behaviour corresponds to a "superstable" steady state.

CHAPTER 6

Model's application to B16 melanoma and 3LL carcinoma cells in response to CENU

Outline

In the recent years several studies have been carried out to perform chloroethylnitrosourea (CENU) chemotherapy for the treatment of B16 melanoma and Lewis lung (3LL) carcinoma tumors in vivo [**56**, **57**, **58**, **59**, **60**]. In this Chapter we apply our proposed ODE-based model for phospholipids to study the effects of such treatments in mouse. For each of these two tumors we have experimental data for three different phases: Control(CTL), Inhibition(INH) and Recovery(REC)[**61**]. In a first step we try to estimate the unknown kinetic parameters, then we perform a complete comparative analysis of parameters in order to learn the predictive statements to explain increases and decreases which one can observe in concentrations.(See the experimental data in Appendix D)

6.1. Model application and Parameter estimation

Our aim is to provide insight into metabolic pathways from biochemical data derived from ^{1}H-NMR spectroscopy-based metabolite profiling of tumors [**61**]. We hypothetize that, by modelling phospholipid derivative content variations between two conditions at steady state, we can give insight, through the values taken by the set of parameters, into the induced regulations of phospholipid metabolism. We thus compare phospholipids metabolism alterations in murine tumors between the baseline and the stable phase of their response to an anticancer agent. Based on the classical hypothesis that pathways of phospholipids metabolism are very similar in liver cells and tumor cells [**34**], we apply our mathematical model to study the effects of such treatments. For each of these two tumors we have experimental data for three different phases: Control(CTL), Inhibition(INH) and Recovery(REC) [**61**](See Fig.6.1). The average concentrations measured experimentally at steady state for each of these phases are shown in Tables 1 and 2.

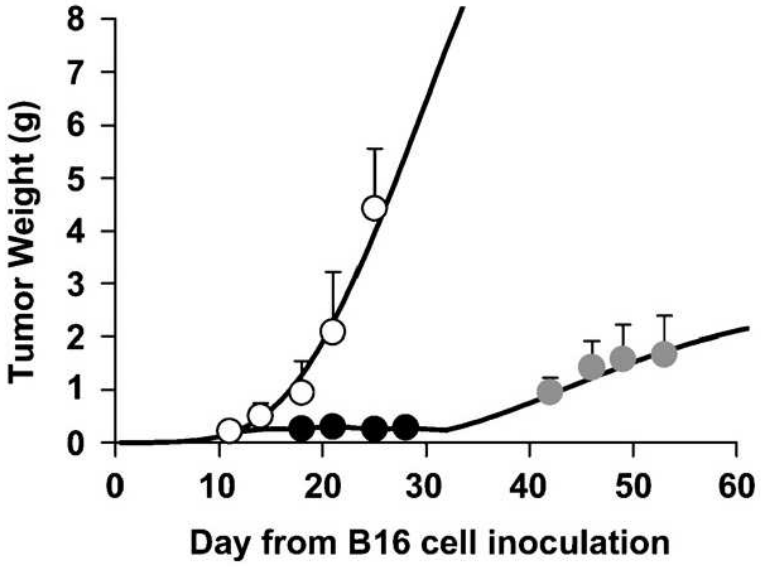

FIGURE 6.1. **Treatment Phases** Growth curves of untreated (white circles) and CENU-treated tumors during the growth inhibition phase to treatment (black circles) and the growth recovery phase (gray circles). CENU was given intratumorally at days 11, 14, and 18. Bars, SD.

TABLE 1. **Average concentrations of B16 melanoma tumor model metabolites**

B16:	CTL	INH	REC
Cho	0.395	0.636	0.518
Eth	0.1	0.102	0.101
PCho	1.091	1.847	1.842
PEth	4.001	9.337	6.304
PtdCho	15.030	25.782	21.915
PtdEth	5.010	8.594	7.305
GPC	0.367	1.561	0.131
GPE	0.703	1.401	0.665

Values are given in $\mu mol.g^{-1}$ melanoma, measured by ^{1}H NMR spectroscopy.

At a first step we try to obtain a possible vector for appropriate parameter values for each phase of treatment, applying the proposed parameter estimation method explained and the same methodology we used for the liver cell metabolites in previous Chapters.(See Chapters 4 and 5). We repeat the parameter estimation process, up to 1000 times with different initial

TABLE 2. **Average concentrations of 3LL carcinoma tumor metabolites**

3LL:	CTL	INH	REC
Cho	0.946	1.746	1.596
Eth	0.1	0.991	0.101
PCho	0.996	1.610	1.542
PEth	3.533	6.458	5.468
PtdCho	10.456	11.470	13.071
PtdEth	3.485	3.823	4.357
GPC	4.643	1.370	2.434
GPE	1.356	1.025	0.873

Values are given in $\mu mol.g^{-1}$ 3LL carcinoma, measured by ^{1}H NMR spectroscopy. doi:10.1002/ijc.21761

vectors of parameters values and for different intervals simultaneously. The average results of parameter estimation for B16 melanoma and 3LL carcinoma tumor cells are shown respectively in Tables 3 and 4.

6.2. Comparative analyses of parameters

Once parameter estimation is done for each phase of treatment; we perform a complete comparative analysis for the rate coefficients (k_i, VM_i) in order to propose the predictive statements which explain the evolutions of concentrations of reactants from one phase to the other (Table 1 and 2). Tables 5 and 6 illustrate the results of the comparative analyses. (from one phase to another, the parameter value decreases (↓), increases(↑) or does not change (-)).

After the comparative analyses, we classify the parameters in different groups, based on the evolution of the parameter during the treatment (CTL → INH) and after the treatment (INH → REC):

(a) **Neutral group**: The parameters which do not change neither during the treatment nor during the early period of after treatment. These are the parameters which are shown in tables 5 and 6, by two consecutive "-" symbols.

(b) **Temporary changed group**: The parameters which are changed during the treatment but they change again in the reverse direction during the early period of after treatment. These are the parameters which are

TABLE 3. **Estimated parameter values for mouse B16 melanoma metabolites**

Cell:	B16-Treated		
Parameter:	CTL	INH	REC
k_1	1.580±0.28	0.975±0.11	0.704±0.28
k_2	1.544±0.19	1.787±0.04	2.402±0.42
k_3	0.664±0.07	0.208±0.08	0.011±0.01
k_4	2.469±0.12	1.907±0.01	2.254±0.14
k_5	0.069±0.04	0.005±0.08	0.113±0.01
k_6	0.041±0.05	0.064±0.02	0.007±0.06
k_7	1.055±0.04	1.002±0.002	1.007±0.04
k_8	0.009±0.04	0.029±0.01	0.082±0.03
k_9	1.115±0.04	1.000±0.001	1.012±0.001
k_{10}	0.921±0.09	0.913±0.19	1.933±0.036
k_{11}	1.016±0.02	1.098±0.09	1.028±0.09
k_{12}	1.000±0.01	1.000±0.001	1.000±0.001
VM_1	3.253±0.08	2.894±0.51	3.148±0.29
KM_1	1.396±0.15	1.345±0.23	0.633±0.11
VM_2	0.290±0.02	0.460±0.10	0.402±0.036
KM_2	15.19±0.03	25.88±0.01	22.04±0.02
VM_3	0.818±0.07	0.871±0.14	0.752±0.151
KM_3	1.559±0.03	2.113±0.31	0.544±0.06
VM_4	3.158±0.35	3.038±0.05	4.570±0.29
KM_4	2.398±0.20	2.900±0.09	1.920±0.31
VM_5	0.317±0.07	0.669±0.15	0.959±0.05
KM_5	15.12±0.02	25.85±0.003	21.97±0.006
VM_6	0.313±0.06	0.742±0.17	0.293±0.05
KM_6	15.15±0.01	25.87±0.01	22.01±0.31
VM_7	2.426±0.01	1.597±0.26	3.623±0.82
KM_7	6.539±0.50	9.419±0.06	8.042±0.45
VM_8	0.410±0.06	0.262±0.01	0.452±0.08
KM_8	5.295±0.01	8.755±0.001	7.482±0.03
VM_9	1.863±0.12	1.159±0.15	2.756±0.27
KM_9	4.130±0.16	9.550±0.17	6.551±0.14
VM_{10}	0.490±0.01	0.335±0.03	0.703±0.25
KM_{10}	1.027±0.07	2.208±0.29	1.427±0.09
VM_{11}	1.980±0.05	3.284±0.26	3.676±0.69
KM_{11}	0.112±0.04	0.287±0.05	0.096±0.02
VM_{12}	1.072±0.18	1.754±0.09	1.299±0.04
KM_{12}	15.13±0.10	25.82±0.005	22.10±0.11

Values (means estimate±SD estimate) are given in $\mu mol.g^{-1}$ tumor for KM_i and in $\mu mol.g^{-1}.s^{-1}$ for VM_i and s^{-1} for k_i.

TABLE 4. **Estimated parameter values for 3LL carcinoma metabolites**

Cell:	3LL-Treated		
Parameter:	CTL	INH	REC
k_1	0.503±0.19	0.204±0.01	0.318±0.05
k_2	1.322±0.05	1.380±0.03	1.420±0.08
k_3	0.197±0.11	0.066±0.006	0.085±0.008
k_4	1.826±0.07	1.720±0.07	1.739±0.19
k_5	0.093±0.01	0.021±0.014	0.014±0.01
k_6	0.059±0.01	0.139±0.04	0.096±0.05
k_7	1.148±0.07	1.127±0.007	1.072±0.14
k_8	0.064±0.01	0.069±0.03	0.089±0.01
k_9	1.100±0.04	1.008±0.04	1.019±0.15
k_{10}	1.013±0.11	1.291±0.14	1.266±0.21
k_{11}	1.009±0.01	0.974±0.012	0.984±0.05
k_{12}	1.000±0.001	1.000±0.001	1.000±0.001
VM_1	1.613±0.18	0.892±0.18	0.946±0.07
KM_1	1.144±0.004	1.836±0.04	1.722±0.16
VM_2	0.585±0.06	0.440±0.06	0.584±0.08
KM_2	10.61±0.006	11.59±0.21	13.17±0.11
VM_3	0.804±0.02	0.732±0.09	0.797±0.01
KM_3	4.681±0.01	1.665±0.13	2.656±0.17
VM_4	3.274±0.13	2.138±0.06	2.375±0.15
KM_4	1.130±0.06	1.761±0.18	1.869±0.15
VM_5	0.646±0.02	0.694±0.06	0.751±0.07
KM_5	10.59±0.001	11.57±0.12	13.14±0.01
VM_6	0.806±0.14	0.662±0.05	0.764±0.07
KM_6	10.60±0.001	11.53±0.08	13.13±0.02
VM_7	2.143±0.08	1.539±0.15	1.699±0.01
KM_7	3.609±0.06	4.165±0.25	4.674±0.26
VM_8	0.448±0.08	0.232±0.007	0.288±0.06
KM_8	3.698±0.01	4.098±0.32	4.599±0.35
VM_9	1.675±0.04	1.506±0.23	1.451±0.19
KM_9	3.517±0.08	6.764±0.27	5.794±0.14
VM_{10}	0.489±0.002	0.272±0.09	0.303±0.09
KM_{10}	1.691±0.05	1.466±0.2	1.012±0.21
VM_{11}	2.348±0.17	2.772±0.05	2.453±0.27
KM_{11}	0.127±0.017	0.134±0.017	0.106±0.008
VM_{12}	1.207±0.08	1.250±0.08	1.334±0.07
KM_{12}	10.54±0.01	11.67±0.1	13.28±0.14

Values (means estimate±SD estimate) are given in $\mu mol.g^{-1}$ tumor for KM_i and in $\mu mol.g^{-1}.s^{-1}$ for VM_i and s^{-1} for k_i.

TABLE 5. Comparative analysis for rate parameters of B16 melanoma.

Cell:	B16(in vitro)		
Parameter:	Std→MDS	MDS→post-MDS	*
k_1	↓	↓	*
k_2	↑	↑	*
k_3	↓	↓	*
k_4	↓	↑	
k_5	↓	-	*
k_6	-	-	
k_7	-	-	
k_8	-	-	
k_9	↓	-	*
k_{10}	-	↑	*
k_{11}	-	-	
k_{12}	-	-	
VM_1	-	-	
VM_2	↑	-	*
VM_3	-	↓	*
VM_4	-	↑	*
VM_5	↑	↑	*
VM_6	↑	↓	
VM_7	↓	↑	
VM_8	↓	↑	
VM_9	↓	↑	
VM_{10}	↓	↑	
VM_{11}	↑	↑	*
VM_{12}	↑	↓	

"↓": parameter value decreased; "↑": parameter value increased; "-": parameter value is fixed. "*": Explicative parameters.

shown in tables 5 and 6, first by ↓ symbol then by ↑ symbol or vice versa.

(c) **Reprogramming group**: The parameters which are definitively changed during treatment , and that do not change anymore during the early period of after treatment. In other words these parameters are able to keep the effect of the treatment. These are the parameters in tables 5 and 6, for which we observe ↓ or ↑ symbols in the first step and "-" symbol in the second step.

Table 6. Comparative analysis for rate parameters of 3LL carcinoma.

Cell:	3LL(in vitro)		
Parameter:	Std→MDS	MDS→post-MDS	*
k_1	↓	↑	
k_2	-	-	
k_3	↓	-	*
k_4	↓	-	*
k_5	-	-	
k_6	↑	↓	
k_7	-	-	
k_8	-	-	
k_9	-	-	
k_{10}	↑	-	*
k_{11}	-	-	
k_{12}	-	-	
VM_1	↓	-	
VM_2	↓	↑	
VM_3	-	-	
VM_4	↓	-	*
VM_5	-	-	
VM_6	↓	↑	
VM_7	↓	-	*
VM_8	↑	-	*
VM_9	↓	↓	
VM_{10}	↓	-	*
VM_{11}	↑	↓	
VM_{12}	-	-	

"↓": parameter value decreased; "↑": parameter value increased; "-": parameter value is fixed. "*": Explicative parameters.

(d) **Definitively changed group**: The parameters which are definitively changed during treatment, and which still change during early period of after treatment. These are the parameters in tables 5 and 6, for which we observe two consecutive ↑ symbols.

(e) **Finally changed group**: The parameters which do not change during the treatment but which change during the early period of after the treatment. These are the parameters in tables 5 and 6, for which we observe first a "-" symbol and then a ↓ or ↑ symbol.

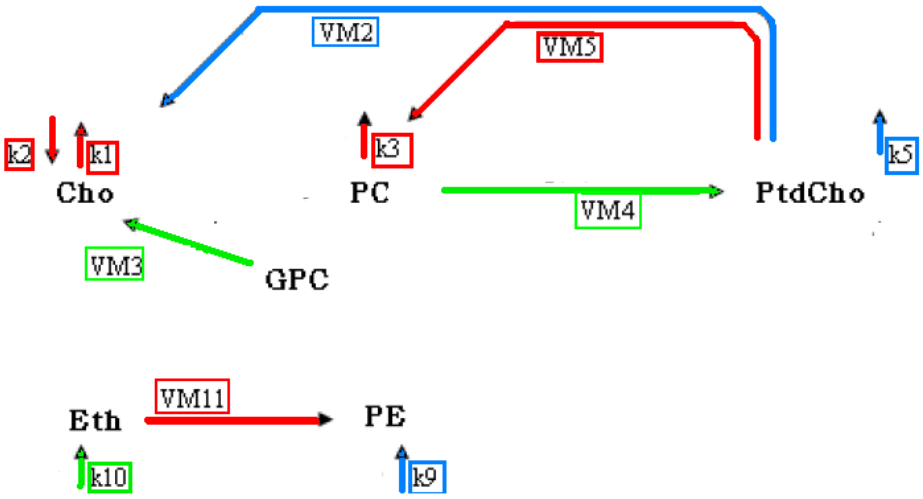

FIGURE 6.2. **Schematic representation of active pathways of the model of phospholipids of B16 melanoma under CENU treatment. Reactants:** Cho(Choline), PC(Phospho-Choline), PtdCho(Phosphatidyle-Choline), PE(Phospho-Ethanolamine), PtdEth(Phosphatidyle-Ethanolamine). **Parameters:** VM (Michaelis maximum reaction rate). The Memory effect group's parameters and the related pathway are shown by blue color. The Definitively changed group's parameters and the related pathway are shown by red color. The Finally changed group's parameters and the related pathway are shown by green color.

6.3. Results

We believe that the parameters of "Reprogramming group", "Definitively changed group" and "Finally changed group" are the most essential parameters of the system which explain the effect of the treatment. These groups are indicated by a star (*) in tables 5 and 6. After the comparative analysis of parameters in the three phases of treatment:

(1) We name the reactions which associate to "Reprogramming group" and "Definitively changed group" parameters, activated reactions. We can determine the activated reactions during CENU treatment; Figures 6.2 and 6.3 show respectively the activated reactions in B16 melanoma and 3LL carcinoma.

(2) We observe that the effect of CENU treatment in B16 melanoma is different from its effect in 3LL carcinoma. In other words the parameters

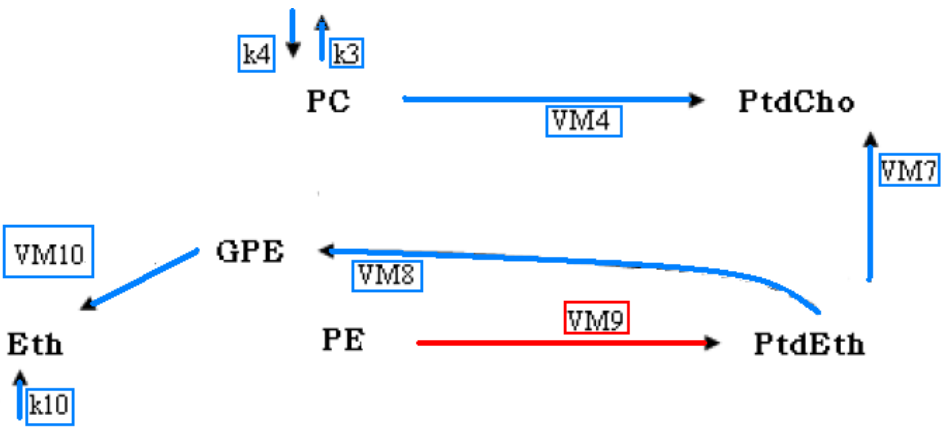

FIGURE 6.3. **Schematic representation of active pathways of the model of phospholipids of 3LL carcinoma under CENU treatment. Reactants:** Cho(Choline), PC(Phospho-Choline), PtdCho(Phosphatidyle-Choline), PE(Phospho-Ethanolamine), PtdEth(Phosphatidyle-Ethanolamine). **Parameters:** VM (Michaelis maximum reaction rate). The Memory effect group's parameters and the related pathway are shown by blue color. The Definitively changed group's parameters and the related pathway are shown by red color.

of "Reprogramming group" and "Definitively changed group" of two tumors are not the same.

(3) We can determine the few parameters which are activated in both tumors during CENU treatment.

(4) We can explain the evolutions of concentrations of reactants, based on changes of parameters from one phase to the other one. Let us explain an example in more details: As it is shown in Table 1, for B16 melanoma, we observe an increase of 5.33 $\mu mol.g^{-1}$ melanoma for Phosphoethanolamine(PEth). The reason is easily explained by our parameter analysis for the change of rates of all the reactions in which PEth plays the role of a substrate or product. Here, PEth concentration increases since VM_{11} is increasing rapidly and VM_9 is decreasing, despite PEMT activity is decreasing. In a similar way we can explain the decreases in GPC and GPE in 3LL carcinoma which is mentioned in [58].

6.4. Conclusion

In the previous Chapter we applied our mathematical analysis of the metabolic pathways which control and command the production of Glycerophospholipids through the enzymatic reactions of PhosphatidylEthanolamine and PhosphatidylCholine, and our analysis showed that the normal cell stands at very special points of equilibrium.

In this Chapter we checked our model against a series of biological experiments in vitro (B16 melanoma and 3LL carcinoma tumor cells under CENU treatment). Our comparative analyses designated a set of kinetic parameters as essential parameters to understand the effect of treatment on each of tumor cells; we observed that this effect is different in different organs and so the essential parameters do. We also could explain the evolutions of concentrations of reactants, based on changes of estimated parameters from one phase to the other one.

CHAPTER 7

Model's application to B16 melanoma cells in response to methionine deprivation

Outline

In this Chapter our goal is to understand the effects of Methionine deprivation stress (MDS) on tumor cells and of its interactions with chemotherapy, a standard treatment of advanced stage cancers. We use our modeling approach to understand the phenomena happening in the treatment. From the experimental data we are able to apply our mathematical model which fits to the experiments (see Appendix E)and explains the respective roles of PEMT. We perform several analyses such as comparative analyses and sensitivity analysis. These analyses designate a set of kinetic parameters as essential parameters to give evidence for the effect of MDS on PEMT enzyme activity.

7.1. Mathematical model and parameter estimation

The PEMT enzyme, a methyltransferase involved in PtdCho synthesis is connected to Met metabolism [**63**]. The action of Met synthesis on phospholipids' metabolism is illustrated in figure 7.1. In this Chapter we analyse the experimentally obtained concentrations of metabolites which are identified by spectroscopy (See Chapter E). These experimental data associates to particular situations of the system of phospholipids; we try to propose a global understanding of the whole system by means of mathematical simulation. In order to analyse the experimental data we use the mathematical approach proposed in Chapter 3. Previously this model has been studied to describe the response of B16 melanoma tumors to a chemotherapy agent such Chloroethylnitrosourea (CENU) which targets phospholipids metabolism; these experimental data was modeled in [**64**].

We use the model of phospholipids metabolism and the ODEs-based chemical kinetic model which was developed in Chapter 3. Next we apply the proposed algorithm in Chapter 4 on experimentally measured concentrations

to estimate the value of the kinetic parameters. For that we use the experimental data which are derived from the concentrations of B16 melanoma cells metabolism, in vitro, measured during different phases of MDS treatment (Tab. 1 and Fig. 7.2.b).

TABLE 1. **Average concentrations of B16 (in vitro).**

B16(In vitro)	Std	MDS	post-MDS
Cho	1.231	1.331	1.017
Eth	0.121	0.122	0.122
PCho	2.582	7.980	3.021
PEth	2.501	10.690	6.841
PtdCho	24.003	36.711	39.673
PtdEth	8.001	12.011	11.081
GPC	0.304	10.989	1.179
GPE	0.750	0.750	0.560

Phases; **Std**: untreated cells in Std medium; **MDS**: cell growth inhibition; **post-MDS:** cell growth recovery after MDS (early period). Values are given in $\mu mol.g^{-1}$ Melanma.

The average results of parameter estimation are shown in table 2. Verifing how spread out are the values to the average value in this table, we observe a low standard deviation.

7.2. Comparative analyses of parameters

In table 2 each of the three vectors (each column) represents the value of the parameters of the model which is associated to one of the three phases of treatment (Std, MDS, and post-MDS). We did a complete comparative analysis for the rate coefficients (k_i, VM_i), in order to study the predictive statements to explain the evolutions of the concentrations of reactants from one phase to the other. These two-step comparisons are shown in table 3. (from one phase to another, the parameter value decreases (↓), increases(↑) or does not change (-)).

After the comparative analyses, we classified the parameters in 4 groups, based on the evolution of the parameter after MDS treatment:

(a) **Neutral group**: The parameters which do not change neither during MDS phase nor during early period of post-MDS phase. These are the few parameters which are shown in table 3, by two consecutive "-" symbols. (k_6, k_7, k_{12}).

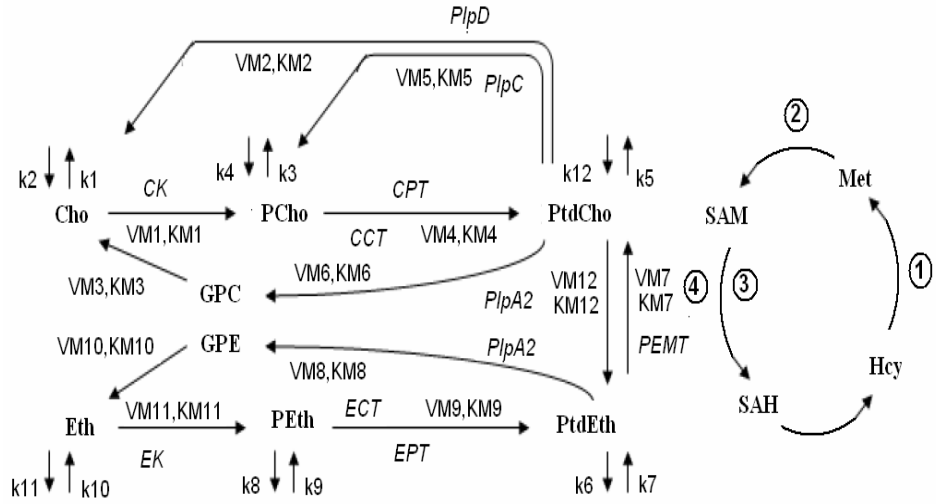

FIGURE 7.1. **Schematic representation of the model of interrelation of Methionine synthesis with Phosphatidylcholine synthesis.** VM_i and KM_i parameters refer to enzymatic reactions while the others represent simple reactions. Input and output arrows indicate external reactions in which the reactant has the role of substrate or product. **Reactants**: Cho(Choline), PC(Phospho-Choline), PtdCho(Phosphatidyle-Choline), GPC(Glycero-PhosphoCholine), Eth(Ethanolamine), PE(Phospho-Ethanolamine), PtdEth(Phosphatidyle-Ethanolamine), GPE(Glycero-PhosphoEthanolamine). **Enzymes:** CK(Choline-Kinase), EK(Ethanolamine-Kinase), CCT/CTP(PhosphoCholine-Cytidyl-Transferase), ECT/EPT(PhosphoEthanolamine-Cytidyl-Transferase), PEMT(PhosphatidyleEthanolamine-N-methyl-Transferase), PlpA2 (PhosphoLipase A2), PlpC(PhosphoLipase C), PlpD(PhosphoLipase D). **Parameters:** VM (Michaelis maximum reaction rate), KM (Michaelis concentration constant), k1-k12 (Rate constants for external reactions). Interrelation in presented in **four steps:** 1)Reaction catalyzed by betaine homocysteine methyltransferas; 2)Reaction catalyzed by methionine adenosyltransferas; 3)Transethylations; 4)Phosphatidylethanolamine-N-methyltransferase (PEMT).

(b) **Temporary changed group**: The parameters which are changed during MDS phase but that are changed again in the reverse direction during early period of post-MDS phase. These are the parameters which are

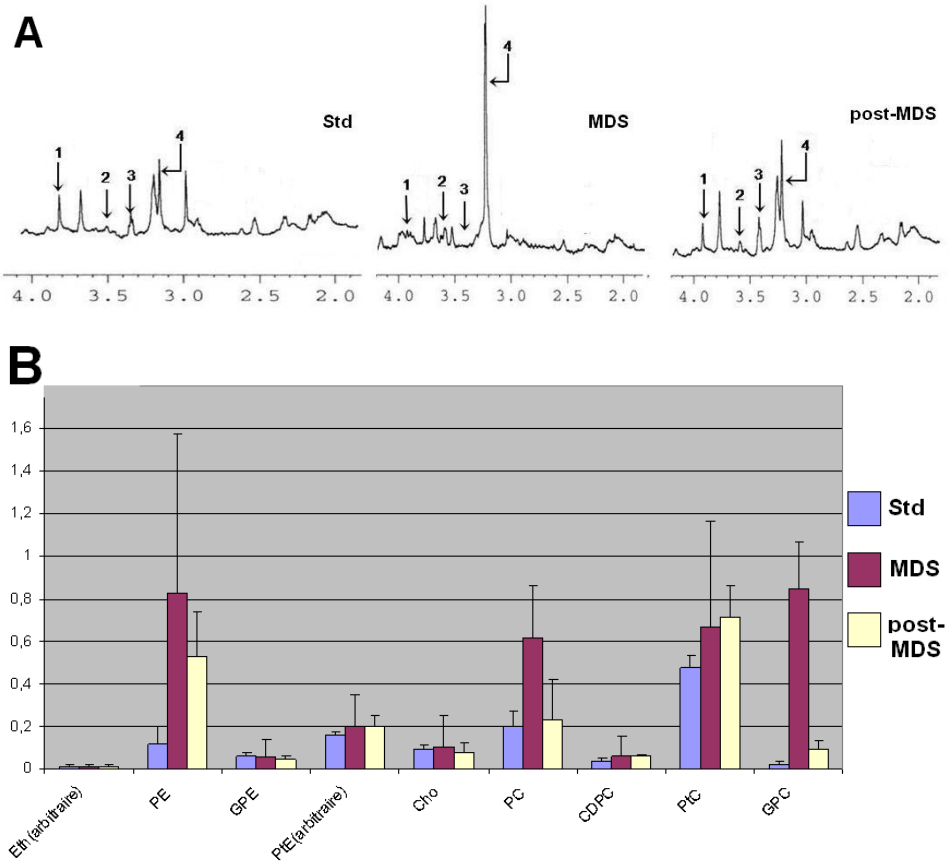

FIGURE 7.2. **A:** ^{1}H-NMR metabolic profiling of the effects of MDS. Typical 1D spectra of: Std spectrum, MDS spectrum at day 4 and post-MDS spectrum after 6 days of reinfusion in Std medium. Chemical shifts are given in ppm; the hyphenated numbers are the chemical shifts of protons to which this proton is scalar coupled: Cho (3.20, 3.55-4.07), PC (3.23, 3.62-4.18), PtdCho (3.23, 3.68-4.39), GPC (3.23, 3.68-4.34), Eth (3.15-3.80), PE (3.22-3.99), PtdEth (3.30-4.20), GPE (3.30-4.12). Identified metabolites were the following: 1, PE; 2, PC; 3, GPE; 4, GPC+PC. Cell culture and ^{1}H-NMR spectroscopy analysis were performed as described under Materials and Methods section. Spectra are representative of three experiments delivering comparable results. **B:** Average concentrations of B16 (in vitro). Phases; Std: untreated cells in Std medium; MDS: cell growth inhibition in MDS group; post-MDS: cell growth recovery after MDS. These concentrations are derived from 1D and 2D spectra.

shown in table 3, with a ↓ symbol followed by ↑ symbol or vice versa. (k_{1-5}, k_7, k_{10-12}, VM_2, VM_3, VM_6, VM_8, VM_{10}, VM_{11}).

(c) **Reprogramming group**: The parameters which are definitively changed in MDS phase, and that do not change anymore during the early period of post-MDS phase. These are the parameters in table 3, for which we observe ↓ or ↑ symbols in the first step and "-" symbol in the second step. (VM_1, VM_4, VM_{12}, k_9, k_8).

(d) **Definitively changed group**: The parameters which are definitively changed in MDS phase, and which still change during early period of post-MDS phase too. These are the parameters in table 3, for which we observe two consecutive ↑ symbols. (VM_5 ,VM_7 , VM_9).

The comparative analysis of the parameters in the three phases of MDS and the dynamic simulations in section p2-2.2.4 show that:

(1) The velocity of the reaction of PtdEth and PtdCho (rate parameter VM_7), in which PEMT plays a key role as enzyme, increases during both MDS and early period of post-MDS phases. On the other hand, the velocity of the consumption of PtdCho decreases during the early period of post-MDS phase. These two events together lead to an increased concentration of PtdCho. These results also are in a good agreement with the experimentally measured increment of the PEMT activity.

(2) We observed the crucial role of the parameters of *Reprogramming group* in the phospholipids' metabolism model. These parameters in which the value changed during the 4 days of MDS treatment, are able to keep the effect of the treatment even during the early period of post-MDS phase. The pathway which keeps this effect is shown in blue color in figure 7.3.

(3) Since the parameters of *Definitively changed group*(VM_5, VM_7 *and* VM_9) were all increased during the early period of post-MDS phase but the parameters VM_1 and VM_4 did not change, we can note that in this phase, PtdCho is not produced from the Choline pathway, but it is produced from the PtdEth methylation. This result is in a good agreement with the result which was shown theoretically in [**64**]; In high concentrations of the PEMT enzyme, the Choline pathway is saturated or blocked, but methylation of PtdEth may relay PtdCho biosynthesis. The pathway which keeps this effect is shown in red color in figure 7.3.

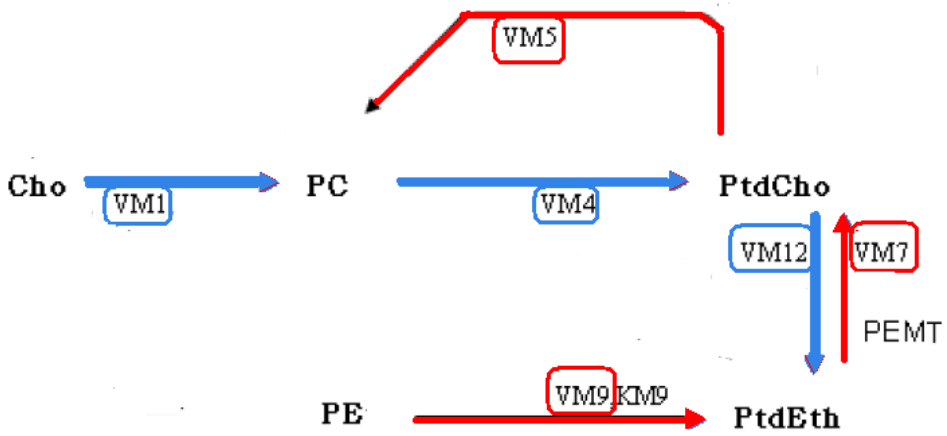

FIGURE 7.3. **Schematic representation of active pathways of the model in each phase. Reactants:** Cho(Choline), PC(Phospho-Choline), PtdCho(Phosphatidyle-Choline), PE(Phospho-Ethanolamine), PtdEth(Phosphatidyle-Ethanolamine). **Parameters:** VM (Michaelis maximum reaction rate). The Memory effect group's parameters and the related pathway are shown in blue color. The Definitively changed group's parameters and the related pathway are shown in red color.

7.3. Sensitivity analysis

Sensitivity analysis provides techniques to identify parameters which have the largest influence on the results obtained from a model. We employ Morris' sensitivity analysis method [65] which is a screening method designed to rank the parameters in order of importance; it can deal with high numbers of parameters and is global as it does not rely on particular parameter values but accounts for their whole range of possible variations. If a small change in a parameter leads to large changes in the results, the model answer is said to be sensitive to this parameter. In other words, influential parameters indicate significant functional reactions (a change in the reaction activity will have an effect) whereas non-influential parameters indicate poor functional reactions (The change has little effect on the model outcome).

Here we use sensitivity analysis to find among parameters k_i and VM_i those that most influence the steady state concentration values of all reactants in phases Std and MDS when parameters KM_i are fixed to the estimated values. As explained in Chapter 5 the maximal velocity of the reaction (VM_i) is dependent on the concentration of the enzyme in the cell

or the extract, but rather a result of regulated gene expression, and thus has to be measured for each phase of treatment again. We note here that the VM_i used in the kinetic models is not the specific activity that is measured with the purified enzyme. Thus, VM_i is dependent on the enzymes concentration and normally needs to be measured or estimated by means of numerical methods *in vivo* or *in vitro*. The binding constant (or KM_i) results from the structure of the enzyme, and thus is independent of the enzyme concentrations. We therefore argue that in many cases it is a legitimate simplification to take the KM_i values from the literature, also from related species if the lack of data requires it. This is the reason why in our sensitivity analysis the parameters KM_i are fixed to the estimated values.

The results of Sensitivity analysis for Std, MDS and early period of post-MDS phases are shown in table 4. The parameters at the top of this table are those that most influence the steady state concentration values of all reactants in each phase. This analysis shows that:

(1) When looking only at parameters k_i (the input and output arrows in figure 7.1), results show that the most influential external reactions are those linked to k_5 , k_{10} *and* k_8 in all phases.
(2) The presence of parameter VM_7 which pertains to the crucial reaction of PtdEth and PtdCho, among the most important parameters of all phases could be still another proof of the important role of the associated enzyme PEMT.
(3) In phase Std we observe VM_3, VM_6, VM_4 , VM_2, VM_5 among the most important VM_i parameters. These are all parameters which pertain to the Choline cycle. In other words in phase Std, the Choline pathway has the greatest influence on the steady state value , while in MDS and early period of post-MDS phases these are not the most important parameters anymore. This could be explained by the fact that in MDS phase the Choline pathway has been inhibited by the treatment and that, as a consequence, the system switches to the other pathways to produce PtdCho.
(4) The parameters k_{12} , k_{11} , k_1 , k_7 , k_6 and k_4 have the least influence on the steady state concentration values, in all three phases.

In summery our mathematical modeling designates parameters VM_1, VM_4, VM_5 , VM_7, VM_9 , VM_{12}, k_9 and k_7 as *essential* parameters to understand the effect of MDS treatment on B16-cells. The activated pathway associated to these parameters witnesses for a metabolomic reprogramming of the B16-cells allowing then to escape cell death during the MDS period.

Therefore these pathways represent candidate targets for combined therapies with MDS.

7.4. Conclusion and Discussion

Once the comparative analyses of parameters and their classification were done, we performed dynamic simulations, using kinetic equations, to study the evolution of the concentrations of reactants along time, for the associated mathematical model of each phase of MDS treatment. In these studies our aim was to compare Std and MDS phases and to see if we are able to define a unique model for both phases in which the explicative parameters are the ones of *Reprogramming group* and *Definitively changed group* (in the above classification). For this aim we performed three sets of dynamic simulations, and in order to obtain a general comparison view of these sets of simulations we fixed all the initial concentrations to 1 μmol.g^{-1}. (Fig. 7.4):

(a) The simulation which is based on parameter values that we found for Std phase (showed by blue color).
(b) The simulation which is based on parameter values that we found for MDS phase. (showed by red color).
(c) At last, the simulation which is based on parameters that we found for Std phase, when we change the value of parameters of *Reprogramming group* and *Definitively changed group* to their value in MDS phase. We denote this model M-Std which means modified Std model. (showed by black color).

We observe that the dynamic simulation of this modified model is very similar to the simulation of the MDS phase model. (Fig. 7.4.) This fact could indicate that one can describe the phospholipids' metabolism model, by defining a unique model which has just a few explicative parameters.

In section 5.6, we proved that in the proposed mathematical model which is based on Michaelis-Menten kinetics, all the evolutions of the cell metabolism are stable (Proof by means of the Jacobian matrix). In this Chapter we observed the stability for a model with diffusions.

In conclusion, this work showed that MDS induces Phospholipids metabolite disorders including PC, GPC and PE form phospholipid metabolism and transmethylation reactions. The MDS treatment allowed us to demonstrate that there was a tumor metabolism reprogramming at the level of the Met

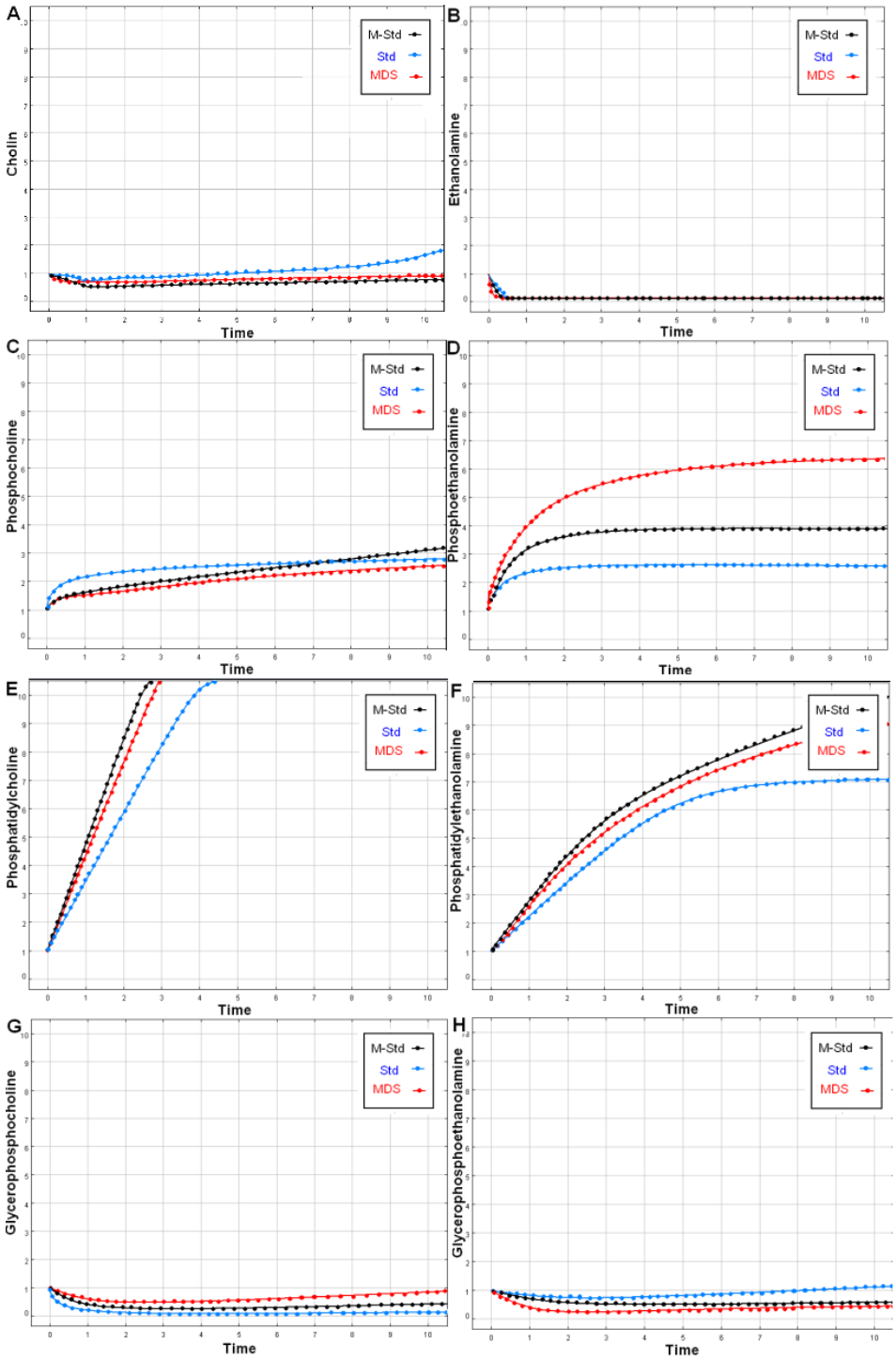

FIGURE 7.4. **Dynamic simulations based on estimated parameters.** (evolution of concentration of each of reactants of the model in time). Models 1) **Std**: model of untreated cells in Std medium (shown by bleu color); 2) **post-MDS**: model of cell growth recovery after MDS. **M-Std**: proposed model for Std in which the explicative parameters are modified. All the initial concentrations are fixed to 1 $\mu mol.g^{-1}$. in order to obtain a general comparison view of the three sets of simulations.

metabolism. These results shed new lights on the understanding of the metabolic consequences of MDS. Our data demonstrate that the metabolomics approach may help:

(1) understanding tumor response to nutritional therapeutics and their association with conventional chemotherapy.
(2) determine potential new therapeutic targets such as PEMT. (We showed the mathematical and biological evidence of the fact that PEMT is a key target for cancer control.)

In this Chapter using an ODEs-based mathematical model, we presented comparative and sensitivity analysis, which:

(1) designated a set of kinetic parameters as essential parameters to understand the effect of MDS treatment on B16-cells.
(2) gave evidence for the effect of MDS on PEMT enzyme activity which has a crucial role in tumor cells.
(3) proposed the activated pathway which witnesses for a metabolomic reprogramming of the B16-cells allowing then to escape cell death during the MDS period. Therefore these pathways represent putative candidate targets for therapies combined with MDS.

Table 2. Estimated parameter values for B16 in vitro.

Cell:	B16(in vitro)		
Parameter:	Std	MDS	post-MDS
k_1	0.664±0.010	1.617±0.020	0.476±0.28
k_2	4.661±0.011	7.856±0.004	5.765±0.012
k_3	0.893±0.005	0.331±0.008	1.295±0.001
k_4	3.357±0.012	1.043±0.014	4.082±0.014
k_5	0.069±0.04	0.018±0.002	0.039±0.001
k_6	0.034±0.001	0.036±0.002	0.052±0.002
k_7	1.011±0.002	1.002±0.002	1.001±0.003
k_8	0.470±0.004	0.140±0.011	0.120±0.013
k_9	2.563±0.004	1.001±0.001	1.042±0.001
k_{10}	5.031±0.009	6.258±0.15	6.167±0.006
k_{11}	0.523±0.002	2.365±0.008	3.470±0.009
k_{12}	1.001±0.01	1.002±0.001	1.001±0.001
VM_1	6.838±0.018	8.421±0.051	8.896±0.029
KM_1	1.232±0.003	1.341±0.003	1.015±0.001
VM_2	3.411±0.032	5.188±0.010	3.522±0.036
KM_2	23.455±0.010	36.008±0.001	40.016±0.002
VM_3	2.312±0.007	3.341±0.004	2.143±0.007
KM_3	0.335±0.002	9.855±0.003	1.180±0.002
VM_4	5.306±0.035	9.578±0.059	9.288±0.029
KM_4	2.391±0.002	7.073±0.004	3.025±0.031
VM_5	3.437±0.021	6.431±0.015	7.808±0.055
KM_5	23.908±0.010	35.776±0.053	39.971±0.013
VM_6	2.312±0.016	3.341±0.017	2.143±0.015
KM_6	24.240±0.010	36.005±0.010	39.015±0.018
VM_7	8.382±0.021	9.804±0.020	10.472±0.022
KM_7	8.005±0.004	11.071±0.006	11.089±0.004
VM_8	1.067±0.003	1.827±0.003	1.489±0.002
KM_8	8.660±0.001	11.011±0.001	11.010±0.003
VM_9	7.950±0.012	9.371±0.015	9.958±0.017
KM_9	2.566±0.006	9.68±0.006	6.551±0.002
VM_{10}	1.067±0.011	1.827±0.030	1.489±0.027
KM_{10}	0.755±0.001	0.750±0.001	0.566±0.001
VM_{11}	9.050±0.052	11.338±0.056	10.637±0.049
KM_{11}	0.112±0.002	0.119±0.002	0.125±0.002
VM_{12}	2.041±0.018	3.075±0.044	3.173±0.042
KM_{12}	24.004±0.018	35.505±0.025	37.905±0.021

Estimated parameter values for B16 which is used in our comparative analysis. Values (means estimate ± SD estimate) are given in $\mu mol.g^{-1}$. tumor for KM_i and $\mu mol.g^{-1}.s^{-1}$ for VM_i and s-1 for k_i.

Table 3. Comparative analysis for rate parameters.

Cell:	B16(in vitro)		
Parameter:	Std→MDS	MDS→post-MDS	*
k_1	↑	↓	
k_2	↑	↓	
k_3	↓	↑	
k_4	↓	↑	
k_5	↓	↑	
k_6	-	-	
k_7	-	-	
k_8	↓	-	*
k_9	↓	-	*
k_{10}	↑	↓	
k_{11}	↑	↑	
k_{12}	-	-	
VM_1	↑	-	*
VM_2	↑	↓	
VM_3	↑	↓	
VM_4	↑	-	*
VM_5	↑	↑	*
VM_6	↑	↓	
VM_7	↑	↑	*
VM_8	↑	↓	
VM_9	↑	↑	*
VM_{10}	↑	↓	
VM_{11}	↑	↓	
VM_{12}	↑	-	*

"↓": parameter value decreased; "↑": parameter value increased; "-": parameter value is fixed. "*": Explicative parameters.

Table 4. The results of Sensitivity analysis for Std , MDS and post-MDS phases.

Std	MDS	early post-MDS
Parameter	Parameter	Parameter
VM_3	VM_{10}	VM_{10}
VM_6	VM_7	VM_8
VM_7	VM_9	VM_9
VM_4	VM_8	VM_7
k_5	k_{10}	VM_6
k_{10}	k_8	VM_3
VM_2	VM_{11}	k_{10}
VM_5	VM_{12}	k_5
VM_9	VM_3	VM_{12}
VM_{10}	VM_4	VM_{11}
VM_1	k_3	k_8
VM_8	VM_6	VM_4
VM_{11}	VM_2	VM_1
k_9	k_5	k_3
k_3	VM_5	VM_2
VM_4	VM_1	VM_5
k_8	k_6	k_2
k_2	k_{11}	k_9
k_4	k_1	k_4
k_6	k_2	k_6
k_7	k_9	k_7
k_1	k_7	k_1
k_{11}	k_4	k_{11}
k_{12}	k_{12}	k_{12}

The parameters at top of this table are those that most influence the steady state concentration values of all reactants in each phase.

CHAPTER 8

Conclusion

Outline

In this Chapter we will point out essential aspects of this work. A short summary and the main results have already been addressed in the last section of each Chapter. The main statements of this thesis are summarized in Section 8.1 and we will respond to consequences for the ultimate goal of constructing models of phospholipid biosynthesis. Finally, Section 8.2 discusses perspectives for future work, which arise from the precedent conclusions.

8.1. Summary and main results

In this dissertation, we studied a model of the phospholipid biosynthesis biochemical reactions which are the core of the system of Glycerophospholipid metabolism in murine cells, in fact in human cells as well. Still the important role of PhosphatidylEthanolamine N-Methyl transferase (PEMT) enzyme on phospholipid biosynthesis is not well studied. Our attempt has been not only to bring serious attention to this issue, but also to present a practical option of using mathematical modeling to help address this issue in a realistic way.

The kinetic model developed for the phospholipid biosynthesis is constructed from acceptable quantitative descriptions of experimental data and is based on the latest experiments of the biologists with whom we colaborated. Even though the kinetic constants of this model have not been experimentally measured, the expected characteristics of the PEMT enzyme were demonstrated in the simulation results.

To construct the mathematical model of the phospholipid biosynthesis we have chosen a dynamic, continuous and deterministic modeling approach. With this model one can represent the behavior of the phospholipids' metabolic pathway; the temporal changes of metabolites are formulated as a generic set of ODEs. Next we applied this model to different experimental

datasets in healthy and tumoral cells; each of these applications consists of parameter estimation process, mathematical simulation of the model and a set of analyses such as stability analysis or sensitivity analysis.

In the first application of the model we considered experimental data of rat's liver cells; given the values of metabolite concentrations we found appropriate parameter values which allowed us to describe the system by means of ODEs. Next we performed several analyses using the developed model such as stability analysis and the time necessary to reach the steady state point. A first interesting result was the global stability of the system which was observed by simulation and then proved by mathematical arguments. A second important result was that we observe on the diagrams that the steady states for healthy cells were precisely the very special points of equilibrium which happened to be a singular point of order two; this fact has been proved for PhosphatidylEthanolamine N-Methyl transferase (PEMT) enzyme which has a crucial role in the tumoral process. Our results provide that all the evolutions of the cell metabolism are stable in the Michaelis-Menten formalism, and the healthy cell behaviour corresponds to a "superstable" steady state.

As a second application of the model, we applied our proposed model to experimental data of proton HRMAS NMR spectroscopy for solid B16 melanoma and Lewis lung (3LL) 3LL carcinoma cells treated by Chloroethyl Nitrosourea (CENU). After performing the estimation of unknown parameters, we proceeded to a complete comparative analysis of the parameters. This analysis in concentrations helped us to find the predictive statements to explain increases and decreases which one can observe. We checked our model against a series of biological experiments and gave evidence for the crucial role of PhosphatidylEthanolamine N-Methyl transferase (PEMT) in tumor cells under CENU treatment. Our results show that the model fits "in vivo" observations and experiments with CENU tumor inhibitor, and provides new hypotheses on metabolic pathway activity based on metabolite profiling of phospholipids derivatives.

In the last application of the model, our study was devoted to the understanding of Methionine deprivation stress (MDS) and of its interactions with chemotherapy, a standard treatment of advanced stage cancers. This

study had a twofold approach to the modeling of the phenomena happening in the treatment. Firstly the biologists we colaborated with, used a metabolomics approach using ^{1}H-NMR spectroscopy to get novel insights into the mechanism of the action of the MDS. To this aim they investigated, in vitro, the growth and metabolic response of B16 melanoma cells to MDS. They showed that MDS provoked a cell growth delay and induced disorders of phospholipid metabolism such as a increase in Glycerophosphocholine (GPC), Phosphocholine (PC) and Phosphoethanolamine (PE) levels and activation of the phosphatidylethanolamine-N-methyltransferase (PEMT) involved in phosphatidylcholine synthesis. After the cessation of MDS, tumor cells metabolism exhibited persistent alterations such as increased PEMT activity. These metabolic events probably explained the increased growth delay induced by the MDS. Secondly from the data they provided, we proposed a mathematical model which fits to these biological experiments and "explains" the respective roles of PEMT. This model proves to be very stable and is very robust w.r.t. reasonable variations that can be induced by experimental errors and individual characteristics. Again in this application we performed several analyses such as comparative analyses and sensitivity analysis. These analyses designated a set of kinetic parameters as essential parameters which give evidence for the effect of MDS on PEMT enzyme activity which has a crucial role in tumor cells and proposed the activated pathway which witnesses for a metabolomic reprogramming of the B16-cells allowing then to escape cell death during the MDS period. Therefore these pathways represent putative candidate targets for therapies combined with MDS.

In conclusion we can mention the advantages of using the ODE-based model that we developed and of the consequent analyses as follow:

(i) Using the model we are able to estimate the kinetic parameters which are not experimentally measured. For different cells and under different treatments we found different values for these kinetic parameters as expected.

(ii) Mathematical simulations of this model help to understand the behaviour of different components of the model in time.

(iii) We determined the essential parameters in different cells (B16 and 3LL). This helped us to find the similar effects of a treatment on specific pathways in these two different cells. Also we found that the effect of

the treatment is not exactly the same in different cells and that the essential parameters are not exactly the same in both families of cells.

(iv) We determined the essential parameters in the same cells (B16) but under two different treatments (CENU and MDS). We observed that the activated pathways after each treatment are different. Also we found the commun parameters in the activated pathway of each treatment where PEMT was one of the most important parameters of the system.

8.2. Discussion and Future work

The last application of the model showed that MDS induces phospholipids metabolite disorders including PC, GPC and PE form phospholipid metabolism and transmethylation reactions. We proposed the activated pathway which witnesses for a metabolomic reprogramming of the B16-cells allowing then to escape cell death during the MDS period. Therefore these pathways represent putative candidate targets for therapies combined with MDS.

The methods applied in this thesis can help to understand tumor response to nutritional therapeutics and their association with conventonal chemotherapy. Also they show the evidence of the fact that PEMT enzyme is a key target for cancer control.

At this point we suggest that interesting investigations to perform in a next step could be:

- Comparing the parameter values in a healthy cell and a tumor cell of the same tissues. Here one of the weeknesses of this study was that we did not have access to experimental values for the same cells before transforming to the tumor cells.
- In the last application of the model we found a set of essential kinetic parameters. In a next step we performed a dynamic simulation of the model in which the only parameters that we change are the ones which we call them essential parameters. In other words we used a model in which the number of parameters is much smaller than in the original model. What we propose from an experimental point of view is that it could be of interest of biologists to apply a new treatment which targets only a few number of chemical reactions associated to these essential parameters.

- During different applications of the model we observed a difference between the values of concentrations of a same reactant. In our model and analyses we tried to explain this changes of concentrations, by finding the changes of the kinetic parameters in different phases (such as different values of VM parameters). From the general form of Michaelis-Menten formula we know that the changes in maximum velocity of a reaction are proportional and could come from the changes in the concentration of enzymes. Therefore it could be interesting first to measure the concentration of enzymes, and second to measure other possible important factors such as temperature or PH in different phases. In that case as a next step in mathematical modeling of such a system, it could be interesting to construct a new model in a more realistic way in which we have other sets of parameters for PH, temperature, etc.

About the simplification of the model, there exists some possibilities:

- One can propose to replace consecutive reactions of a specific pathway by only one hypothetical reaction. In other words is it possible to simply delete the intermediate reactions and reactants? In our model we used experimental data in order to not loose the accuracy of the model; this simplification we used only for two intermediate reactions which are mentioned in literature.
- Another simplification for the mathematical model could be to assume that all reactions follow just the mass action law and that there is a need to use the Michaelis-Menten formula in equations. After applying this simplification we found that it may help to have a smaller number of unknown parameters in the ODE-based mathematical model, but on the other hand it wont help us to find precise information about the essential parameters in order to compare different treatments. Therefore in our model we assumed the Michaelis-Menten formula for enzymatic reactions.
- In most mathematical models for other similar metabolic pathways which are already published, the modelers assumed that the system of reactions is a closed system, which means that they assume just the internal reaction between given reactants. This will of course help to have a smaller number of parameters in the mathematical system. But in our methodology we assumed that the model is open. This means that there are also interactions between internal reactants of our model with the external reactants, which is the

case in the reality. We showed this fact with external or internal fleshes on graph of reactions. On the other hand, comparative and sensitivity analyses show that a few number of essential parameters are associated to this external reactions. This shows the importance of adding this reactions to the model.

APPENDIX A

Chemical reactions and enzyme kinetics

Outline

This Appendix introduces some basic biochemical definitions about different types of chemical reactions, systems of chemical reactions and enzyme kinetics. Furthermore this Appendix describes some basic building blocks from which we constructed our mathematical model: concepts of reaction rate and different rate laws such as mass action law and Michaelis-Menten kinetic. (Note that most of definitions in this Appendix are taken from Wikipedia documents and Lecture notes of D. Gonze and M. Kaufman [70])

A.1. Chemical Reactions

A chemical reaction is the process that converts a fixed collection of metabolites, the reactants, to another fixed collection of metabolites, the products. Chemical reactions can consist of one reactant (monomolecular reaction), two reactants (bimolecular reaction), or a greater number of reactants (trimolecular reaction, etc.). Most of the chemical reactions in the systems studied in this dissertation are monomolecular reactions. In special cases, such as open systems, there are reactions with zero reactant.

A chemical reaction equation consists of reactants followed by an arrow pointing to the products, as in:

$$CO_2 \ + \ H_2 \rightarrow CO \ + \ H_2O \tag{11}$$

This particular chemical reaction is an example of an oxidation-reduction reaction in which CO_2 and H_2 have the role of substrates and CO and H_2O are the products of the reaction.

A chemical reaction can require more than one instance of a reactant, or produce more than one instance of a product. The stoichiometry is the number of instances of a reactant or product in a single chemical reaction.

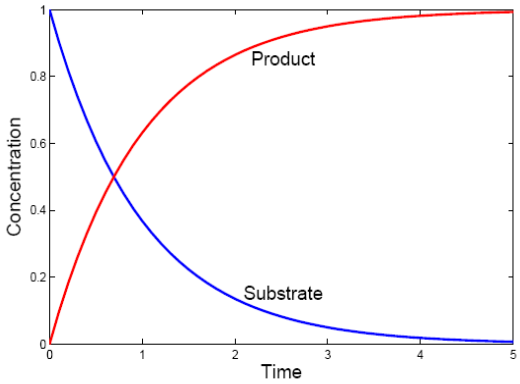

FIGURE A.1. **Time evolution of the concentration of the substrate and product.**

In order to declare the stoichiometry of each metabolite in the chemical reaction we write a number before that metabolite. For example, the reaction equation,

$$2Fe^{3+} \ + \ Zn \rightarrow 2Fe^{2+} \ + \ Sn^{2+}, \tag{12}$$

corresponds to the chemical reaction equation with two copies of the metabolite Fe^{3+} and two copies of the metabolite Fe^{2+}.

The chemical reactions given so far are irreversible chemical reaction equations. An irreversible chemical reaction equation only proceeds from the chemical reactants to the chemical products. A reversible chemical reaction equation can proceed in both directions and we represent it with a two-way arrow, as in the following reaction which is equivalent to a pair of irreversible chemical reaction equations.

$$N_2 \ + \ 3H_2 \rightleftharpoons 2NH_3, \tag{13}$$

Most reactions in the cell are reversible. However, the reversible reactions generally have an equilibrium point that favors one of the reactions over the other at any moment. Wa call the set of chemical reactions that take place within an enclosed universe, the system of chemical reactions (or chemical system). When modeling big chemical systems it is difficult to represent every chemical species that exist inside the cell; we then try to simplify the model by choosing a limited number of chemical species that

play an important role in the problem and its simulations. Furthermore in the model studied in this dissertation we propose to take into account two types of reactions: "synthesis" and "degradation". This comes from the fact that sometime areaction indicates that a chemical species spontaneously appears or disappears in the chemical system. We name such a system "open". Open chemical systems exchange energy and matter between the system and its containing environment. Similarly, if there is no synthesis or degradation in a system we name such a system "closed".

When no reactant takes part in "synthesis" reactions we write an empty space for the reactants, " $\rightarrow X$" in its reaction equation. Similarly, when no products takes part in "degradation" reactions we write an empty space for the products, "$X \rightarrow$ ". These equations in a chemical system represent the transportation of species into and out of the enclosing universe.

A.2. Reaction rate

Consider a typical elementary chemical reaction in which m molecules of A react with p molecules of B:

$$mA \ + \ pB \rightarrow qC \ + \ rD \tag{14}$$

The **rate law** for this chemical reaction is given by the mass action law:

$$v = k[A]^m[B]^p \tag{15}$$

Note that the sum m+p is called the **order of a reaction**. In such a reaction, *the variation in time* of the concentration of the metabolites is given by,

$$\frac{\partial A}{\partial t} = \frac{\partial B}{\partial t} = -k[A]^m[B]^p \ and \ \frac{\partial C}{\partial t} = \frac{\partial D}{\partial t} = k[A]^m[B]^p \tag{16}$$

The negative sign in the right-hand side of these equations stands for the consumption of metabolites A and B and the positive sign stands for production of metabolites C and D. The **rate constant k** accounts for the probability that the molecules are well oriented and have enough energy to react.

Consider now the following general reaction, in which for each n molecules (moles) of X, p molecules (moles) of X are recovered at the end:

$$nX \ + ... \rightarrow pX \ + ... \tag{17}$$

When we write the evolution of the concentration of X, we must take into consideration the fact that each time this reaction occurs, only $p - n$ molecules of X are transformed or are created. So the evolution equation for the concentration of X in both cases is:

$$\frac{\partial X}{\partial t} = \eta v \ with \ \eta = p - n, \ andvisanexpressionin[X] \tag{18}$$

η is called the **stoechiometric coefficient**. This coefficient is positive if, globally, the species is produced (p > n) and negative if the species is transformed (n > p).

For example, for the following reaction:

$$2A \ + \ 3B \rightarrow 4A \ + \ B \ + \ C \tag{19}$$

the stoechiometric coefficients of the different metabolites are:

$$\eta_A = 4 - 2 = 2, \ \eta_B = 1 - 3 = -2, \ \eta_C = 1 - 0 = 1 \tag{20}$$

and the evolution in time of metabolites are:

$$\frac{\partial A}{\partial t} = 2k[A][B]^2, \ \frac{\partial B}{\partial t} = -2k[A][B]^2, \ \frac{\partial C}{\partial t} = k[A][B]^2 \tag{21}$$

A.3. System of chemical reactions

We are usually interested by systems of coupled chemical reactions (also known as chemical systems). The variation of a given metabolite X_i that is involved in R reactions is defined by:

$$\frac{\partial X_i}{\partial t} = \sum_{r=1}^{R} \eta_{ir} v_r = \eta_{ir} v_r + \eta_{i2} v_2 + ... + \eta_{iR} v_R \tag{22}$$

where

v_R= rate of the different reactions ($r = 1, 2, ...R$).
$\eta_{ir} = p_{ir}$ - n_{ir}= stoechiometric coefficient of compound X_i in reaction r.

Table 1 illustrates an example of a system of chemical reactions:

TABLE 1. Example: System of chemical reactions.

r	reaction	rate	η_{Xr}	η_{Yr}
1	$A \xrightarrow{k_1} B$	$v_1 = k_1 A$	η_{X1}=1	η_{Y1}=0
2	$B + X \xrightarrow{k_2} Y + C$	$v_2 = k_2 BX$	η_{X2}=-1	η_{Y1}=1
3	$2X + Y \xrightarrow{k_3} 3X$	$v_3 = k_3 X^2 Y$	η_{X3}=1	η_{Y3}=-1
4	$X \xrightarrow{k_1} D$	$v_4 = k_4 X$	η_{X4}=-1	η_{Y4}=0

The evolution equations for X and Y are given by

$$\begin{cases} \frac{\partial X}{\partial t} = k_1 A + k_2 BX + k_3 X^2 Y - k_4 X \\ \frac{\partial Y}{\partial t} = k_2 BX - k_3 X^2 Y \end{cases}$$

A.4. Enzyme kinetics

A.4.1. Enzymes. Enzymes are generally proteins that catalyze chemical reactions by increasing or decreasing the rates of reactions. Although enzymes help to convert substrates into products, they themselves are not modified by the reaction; it means that enzymes are not consumed by the reactions they catalyze, nor do they alter the equilibrium of these reactions. Enzymes are particularly efficient at **speeding up** biological reactions. Most enzyme reaction rates are up to millions of times faster than in un-catalyzed reactions.

Enzymes work by lowering the free activation energy for a reaction, thus increasing the rate of the reaction. As a result, products are formed faster and reactions reach the equilibrium state more rapidly (Fig. A.2).

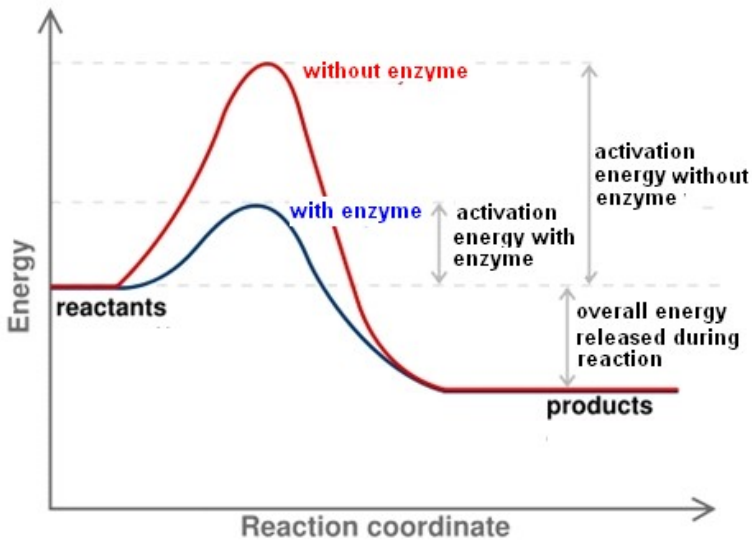

FIGURE A.2. **Activation Energy:** diagram of a catalytic reaction showing difference in activation energy in uncatalysed and catalysed reaction (taken from Wikipedia: Mechanisms of catalysis)

An example of an enzymatic reaction is the conversion of sucrose to fructose and glucose, catalysed by the enzyme sucrase which in shown in figure A.3. The active site of enzyme has a specific shape that only a particular substrate fits into. When enzyme, sucrase (shown by purple color), and substrate, sucrose (shown by yellow color), are joined they react and the substrate converts into the product, glucose (shown by orange color) and fructose (shown by pink color) . Finally the enzyme and new product separate (Enzyme left unchanged).

A.4.2. Michaelis-Menten equation. Enzymatic reactions do not follow the mass action law directly. If we apply mass action law directly to the reaction with the enzyme, the reaction velocity has to increase linearly as the substrate increases. While in an enzymatic reaction when the concentration of substrate is increased, the rate of the reaction increases only to a certain extent, reaching a maximal reaction velocity at high substrate concentration. Based on experimental observations, Leonor Michaelis and Maud Menten (1913) have proposed the following mechanism for the enzyme-catalysed biochemical reactions to explain this saturation in speed [**71**]:

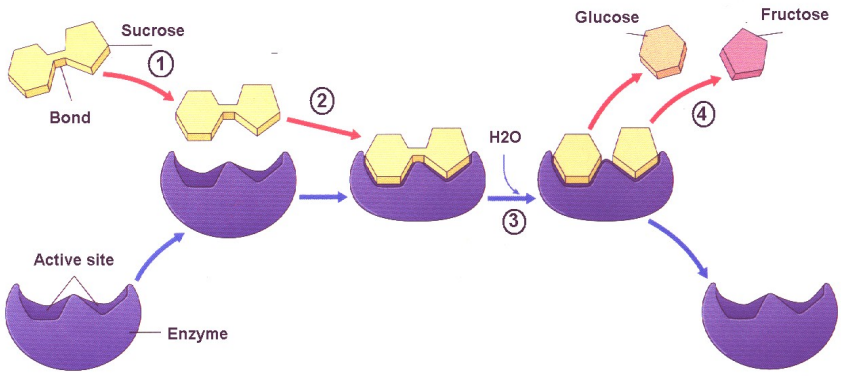

FIGURE A.3. **Conversion of sucrose to glucose.** 1: The substrate, sucrose, consists of glucose and fructose bonded together. 2: The substrate binds to the enzyme, forming an enzyme-substrate complex. 3: The binding of the substrate and enzyme places stress on the glucose fructose bond and the bond breaks. 4: Products are released and the enzyme is free to bind other substrates.

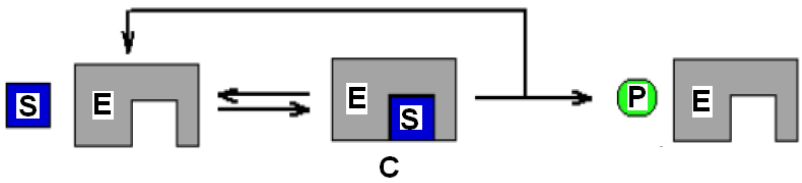

FIGURE A.4. **Michaelis-Menten mechanism** for the enzyme-catalysed reactions to explain this saturation in speed. S(Substrate), P(Product), E(Enzyme), C(enzyme-substrate Complex) (see [71])

This reaction and the evolution equation for the different metabolites (following the mass action law) can be written as:

$$E \ + \ S \overset{k_1, k_{-1}}{\leftrightarrow} C \overset{k_2}{\rightarrow} E \ + \ P \tag{23}$$

FIGURE A.5. **Maud Menten and Leonor Michaelis**, who together pioneered the development of enzyme kinetics by formulating the Michaelis-Menten equation to describe the steady state action of enzymes.

$$\begin{cases} \frac{\partial S}{\partial t} = -k_1[E][S] + k_{-1}[C] \\ \frac{\partial E}{\partial t} = -k_1[E][S] + k_{-1}[C] + k_2[C] \\ \frac{\partial C}{\partial t} = k_1[E][S] - k_{-1}[C] - k_2[C] \\ \frac{\partial P}{\partial t} = k_2[C] \end{cases}$$

where C is the complex of enzyme E and substrate S.

Michaelis and Menten in their original analysis, assumed that the substrate S is in instantaneous equilibrium with the complex C, i.e.

$$k_1, k_{-1} >> k_2 \tag{24}$$

Therefore

$$k_1[E][S] = k_{-1}[C] \tag{25}$$

Since $E_T = E + C$, we find that:

$$C = \frac{[E_T][S]}{\frac{k_{-1}}{k_1} + [S]} \tag{26}$$

Hence, the product P of the reaction is produced at a rate

$$v = \frac{\partial P}{\partial t} = k_2[C] = V_{max}\frac{[S]}{K_S + [S]} \tag{27}$$

where

$$V_{max} = k_2[E_T] \; and \; K_S = \frac{k_{-1}}{K_1} \tag{28}$$

A.4.3. Briggs-Haldane equation. Based on the same reaction mechanism (fig. A.4), Briggs and Haldane (1925) suggested an alternative hypothesis: if the enzyme is present in "catalytic" amounts (i.e. E << S), then, very shortly after mixing E and S, a steady state is established in which the concentration of ES (variable C in system of equations) remains essentially constant with time [**72**] (see figure A.6):

$$\frac{\partial C}{\partial t} = \frac{\partial E}{\partial t} = 0 \tag{29}$$

We define $[E_T]$ the total concentration of enzyme: $[E_T]$ = [E] + [C] = constant.

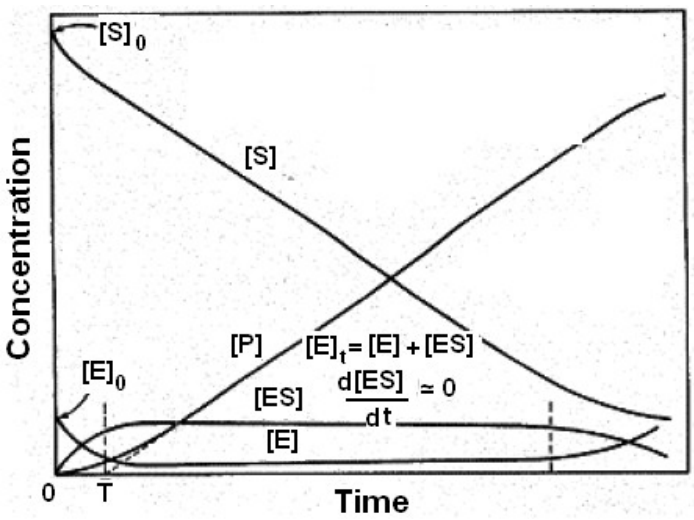

FIGURE A.6. **Evolution of the concentration in an enzyme-catalyzed reaction.** E: Enzyme, S: Substrate, ES: enzyme-substrate complex, P: Product. ([**70**, **72**])

This hypothesis is the quasi-steady state approximation. This assumption implies that:

$$k_1[E][S] - k_{-1}[C] - k_2[C] = 0 \tag{30}$$

From this equation, with $[E_T] = [E] + [C]$ we can extract C:

$$C = \frac{k_1[E_T][S]}{k_1[S] + (k_{-1} + k_2)} = \frac{[E_T][S]}{[S] + \frac{(k_{-1}+k_2)}{k_1}} \tag{31}$$

When we replace this expression for C in the rate of production of P, we obtain:

$$v = \frac{\partial P}{\partial t} = k_2[C] = \frac{k_1[E_T][S]}{k_1[S] + (k_{-1} + k_2)} = \frac{k_2[E_T][S]}{[S] + \frac{(k_{-1}+k_2)}{k_1}} \tag{32}$$

which is usually written as:

$$v = V_{max}\frac{[S]}{[S] + K_M} \tag{33}$$

where

$$K_M = \frac{k_{-1} + k_2}{k_1} \; and \; V_{max} = k_2[E_T] \tag{34}$$

The rate is thus similar to the rate of the equilibrium hypothesis (Michalis-Menten equation); only K_M has a slightly different meaning. We see that when k_1, $k_{-1} >> k_2$, we have $K_M \rightarrow K_S$. Note that K_M is usually called the **Michalis-Menten constant**, although the exact meaning of this constant is rarely specified.

If $[S] << K_M$, we observe a first order kinetic (linear relation between v and S):

$$v = k[S] \tag{35}$$

where

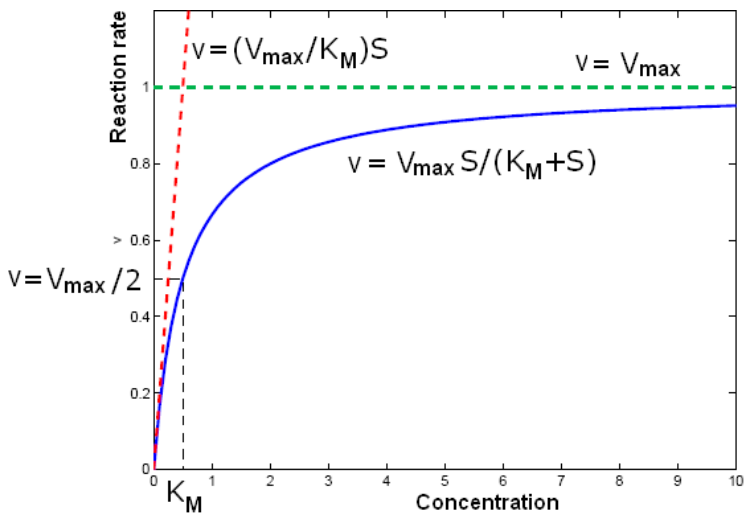

FIGURE A.7. **Michalis-Menten kinetic.** v: reaction rate, V_{Max}: maximum reaction rate, K_M: inverse of enzyme affinity, S: substrate's concentration. (see [**71**])

$$k = \frac{V_{max}}{K_M} \tag{36}$$

If S >> K_M, we observe a zero-order kinetic (constant rate v):

$$v = V_{max} \tag{37}$$

APPENDIX B

Parameter estimation methods

B.1. Forward or bottom-up modeling

Before the rapid development of high-throughput experimental tools, essentially all metabolic models were developed from "local" kinetic information of biochemical or physiological responses in a reductionist manner. Specifically, biologists worked on characterizing one particular enzyme or transport step at a time in the traditional manner. They purified the enzyme, studied its characteristics, determined optimal temperature and pH ranges, and quantified cofactors, modulators, and secondary substrates. Isolated from these laboratory experimenters, modelers converted this information into a mathematical rate law. One can merge all information about rate laws into an integrative mathematical model. This forward process might lead to a model representation of the pathway that exhibits the same features as reality, at least qualitatively, if not quantitatively [**73**, **74**, **75**]. The strategy consists of setting up a symbolic model, estimating local parameters, studying the integration of all individual rate laws into a comprehensive model, testing the model, and making refinements to some of the model structure and the parameter values.

While theoretically straightforward, there are several disadvantages to this approach. The main issue is that a considerable amount of local kinetic information is needed and that this information is often obtained from different organisms, different species, and collected under different experimental conditions. Therefore, more often than not the "integrated result" is not consistent with biological observations. Furthermore, this process of construction and refinement is very labor intensive and requires a combination of biological and computational expertise that is still rare [**74**, **75**].

B.2. Using steady-state data

If a system operates preferentially at a steady state, the parameters of the model can be estimated using steady-state data, including steady-state concentrations and fluxes of material flows at steady state. Estimations of

parameter values from steady-state data are generally based on observing how a biochemical system responds to small perturbations around the steady state.

B.3. Inverse or top-down modeling

Much of the information necessary for parameter estimation depends not only on steady-state measurements or simple perturbations around the steady-state, but on measurements for all metabolites at sequential points in time that may include considerable deviations from the steady state. Modern high-throughput techniques of biology are capable of producing this type of time series data and have begun to offer distinct alternative options for modelling metabolic systems, namely the "top-down" or "inverse" approach. The experimental tools which allow the generation of dynamic metabolite concentration profiles presently include nuclear magnetic resonance (NMR), mass spectrometry (MS), high performance liquid chromatography (HPLC), and flow cytometry (see review in [**73**]). In contrast to the "local" data obtained from traditional experiments, the clear advantages of using "global" data are that the information is collected within the same organism, obtained under the same experimental condition, and sometimes even *in vivo*. These data contain enormous information on the structure and regulation of the biological system they describe. However, this information is mostly implicit, and it is very challenging to extract it from these data because the complexity and nonlinearity of biological networks.

APPENDIX C

Stability analysis in dynamic models

Outline

The analysis of the stability of the steady state is an important aspect for the further interpretation of dynamic models. Only if the model has a stable steady state can a sensitivity analysis of its variables be performed. In this Appendix we give an introduction to the stability analysis of dynamic models. (This Appendix is inspired by a number of books and lecture notes [**76**, **77**, **78**])

C.1. Stability Analysis of Dynamic Models

In the following conditions for the stability of a steady state of a dynamic model are obtained using Lyapunov's stability criterion ([**79**]) and linear stability analysis. In order to do this the concepts of eigenvectors and eigenvalues of a square matrix are needed so a brief introduction to these concepts is given first.

C.1.1. Eigenvectors and eigenvalues of square matrices. Eigenvectors and eigenvalues are defined as follows:

Definition C.1 (Eigenvalues and eigenvectors). Let A be an $n \times n$ matrix. A scalar λ is an eigenvalue of A if there is a nonzero column vector v in n-space such that $Av = \lambda v$. The vector v is then an eigenvector of A corresponding to λ.

The eigenvalues and eigenvectors have the following useful property [**80**]:

Theorem C.2 (Matrix summary of eigenvalues of A). *Let A be an $n \times n$ matrix and let $\lambda_1, \lambda_2, ..., \lambda_n$ be (possibly complex) scalars and $v_1, v_2, ..., v_n$ be nonzero vectors in n-space. Let C be the $n \times n$ matrix having v_j as jth column vector, and let D be the diagonal matrix with $\lambda_1, \lambda_2, ..., \lambda_n$ on its main diagonal and zeros everywhere else*

$$D=\begin{bmatrix} \lambda_1 & & & 0 \\ & \lambda_2 & & \\ & & \ddots & \\ 0 & & & \lambda_n \end{bmatrix}$$

Then $AC = CD$ if and only if $\lambda_1, \lambda_2, ..., \lambda_n$ are eigenvalues of A and v_j is an eigenvector of A corresponding to λ_j for $j = 1, 2, ..., n$.

The theorem above is easily proved by using the definition of eigenvalues and eigenvectors.
Furthermore when the matrix C is invertible it can be used to diagonalise A, i.e.:

$$C^{-1}AC = D \tag{38}$$

Conversely, also provided that C is invertible:

$$A = CDC^{-1} \tag{39}$$

C will be invertible if and only if A has n independent eigenvectors.

C.1.2. Linear stability analysis and Lyapunov's criterion for stability. The balancing of the intermediates in a given pathway yields a differential equation for each metabolite of the form:

$$\frac{\partial x_i}{\partial t} = f_i(x_1, x_2, ..x_m; c_1, c_2, ..c_q; p_1, p_2, ..p_l) \tag{40}$$

Here x_1 to x_m are the concentrations of m balanced metabolites, i.e. the dependent variables and c_1 to c_q are the q independent metabolites. p_1 to p_l represent the l parameters. Note that the concentrations of independent metabolites c are predefined functions of time. As such they represent the part of f_i directly dependent on time. They might be regarded as "time dependent parameters".
When balance equations are defined for all x_i the resulting system of differential equations can be written in vector notation as:

$$\frac{\partial \mathbf{x}}{\partial t} = f(\mathbf{x}; \mathbf{c}; \mathbf{p}) \tag{41}$$

The function f is given by the kinetic rate equations multiplied by the appropriate stoichiometric coefficients.

Consider the above system of differential equations. Suppose the system has a steady state given by:

$$\frac{\partial \mathbf{x}}{\partial t} = f(\mathbf{x}^0; \mathbf{c}^0; \mathbf{p}) = \ 0 \tag{42}$$

where the superscript ^{0} refers to the steady state concentration values. When analyzing the steady state the independent metabolite concentrations, c^0, are considered to stay constant so they can be included in the parameter vector. An extended parameter vector $\mathbf{p}^{\#} = [\mathbf{c}^0 \mid \mathbf{p}]$ is therefore defined so that Eq. 42 can writes as

$$\frac{\partial \mathbf{x}}{\partial t} = f(\mathbf{x}^0; \mathbf{p}_{\#}) = \ 0 \tag{43}$$

Suppose now that the stationary state x^0 is perturbed by $\delta x = \xi$. The metabolite concentrations will then be given by:

$$\mathbf{x} \ = \ \mathbf{x}^0 + \xi(t) \tag{44}$$

The time evolution of metabolite x_i is given by:

$$\frac{\partial (x_i^0 + \xi_i)}{\partial t} = f_i(\mathbf{x}^0 + \xi; \mathbf{p}^{\#}) \tag{45}$$

By doing a Taylor expansion of f_i around x_i^0, f_i can be expressed as:

$$f_i(\mathbf{x}^0 + \xi; \mathbf{p}^{\#}) = f_i(\mathbf{x}^0; \mathbf{p}^{\#}) + \sum_j^m \left[\frac{\partial f_i}{\partial x_j}\right]_0 \xi_j + \dots \tag{46}$$

The subscript $_0$ on the partial derivatives indicates that they are evaluated at the stationary state x^0. The higher order terms in the Taylor polynomial can be neglected since ξ is small and one therefore only needs to consider the linear terms (hence *linear* stability analysis). By linearity

$$\frac{\partial (x_i^0 + \xi_i)}{\partial t} = \frac{\partial x_i^0}{\partial t} + \frac{\partial \xi_i}{\partial t}; \tag{47}$$

Hence Eq. 45 and 46 can be combined to get

$$\frac{\partial x_i^0}{\partial t} + \frac{\partial \xi_i}{\partial t} = f_i(\mathbf{x}^0; \mathbf{p}^{\#}) + \sum_j^m \left[\frac{\partial f_i}{\partial x_j}\right]_0 \xi_j. \tag{48}$$

Since by definition

$$\frac{\partial x_i^0}{\partial t} = f_i(\mathbf{x}^0; \mathbf{p}^{\#}) = 0 \tag{49}$$

Eq. 48 reduces to

$$\frac{\partial \xi_i}{\partial t} = \sum_j^m \left[\frac{\partial f_i}{\partial x_j}\right]_0 \xi_j \tag{50}$$

Thus $\xi_i(t)$ can be expressed as a linear combination of partial derivatives of f. Eq. 50 written in matrix notation for all ξ_i becomes:

$$\frac{\partial \xi}{\partial t} = \mathbf{J}\xi \tag{51}$$

$\mathbf{J}$ is the matrix of partial derivatives of f often referred to as the Jacobian:

$$\text{J}=\begin{bmatrix} \frac{\partial f_1}{\partial x_1} & \cdots & \frac{\partial f_1}{\partial x_m} \\ \vdots & \ddots & \vdots \\ \frac{\partial f_m}{\partial x_1} & \cdots & \frac{\partial f_m}{\partial x_m} \end{bmatrix}$$

where the partial derivatives are evaluated at x^0.

If the eigenvectors of $\mathbf{J}$ are independent Eq. 39 can be used to obtain a general solution of Eq. 51. The $m \times m$ matrix $\mathbf{J}$ has m eigenvalues and eigenvectors. Let $\mathbf{D}$ be the diagonal matrix of the eigenvalues of $\mathbf{J}$:

$$\text{D}=\begin{bmatrix} \lambda_1 & & & \\ & \lambda_2 & & \\ & & \ddots & \\ & & & \lambda_n \end{bmatrix}$$

and let **C** be the matrix made up of the eigenvectors **v** of **J** where $\mathbf{v}_j$ is the jth column in **C**:

$$\text{C}=\begin{bmatrix} | & | & & | \\ v_1 & v_2 & \cdots & v_m \\ | & | & & | \end{bmatrix}$$

According to Eq. 39 **J** can be expressed as:

$$J = CDC^{-1} \tag{52}$$

Substituting for **J** in Eq. 51 the differential of ξ becomes:

$$\frac{\partial \xi}{\partial t} = CDC^{-1}\xi \tag{53}$$

Define now a dummy variable

$$y = C^{-1}\xi \tag{54}$$

so that Eq. 53 can be written as

$$\frac{\partial y}{\partial t} = Dy \tag{55}$$

Since **D** is a diagonal matrix the system of differential equations in Eq. 55 can be readily solved. For each y_i one gets:

$$\frac{\partial y_i}{\partial t} = \lambda_i y_i \tag{56}$$

which has the general solution:

$$y_i(t) = k_i e^{\lambda_i t} \tag{57}$$

where k_i is a scalar. In vector notation for all y_i:

$$\text{y}=\begin{bmatrix} k_1 e^{\lambda_1 t} \\ k_2 e^{\lambda_2 t} \\ \vdots \\ k_m e^{\lambda_m t} \end{bmatrix};$$

ξ can now be substituted back in again using Eq. 54 to get the general solution of Eq. 51:

$$\xi = \mathrm{C} \begin{bmatrix} k_1 e^{\lambda_1 t} \\ k_2 e^{\lambda_2 t} \\ \vdots \\ k_m e^{\lambda_m t} \end{bmatrix}.$$

With the general solution for the time evolution of the perturbation ξ, a conclusion on the stability of the steady state can now be arrived at. According to Lyapunov's theory the stability depends on whether the perturbation ξ will grow or decay with time. It is seen from the last equation that the only time dependent terms are the exponentials. Thus the stability of the system depends only on the eigenvalues of the Jacobian matrix. If one or more of the eigenvalues have a positive real part the associated solutions will grow exponentially. The stability criterion can therefore be formulated as:

THEOREM C.3 (Stability criterion). *A steady state is stable if, and only if, the eigenvalues of the associated Jacobian matrix all have negative real parts.*

Thus, the stability is evaluated by calculating the eigenvalues of the Jacobian of the system of ODEs. The issue of stability of mathematical models is common in all engineering disciplines and the theorem above is well known.

An almost complete classification of different types of fixed points based on the type of their eigenvalues (complex or real) and the sign of their breal parts (negative or positive) is shown in figure C.1:

A conjugate pair of complex eigenvalues signifies that the system is able to oscillate (focus). The only problem is with systems which have one or more eigenvalues with real part zero. If a zero eigenvalue is found, the test gives no conclusion on the stability.

Eigenvalues	**Fixed point**	**Flow**
complex with positive real parts	unstable focus	
complex with negative real parts	stable focus	
real and positive	unstable node	
real and negative	stable node	
one positive and one negative	saddle point	

FIGURE C.1. Classification of planar systems based on their eigenvalues

APPENDIX D

Experimental data of CENU

D.1. B16 melanoma and 3LL carcinoma cells in response to CENU

D.1.1. In vivo experiments: Treatment protocol. Six to eight weeks old C57BL6/6J male mice were purchased from IFFA CREDO, (L'Arbresle, France). Mice were shaved before s.c. injections into their flank of 5×10^5 tumor cells(B16 melanoma or 3LL cells). B16 melanoma or 3LL tumors became palpable at days 8-10 after cell inoculation. Mice were divided into two groups, a Control (CT) group, which received sham injections of saline solution, and a Treated (TR) group. The TR group received intratumor chloroethylnitrosourea (CENU) injections at a dose of 15 μg/g body weight. CENU was injected at days 11, 14, and 18 from B16 cell inoculation.
At defined times of tumor evolution (days 10, 12, 15, 20, 24, and 29 after B16 cell inoculation for CT and TR tumors and prolonged to days 35, 43, and 54 for TR tumors), three mice of each group were sacrificed according to institutional guidelines for animal welfare and experimental conduct. Tumors were dissected and weighed. The dissection of the s.c. tumor took <2 min. A piece of the tumor <50 mg of the whole tumor was immediately prepared for NMR Spectroscopy as described below or frozen at $-80\,^{\circ}$C in case of delayed examination.
Tumor growth curves were fitted to the Gompertz function and modified for the TR group to include a growth delay period. Ranges for maximum attainable weights and other model parameters obtained in CENU-treated melanoma models have been published previously [**62**].

D.1.2. Model application. The aim of this section is to provide insights into metabolic pathways from biochemical data derived from ^{1}H-NMR spectroscopy-based metabolite profiling of tumors [**61**]. Proton two-dimensional NMR spectroscopy analysis has been shown to cover very well the subset of phospholipid derivatives [**56, 58, 81**], including the most concentrated phospholipids (phosphatidylcholine and phosphatidylethanolamine), water-soluble precursors (choline, phosphocholine, cytidyl-diphosphocholine,

ethanolamine, phosphoethanolamine, cytidyl-diphosphoethanolamine), phospholipid hydrolysis products (glycerophosphocholine, glycerophosphoethanolamine), and oxidization products (betaine).

Besides these technical conveniences, phospholipid metabolism is crucial for the build-up of cellular membranes thus for tumor cell proliferation, a major phenotypic feature of tumors. Recently, as an anticancer treatment strategy, it was proposed to inhibit key-enzymes of phospholipid metabolism (choline-kinase) to slow down tumor cell proliferation [**82**].

We hypothetized that, by modelling phospholipid derivative content variations between two conditions at steady state, we could give insight, through the used set of parameters, into the induced regulations of phospholipid metabolism. We thus compared phospholipids metabolism alterations in murine tumors between baseline and the stable phase of their response to an anticancer agent. Based on the classical hypothesis that pathways of phospholipids metabolism are very similar in liver cells and tumor cells [**34**], we applied our mathematical model to study the effects of such treatments. For each of these two tumors we have experimental data for three different phases: Control(CTL), Inhibition(INH) and Recovery(REC) [**61**](See Fig.6.1). The average concentrations measured experimentally at steady state for each of these phases are shown in Tables 1 and 2 of Chapter 6.

APPENDIX E

Experimental data of MDS

E.1. B16 melanoma cells and response to methionine deprivation (MDS)

E.1.1. Chemicals. S-Adenosyl-[$^{14}CH_3$]-Met (specific activity 60 mCi/mmol) was from Amersham Biosciences (Buckinghamshire, UK). Acetone, acetonitrile and methanol of HPLC grade were from SDS.

E.1.2. Cell culture and treatment. B16-F10 melanoma cells were maintained as monolayers in 75 cm^2 culture flasks in medium RPMI (SIGMA) either supplemented with 100 μM Met and completed with 10% fetal calf serum (SIGMA) which is considered as standard (Std) condition or non-supplemented in Met (MDS) completed with 10% dialyzed fetal calf serum (Gibco) which is considered as MDS condition. All media were completed with 100 μM folic acid, 1.5 μM cyanocobalamin, 1 mM sodium pyruvate, 4 μg/ml gentamicin (Gibco), 1X non-essential amino-acid solution, 2 μM glutamine and 1X vitamin cocktail (Gibco). Cells were maintained in culture with 5% CO_2 and 90% humidity at 37°C. Cells were separated in 2 groups. The first one Std group was grown in Std medium. The second one MDS group was grown in Met-deficient medium for 4 days. Then after 4 days of MDS, these cells were replaced in Std medium supplemented with 100 μM Met, thus these cells were in post-MDS condition. During post-MDS condition we define two periods: first one is early phase (2 days after MDS) and the second one is late phase (6 days after MDS). Cells were harvested and conserved at -80°C until analysis.

E.1.3. ^{1}H-NMR Spectroscopy analysis. Analysis was performed on a small bore Bruker DRX 500 magnet, equipped with an Proton High Resolution Magic Angle Spinning (HRMAS) probe. Samples, consisting of a piece of intact melanoma tissue below 50 mg or of pellet of intact cells, were inserted into 4 mm diameter zirconia rotors, and rotated at 4 kHz. Metabolite profiling was performed based on a technique using both one-dimensional ^{1}H saturation recovery sequence (repetition time: 10 s, spectral

width: 10 ppm, complex data points: 16 K, number of samples: 64, water signal presaturation at low power) and two-dimensional ^{1}H-^{1}H total correlation spectroscopy sequence (repetition time: 1 s, spectral width: 6 ppm $\times$ 6 ppm, complex data points: 2 K 256 points, number of samples: 16, spin lock duration: 75 ms, water signal presaturation at low power). 2D-based NMR spectroscopy quantification was performed using the technique reported in previous article [**83**].

E.1.4. Methionine concentration measurement. The method used derivatization of intracellular methionine by dabsyl chloride [**84, 85**] and High Pressure Liquid Chromatography (HPLC). The standard used was the non metabolisable amino acid norleucine. The HPLC separation of dabsylated amino acids was performed on a Hewlett Packard Series 1100 system using a 3 μm Supelcosil LC Dabs column (150 4.6 mm I.D.) protected with a 5 μm Supelcosil LC 18T (20 $\times$ 4.6 mm I.D.) guard column. The injection volume was 5 μl and detection was performed at 436 nm. Data collection and peak integration were done with the Enhanced Integrator System of the HP ChemStation.

E.1.5. Phosphatidylethanolamine-N-methyltransferase activity (PEMT). Cells pellets were sonicated on ice in lysis buffer (50 mM Tris-HCl, pH 8; 100 mM NaCl) containing protease inhibitor mixture (Roche, Mannheim, Germany). After centrifugation (14000 x g, 15 min at 4°C), the supernatant was assessed for protein concentration. Intracellular protein concentration was determined with Coomassie Blue at $\lambda = 595$ nm. PEMT enzyme activity was assessed as reported [**86**]. The substrate for PEMT activity was L-α-phosphatidylethanolamine from egg yolk (Sigma) dissolved at the concentration of 1.7 mg/l in 5 mM Tris-HCl pH 9.2 containing 0.06% Triton X100. PEMT enzyme activity was assessed using S-Adenosyl-[$^{14}CH_3$]-Met (specific activity 60 mCi/mmol) (Amersham Biosciences, Buckinghamshire, United Kingdom). Results are expressed in Units. One Unit represents 1 pmole methyl residue transferred/min/mg protein.

E.1.6. Statistical analysis. NMR spectroscopy phospholipid derivatives measurement were expressed as mean $\pm$ SEM and tested for statistical significance analysis with the Mann-Whitney U-test (SEMSTAT, International SEMATECH, TX).

E.2. Biological global effect of MDS

E.2.1. Cell proliferation. Std B16 melanoma cells (Std group) grew exponentially in Std medium . In the MDS group, after 4 days of MDS, cell proliferation was arrested. After replacing cells in Std medium (post-MDS), cell proliferation rate returned at the level of Std cells.(Fig.E.1).

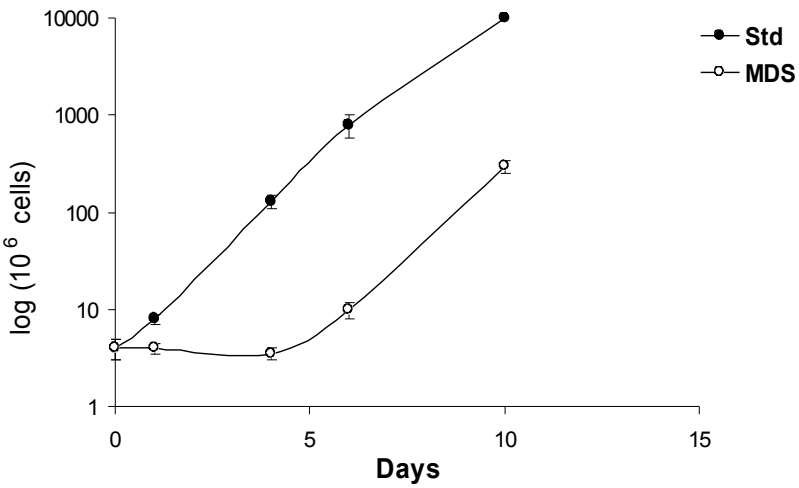

FIGURE E.1. **MDS inhibitory effect on B16 melanoma cells proliferation.** The first group (Std) was cultivated in Std medium. The second group (MDS) was cultivated in MDS medium for 4 days and replaced in Std medium. Then cells were cultivated in Std medium. Results are the mean of three independent experiments. **; p ¡ 0.01, MDS *vs* Std.

E.2.2. ^{1}H-NMR spectroscopy analysis of the metabolic response to MDS. Figure 7.2.a depicts ^{1}H-NMR spectrum of Std cells metabolic profile. After 4 days of MDS, cells from the UN MDS group showed a decrease content. PtdCho pool was not altered but there was an increase of GPC pool, suggesting as hydrolysis of PtdCho. After replacing cells in Std medium, during the post-MDS phase, metabolic profile returned at the level of Std cells at day 10.

E.2.3. Methionine measurement (HPLC-based). We next evaluated the effect of MDS on tumor cells methionine. Cells metabolic response of Sdt group was compared to that of MDS group . After 4 days of MDS, Met pool was depleted, with a drop of 75% ($p < 0.01$). After the cessation of MDS, there was a return to baseline values.

E.2.4. PEMT activity in response to MDS. During MDS, PEMT activity was increased, and remained elevated during the early period of post-MDS phase (p ¡ 0.05, Fig. E.2). PEMT enzyme activity was assessed by using S-Adenosyl-[$^{14}CH_3$]-Met (specific activity 60 mCi/mmol, from Sigma). Results were expressed in unit. One unit represented 1 pmole methyl residue transferred/min/mg protein.

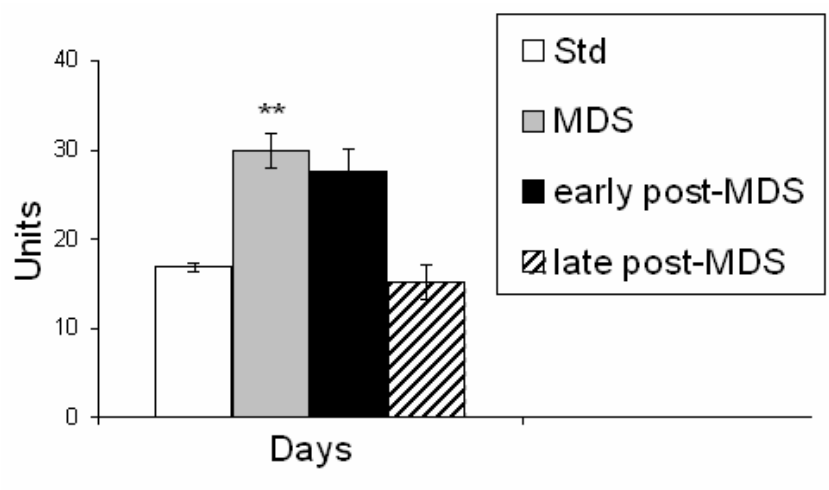

FIGURE E.2. **Effect of MDS and its association with chemotherapy on phosphatidylethanolamine-N-methyltrasferase activity.** PEMT activity was assessed *in vitro* and the incorporation of [$^{14}CH_3$]-methyl groups in phosphatidylethanolamine was determined. One Unit represents 1 pmole methyl residue transferred/min/mg protein. *; $p < 0.05$, when compared to UN Std; **; $p < 0.01$, when compared to UN Std; Mann-Whitney test. Results are the mean of three independent experiments

E.2.5. Biological response to MDS. We showed that untreated B16 melanoma cells express a functional PEMT enzyme and its activity was in agreement with values found in hepatoma cell lines [87]. Here we showed that MDS induced disorders of transmethylation reactions as attested increased activity of PEMT. The latter may aim at compensating for decreased availability of Met for transmethylation of phosphatidylethanolamine. This suggests that the preservation of the PtdCho is mandatory. The pool of PtdCho homeostasis is critical for cell survival, it has been shown that in response to phospholipid overload, e.g., because of an excess in the culture medium, cells protect themselves through phospholipases A2 (PLA2) activation and base-exchange activation [88]. The PEMT pathway is an accessory

pathway for PtdCho biosynthesis, with the CDP-Cho pathway as the major route [89, 90]. This pathway is unable to compensate for a severely failing CDP-Cho pathway [88] and it was shown to remodel the PtdCho pool of hepatocytes with more poly-unsaturated fatty acids (PUFA), thus providing cells with bioactive lipids [90]. Thus, the rise of PEMT activity in response to MDS suggested a downregulation of the Kennedy pathway. However the modification of transmethylation reactions in response to MDS might be the consequence of the decrease of the SAM/SAH ratio, or a compensation for the low availability of substrates [91].
The activation of the PEMT in response to MDS might also reflect the need for bioactive lipids and for maintaining PtdCho homeostasis, which is a critical factor for cell survival [90, 88]. However further investigations are needed to understand the critical role of the PEMT in tumor cell proliferation arrest. This enzyme might play an important role in cancer physiology or in tumor response to therapy.

E.2.6. Metabolic insight into the combined therapy. The PEMT pathway has not been much studied in tumor cells due to its small contribution and its role is less well understood. Increased expression of PEMT was shown to be associated with decreased cytidine-diphosphate-choline (CDP-Cho) pathway activation [87], decreased rate of cell proliferation [89] and induction of apoptosis [90]. Moreover it was reported that the PEMT activity was decreased in hepatoma tumors [89]. We showed that the combination of MDS and CENU treatment induced an up-regulation of PEMT activity which was responsible for PtdCho hydrolysis.[63]. The excess of PtdCho might be hydrolyzed through the activation of phospholipase A2, producing GPC which, in turn, could give poly-unsaturated fatty acids and ceramide [92, 93]. CENU treatment and MDS are both DNA hypomethylation inducers and DNA hypomethylation would result in gene overexpression [94]. As a consequence, some genes coding for methyltransferase might have been upregulated and among them, PEMT expression.

The inhibition of Akt phosphorylation induced by MDS alone support this hypothesis [95]. One of the Akt regulator is the protein phosphatase 2A (PP2A) which regulates cell proliferation, or resistance to apoptosis [96]. To be active, PP2A needs to be methylated on its catalytic subunit by a specific methyltransferase, leucine carboxymethyltransferase-1 (LCMT-1) [96]. The

LCMT-1 activity might have been also upregulated in reponse to the therapeutic association by ceramide, through the degradation of the PtdCho pool originating from PEMT activity, which are known PP2A activators [**97, 98**].

APPENDIX F

Basis for a new software for biological networks modeling

Outline

In this Chapter we describe the basis for a new software for biologial networks modeling. We named this software MPAS (Metabolic Pathway Analyser Software). First we study the reasons for such a software and the goals we want to achieve; then we give some details about the development tools and finally we comment in a few words about advantages of this software.

F.1. Introduction

The techniques most frequently used in biology for the study of metabolism (nuclear magnetic resonance (NMR), mass spectrometry(MS), chips, etc) only provide partial informations about networks. Then the expert has to reconstruct the interaction networks between the metabolites for which we have information. In addition, each of these techniques has its limits and only provides data for a particular aspect of metabolism. By combining the results of these different techniques, we hope to overcome these limitations and to contribute to derive new and more comprehensive models.

F.2. Goal

Our goal is to develop a new innovative software to merge data from exploration techniques for the large-scale cellular metabolism. This strategy will model the evolution of cellular metabolism in the context of a pathology or a particular physiological environment. For example, it will be possible to identify targets to initiate the specific therapy strategies to the studied pathology according to the results of biomarker tests.

F.3. Data and Methods

The data that we have are of four types: *Promotology* (we realized a software for the promotology analysis of the regulation of genes in a pathology, giving a list of genes which are potentially co-regulated with the genes of interest), *Transcriptomics*, *Metabolomics* et *Proteomics*. The intersection of the results of these techniques should help to overcome some of their limits and to derive the new information.

This software will give the possibility to rebuild all possible reactions between the metabolites of interest (identified by NMR spectra or MS, DNA chips, or promotology).(Fig. F.1)

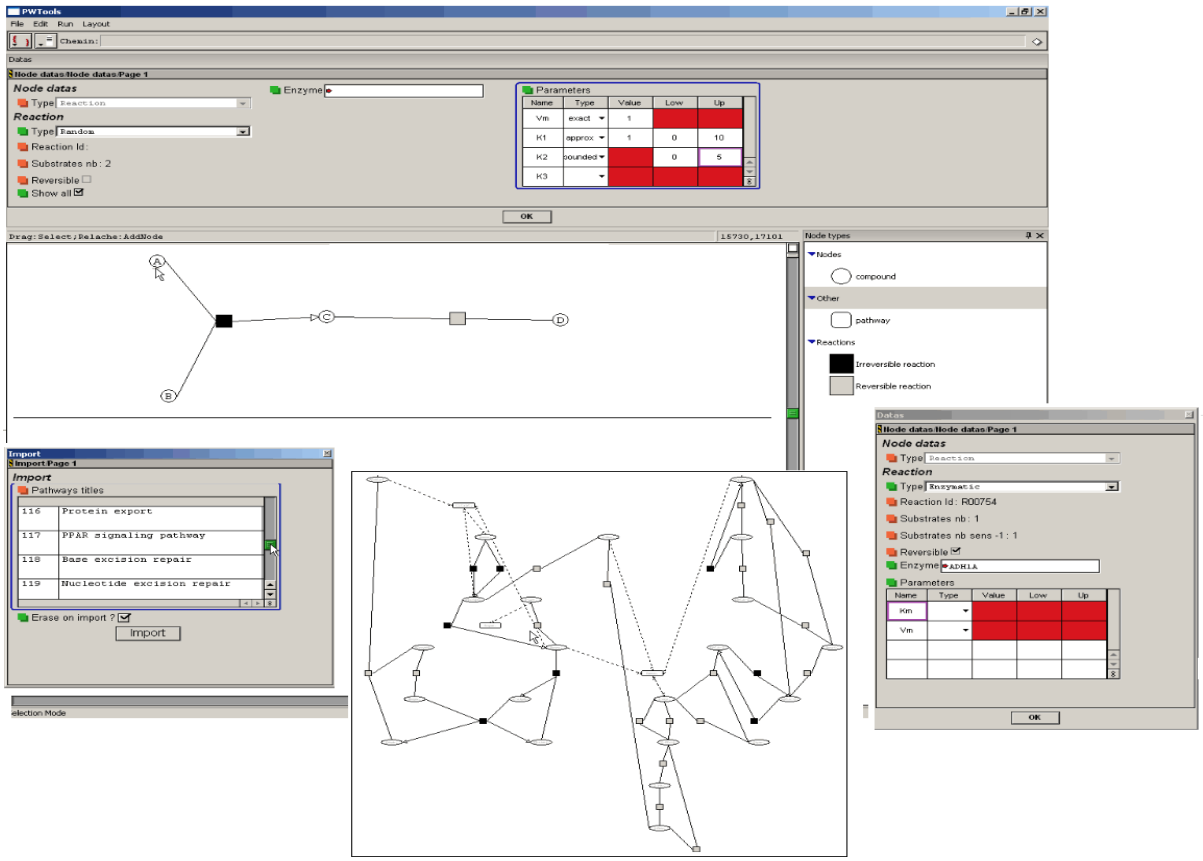

FIGURE F.1. A general schema of the first version of MPAS.

The software will be based on a combination of different public databases like KEGG (Kyoto Encyclopedia of Gene and Genomes) or BiGG. KEGG

is a collection of online databases dealing with genomes, enzymatic pathways and biological chemicals. The pathway database of KEGG records networks of molecular interactions in the cells and variants of them specific to particular organisms. The KEGG database can be used for modeling and simulation, browsing and retrieval of data. It is a part of the so-called systems biology approach.

In MPAS software, the database will also record the results of simulations. These results can then be exported in the standard file formats used in modeling : SBML (Public database for Biomodels) or BioPax(Online database Biological Pathway Exchange).

SBML is a computer-readable format for the implementation of models of biochemical systems. It is based on XML and uses MathML to encode mathematical formulas. It is widely applicable to most biochemical systems and readable by a multitude of software tools. An advantage as well as a disadvantage of SBML is its wide applicability and neutrality towards software encoding. This allows a wide variety of programs to use SBML while each program can process the model differently. Thus, two SBML-compliant programs need not necessarily produce the same output when performing similar tasks (e.g. simulation of the model) on a model. For detailed information about SBML, see [**66**, **67**].

F.4. Development tools

We chose to develop this software in C++ because of a better fluency and execution's speed, in compare to many available softwares of graphs representation in the market which are written in Java. This software is included in an information system which is capable to handle the set of our biological and bioinformatics data. For the reconstruction of metabolic pathways, the software uses a MySQL database managed by a server in Ruby on Rails. The database schema is provided by the DTD of KGML files(XML files produced by Kegg for metabolic pathways export). The database contains all human metabolic pathways in Kegg and BIGG. An API service is implemented on the database management server, allowing to query it via a REST interface. This will give the facility to connect easily the new softwares on this database. The simulation of biological networks, parameter estimation, mathematical analyses and also all graphics will be done by a direct inclusion of Matlab software.

F.5. Graph construction

It is possible to construct a graph in different ways. It is possible to build the graph of reactions manually by introducing compounds and reactions between these compounds graphically. We can also import the graph of reactions of a human metabolic pathway directly. The software retrieves the requested metabolic pathway from KEGG or BiGG, and retranscribes it on the screen as a graph. It is also possible to provide a list of the genes of interest. The software will find the metabolic pathways where these genes are involved. It is also possible to edit a graph of reactions which is imported automatically, by adding or removing compounds or reactions.(See figure F.1)

F.6. Analyses

- From the complex metabolic network established by the software, the system of ordinary differential equations which corresponds to this network is automatically created.

- The user may choose the biochemical laws which will be used for the construction of this system.

- One can enter the parameter values which are known (probably found in biological experiments).
  (See figure F.1)
- The unknown parameters are predicted by the software with the numerical methods and will be presented in a table.

- The results of the simulation of systems and different analyses are presented as diagrams: changes in metabolite concentrations over time, evolution of concentration of a metabolite in relation to another, phase spaces, stability curves of the system, speed of reaching the steady state for each of the metabolites, etc.(See figure F.2)

F.7. Rate laws to construct the equations

The user can choose the type of multi-substrate reactions:

- Non-Enzymatic reaction
- Random mechanism
- Ordered mechanism

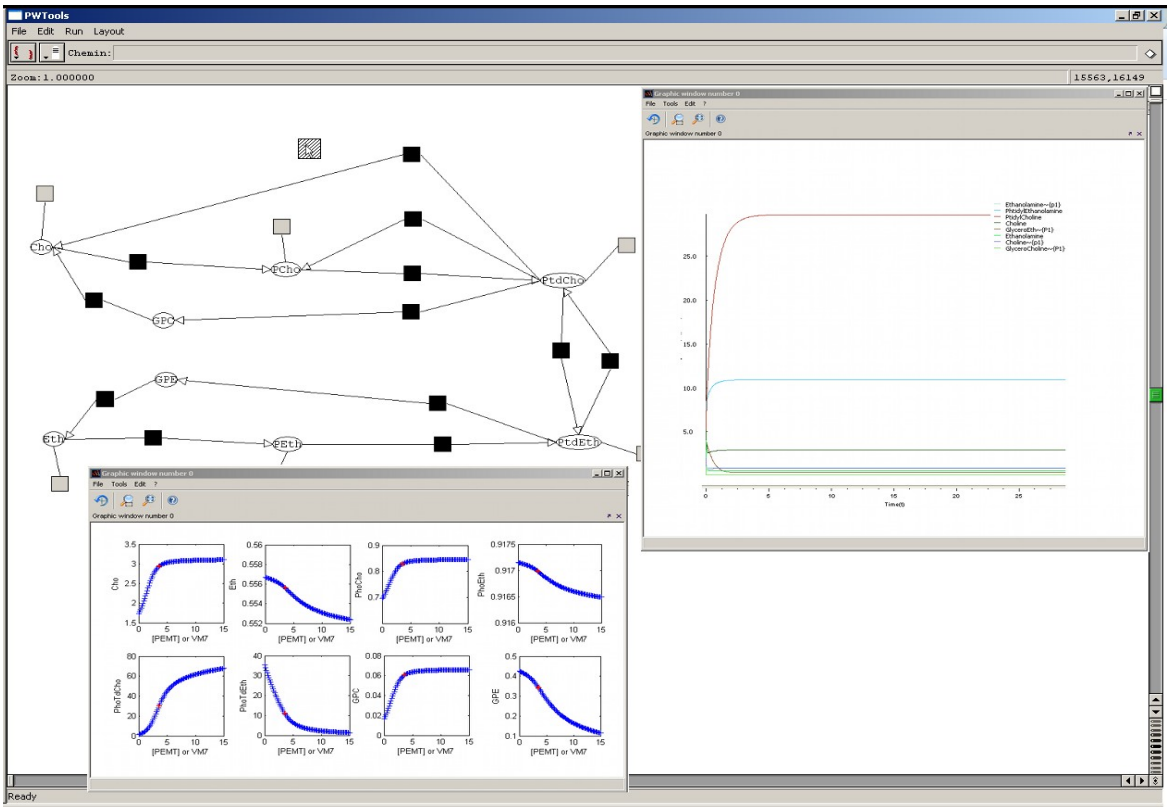

FIGURE F.2. An example of MPAS application to model phospholipid biosynthesis.

- Ping-Pong mechanism

F.7.1. Non-enzymatic reaction. In the non-enzymatic multi-substrate reaction , the Michaelis-Menten formula is of the form:

$$v = k.[A].[B].[C]... \tag{58}$$

F.7.2. Random Mechanism and Ordered Mechanism. In the random-mechanism and ordered-mechanism , with n substrates, the Michaelis-Menten formula is of the form:

$$v = \frac{V_{max}.[S_1].[S_2]...[S_n]}{K_1 + ... + K_i.[S_i] + ... + K_{i+k}.[S_i].[S_j] + ... + K_{2^n-1}.[S_1]...[S_{n-1}] + ... + [S_1]...[S_n]} \tag{59}$$

For example if n=2 :

$$v = \frac{V_{max}.[S_1].[S_2]}{K_1 + K_2.[S_1] + K_3.[S_2] + [S_1].[S_2]} \tag{60}$$

F.7.3. Ping-Pong Mechanism. In the ping-pong- mechanism , with **n** substrates,the Michaelis-Menten formula is of the form:

$$v = \frac{V_{max}.[S_1].[S_2]...[S_n]}{K_1.[S_1]...[S_{n-1}] + ... + K_n.[S_2]...[S_n] + ... + [S_1].[S_2]...[S_n]} \tag{61}$$

For example if $n = 3$:

$$v = \frac{V_{max}.[S_1].[S_2].[S_3]}{K_1.[S_1].[S_2] + K_2.[S_1].[S_3] + K_3.[S_2].[S_3] + [S_1].[S_2].[S_3]} \tag{62}$$

F.8. Inhibitors

This happens sometimes in the KEGG database or at the request of user, to add an inhibition to a reaction. The inhibitor (I) can bind to either E (Enzyme) or ES (Enzyme-Substrate complex) with the dissociation constants K_i or K_I, respectively. So there are several possibilities for **Inhibitor** :

- Competitive inhibitor
- Uncompetitive inhibitor
- Noncompetitive inhibitor
- Mixed inhibition

F.8.1. Competitive inhibitor. the substrate and inhibitor cannot bind to the enzyme at the same time. This usually results from the inhibitor having an affinity for the active site of an enzyme where the substrate also binds; the substrate and inhibitor *compete* for access to the enzyme's active

site.

$$v = \frac{V_{max}.[S]}{[S] + K_m.(1 + \frac{[I]}{K_i})} \tag{63}$$

F.8.2. Uncompetitive inhibitor. the inhibitor binds only to the substrate-enzyme complex, it should not be confused with non-competitive inhibitors.

$$v = \frac{\frac{V_{max}}{(1+\frac{[I]}{K_I})}.[S]}{[S] + \frac{K_m}{(1+\frac{[I]}{K_I})}} \tag{64}$$

Inhibition by the substrate is a special case of this group in which two molecules of substrate bind to the enzyme but can not be transformed into the product:

$$v = \frac{V_{max}.[S]}{[S] + K_m + \frac{[S]^2}{K_I}} \tag{65}$$

F.8.3. Mixed inhibition. The inhibitor can bind to the enzyme at the same time as the enzyme's substrate. However, the binding of the inhibitor affects the binding of the substrate, and vice versa. This type of inhibition can be reduced, but not overcome by increasing concentrations of substrate. Although it is possible for mixed-type inhibitors to bind in the active site, this type of inhibition generally results from an allosteric effect where the inhibitor binds to a different site on an enzyme. Inhibitor binding to this allosteric site changes the conformation (i.e., tertiary structure or three-dimensional shape) of the enzyme so that the affinity of the substrate for the active site is reduced.($K_i \neq K_I$.)

$$v = \frac{\frac{V_{max}}{(1+\frac{[I]}{K_I})}.[S]}{[S] + K_m.\frac{(1+\frac{[I]}{K_i})}{(1+\frac{[I]}{K_I})}} \tag{66}$$

F.8.4. Noncompetitive inhibitor. is a form of mixed inhibition where the binding of the inhibitor to the enzyme reduces its activity but does not affect the binding of substrate. As a result, the extent of inhibition depends only on the concentration of the inhibitor.

$$v = \frac{\frac{V_{max}}{(1+\frac{[I]}{K_i})} \cdot [S]}{[S] + K_m} \tag{67}$$

We plan to include the other simulation methods or study of biological networks such as calculating elementary modes to this software[68], such as Petri nets[69].

Bibliography

[1] A. Krogh, The number and distribution of capillaries in muscle with calculations of the oxygen pressure head necessary for supplying the tissue, *J. Physiol.*, 52, pp. 409-15, 1919.

[2] B.J. Mcguire and A. Secomb, Estimation of capillary synthase from rat kidney and rat brain, *J. Biol. Chem.*, 248, pp. 8022-30, 1973.

[3] R.N. Pittman, Oxygen transport and exchange in the microcirculation, *Microcirculation*, 12, pp. 59-70, 2005.

[4] D.A. Beard and H. Qian, English Book: Chemical Biophysics, Quantitative analysis of cellular system, *Cambridge Texts in Biomedical Enineering*, ISBN: 978-0-521-87070-2, 2008.

[5] A. Kriete and R. Eils, Computational systems biology, *Academic Press*, pp. 28-17, 2006.

[6] R.G. Sargent , Validation and verification of simulation models, *IEEE Computer Society Press*, pp. 28-17, 2004.

[7] H. Kitano, Computational systems biology, *Nature*, 420, pp. 206-210, 2002.

[8] H. Kitano, Computational systems biology in cancer: modeling methods and applications, *Gene regulation and systems biology*, 1, pp. 91-110, 2007.

[9] A. Farooqui, L. Horrocks and T. Farooqui , Glycerophospholipids in brain: their metabolism, incorporation into membranes, functions and involvement in neurological disorders, *Chem. Phys. Lipids*, 106, pp. 1-29, 2000.

[10] C. Gupta, Phospholipids in disease, *Newyork: Marcel Dekker*, 46, pp. 895-908, 1993.

[11] A. Regev, W. Shapiro, Representation and simulation of biochemical processes using the pi-calculus process algebra, *Proceedings of the sixth Pacific Symposium of Biocomputing*, pp. 459-70, 2001.

[12] M. Nagasaki, S. Onami, S. Miyano and H. Kitano, Bio-calculus: Its concept and an application for molecular interaction, *Computational Molecular Biology*, 30, 2000.

[13] R. Hofestadt and S. Thelen, Quantitative modelling of biochemical networks, *In Silico Biology IOS Press* , 1, pp. 39-53, 1998.

[14] L. Cardelli, Technical report of artificil biochemistry, *Microsoft research, University of Trento center of computational and systems biology* , pp. 1-43, 2006.

[15] M. Israel and L. Schwartz, English Book: Cancer,a dysmethylation syndrome, *Publisher:John Libbey*, ISBN: 2-7420-0597-8, 2005.

[16] E. Kennedy and B. Roelofsen, The biosynthesis of phospholipids in Lipids and Membranes: Past, Present and Future, *Elsevier Science*, pp. 171-206, 1986.

[17] D.E. Vance Phosphatidylcholine Metabolism, *CRC Press*, 22,pp. 33-46, 1989.

[18] H. Kanoh, M. Kai and I. Wada, Phosphatidic acid phosphatase from mammalian tissues: discovery of channel-like proteins with unexpected functions, *Biochim. Biophys. Acta.*, 1348,pp. 56-62, 1997.

[19] C.L. Jelsema and D.J. More, Distribution of phospholipid biosythetic enzymes among cell components of rat liver, *J Biol Chem*, 253,pp. 7960-71, 1978.

[20] M. Miller and C. Kent, Characterization of the pathways for phosphatidylethanolamine biosynthesis in Chinese hamster ovary mutant and parental cell lines, *J Biol Chem*, 261,pp. 9753-61, 1986.

[21] J.L. Reed, I. Famili, I. Thiele and B. Palsson, Towards multidimensional genome annotation, *Nat Rev Genet.*, 7,pp. 130-41, 2006.

[22] N.C. Duarte, S.A. Becker, N. Jamshidi, I. Thiele, M.L. Mo, T.D. Vo, R. Srivas and B. Palsson, Global reconstruction of the human metabolic network based on genomic and bibliomic data, *Proc Natl Acad Sci U S A.*, 104,pp. 1777-82, 2007.

[23] P.H. Raven, G.B. Johnson, J.B. Losos and S.R. Singer, Biology (seventh edition), *McGraw-Hill* , 2005.

[24] R. Sundler, G. Arvidson and B. Akesson, Pathway for the incorporation of choline into rat liver phosphatidylcholine in vivo. *Biochim. Biophys. Acta*, 280,pp. 559-68, 1972.

[25] R. Sundler and B. Akesson, Biosynthesis of phosphatidylethanolamines and phosphatidylcholines from ethanolamine and choline in rat liver, *Biochem. J.*, 146,pp. 309-315, 1975.

[26] S.A. Henry and J.L. Patton-Vogt,Genetic regulation of phospholipid metabolism in yeast, *Progress in Nucleic Acid Research and Molecular Biology*, 61,pp. 133-79, 1998.

[27] J.K. Blusztajn, Choline a vital amine, *Science*, 281,pp. 794, 1998.

[28] S.H. Zeisel, Choline A nutrient that is involved in the regulation of cell proliferation, cell death, and cell transformation, *Adv Exp Med Biol*, 399,pp. 131, 1996.

[29] J.L. Patton Vogt, P. Griac, A. Sreenivas, V. Bruno, S. Dowd, M.J. Swede and S.A. Henry, Role of the yeast phosphatidylinositol/phosphatidylcholine transfer protein (Sec14p) in phosphatidylcholine turnover and INO1 regulation, *J. Biol. Chem.*, 272,pp. 20873, 1997.

[30] R. Sundler and B. Akesson, Regulation of phospholipid biosynthesis in isolated rat hepatocytes, *Biochem. J.*, 146,pp. 309-15, 1975.

[31] R. Sundler, The phospholipid substrates in the Ca2+ -stimulated incorporation of nitrogen bases into microsomal phospholipids, *Biochim.Biophys.Acta*, 306,pp. 218-26, 1973.

[32] D.E. Vance and C.J. Walkey, Roles for the methylation of phosphatidylethanolamine, *Curr. Opin. Lipidol.*, 9,pp. 125-30, 1998.

[33] D.E. Vance, M. Houweling, M. Lee and Z. Cui,Phosphatidylethanolamine methylation and hepatoma cell growth, *Anticancer Res.*, 16,pp. 1413-16, 1996.

[34] F. Podo, Tumor phospholipid metabolism, *NMR Biomed*, 12,pp. 413, 1999.

[35] E. Ackerstaff, BR. Pflug, J.B. Nelson and Z.M. Bhujwalla, Detection of increased choline compounds with proton nuclear magnetic resonance spectroscopy subsequent to malignant transformation of human prostatic epithelial cells, *Cancer Res.*,61,pp. 3598, 2001.

[36] N.V. Reo, M. Adinehzadeh and B.D. Foy, Kinetic analyses of liver phosphatidylcholine and phosphatidylethanolamine biosynthesis using (13)C NMR spectroscopy, *Biochim. Biophys. Acta*, 1580,pp. 171-88, 2002.

[37] A.A. Farooqui, L.A. Horrocks and T. Farooqui, Glycerophospholipids in brain:their metabolism,incorporation into membranes,functions, and involvement in neurological disorders, *Chem. Phys. Lipids*, 106,pp. 1-29, 2000.

[38] C.M. Gupta, Phospholipids in disease, *G.Cevc, editor. Phospholipids handbook. New York: Marcel Dekker*, pp. 895-908, 1993.

[39] J. Kanfer and E.P. Kennedy, Metabolism and function of bacterial lipids.II. Biosynthesis of phospholipids in escherchia coli, *J Biol Chem.*, 239,pp. 1720-6, 1964.

[40] S.R. Veflingstad, P. Dam, Y. Xu and E.O. Voit, Microbial pathway models. Computational Methods for Understanding Bacterial and Archaeal Genomes, *Imperial College Press.*,2008.

[41] S. Schuster , T. Dandekar and D.A. Fell, Detection of elementary flux modes in biochemical networks: a promising tool for pathway analysis and metabolic engineering, *Trends Biotechnol*, 17,pp. 53, 1999.

[42] I.H. Segel, Enzyme Kinetics: Behavior and Analysis of Rapid Equilibrium and Steady-State Enzyme Systems,*Wiley-Interscience, Malden, MA* ,1975.

[43] W. Karush, W. Kuhn and W. Tucker, Characterization of the pathways for Nonlinear Programming, the Karush-Kuhn-Tucker Theorem, *University of California Press*, 2,pp. 481- 92, 1951.

[44] W. Karush , Minima of Functions of Several Variables with Inequalities as Side Constraints, M.Sc. Dissertation. *Dept. of Mathematics, Univ. of Chicago, Chicago, Illinois*, 1939.

[45] K.A. Clements, P.W. Davis and K.D. Frey, An interior point algorithm for weighted least absolute value power system state estimation, *IEEEPES Winter Meeting*, 1991.

[46] E. Silberberg and W. Suen, The Structure of Economics, A Mathematical Analysis, *McGraw-Hill*, pp. 253, 2001.

[47] J.J. More and S.A. Vavasis, On the solution of concave knapsack problems, *Mathematical Programming*, 49 ,pp. 397, 1990.

[48] H. Luss and S.K. Gupta, Allocation of effort resources among competing activities, *Operations Research*, 23 ,pp. 360-66, 1975.

[49] R.M. May, Stability and complexity in model ecosystems, *Princeton University Press*, 1973.

[50] J. Tyson , Modeling the cell division cycle: cdc2 and cyclin interactions *Cell Biology*, 88,pp. 7328-32, 1991.

[51] C.W. Gear , Numerical initial value problems in ordinary differential equations *Prentice-Hall, Englewood Cliffs, NJ*, 1971.

[52] M. Adinehzadeh and N.V. Reo, Effects of Peroxisome Proliferators on Rat Liver Phospholipids: Sphingomyelin Degradation May Be Involved in Hepatotoxic Mechanism of Perfluorodecanoic Acid, *Chem. Res. Toxicol.*, 11,pp. 428-40, 1998.

[53] M. Adinehzadeh and N.V. Reo, NMR analysis of liver phospholipids: temperature dependence of 31P chemical shifts and absolute quantitation, *Biol. Med.*, 3,pp. 171-6, 1996.

[54] Z. Cuia and M. Houwelingb, Phosphatidylcholine and cell death, *Biochimica et Biophysica Acta*, 2003.

[55] L. Tessitor et al., Expression of phosphatidylethanolamine N-methyltransferase in human hepatocellular carcinomas, *J. Oncology*, 65,pp. 152-8, 2003.

[56] D. Morvan, A. Demidem, J. Papon and J.C. Madelmont, Quantitative HRMS Proton Total Correlation Spectroscopy Applied to Cultured Melanoma Cells Treated by Chloroethyl Nitrosourea: demonstration of phospholipid metabolism alternation, *Mgan Reson Med* , 49,pp. 241-48, 2003.

[57] D. Morvan, A. Demidem, S. Guenin and J.C. Madelmont, Methionine-Dependence Phenotype of Tumors: Metabolite profiling in a Melanoma model using L-[methyl-13C]methionine and high-resolution magic angle spinning 1H-13C nuclear magnetic resonance spectroscopy, *Mgan Reson Med* , 55,pp. 948-96, 2006.

[58] Bystander effects are induced by CENU treatment and associated with altered protein secretory activity of treated tumor cells. A relay for chemotherapy?, *Int J. of Cancer*, 119,pp. 992-1004, 2006.

[59] P. Merle, D. Morvan, J.C. Madelmont, D. Caillaud and A. Demidem, CENU treatment induced bystander effects which are effective on parental and non-parental tumors and have a phospholipid metabolism proton NMR spectroscopy signature, *Int J. Oncol.*, 29,pp. 637-42, 2006.

[60] P. Merle, D. Morvan, J.C. Madelmont, D. Caillaud and A. Demidem, Chemotherapy-induced Bystander Effect in Response to Several Chloroethylnitrosoureas: An origin independent of DNA damage?, *Anticancer Research*, 28,pp. 21-7, 2008.

[61] D. Morvan and A. Demidem, Metabolomics by proton nuclear magnetic resonance spectroscopy of the response to chloroethylnitrosourea reveals drug efficacy and tumor adaptive metabolic pathways, *Cancer Res.*, 67,pp. 2150-59, 2007.

[62] A. Demidem, D. Morvan, Papon J. Papon, M. De Latour and J.C. Madelmont, Cystemustine induces redifferentiation of primary tumors and confers protection against secondary tumor growth in a melanoma murine model, *Cancer Res.*, 61,pp. 2294-300, 2001.

[63] S. Guenin, D. Morvan, E. Thivat, G. Stepien and A. Demidem, Combined methionine stress and Chloro-ethylnitrosourea treatment have a time-dependent synergy effect which NMR-based metabolomics explains by methionine metabolism reprogramming of melanoma tumors, *Nutr. Cancer.*, 61,pp. 518-29, 2009.

[64] M. Behzadi, A. Demidem, D. Morvan, L. Schwartz, G. Stepien, J.M. Steyaert, A model of phospholipid biosynthesis in tumor in response to an anticancer agent in Vivo, *J Integrative Bioinfo.*, 7,pp. 129, 2010.

[65] M.D. Morris, Factorial sampling plans for preliminary computational experiments, *Technometrics*, 33,pp. 161-74, 1991.

[66] M. Hucka et al., The Systems Biology Markup Language (SBML): A Medium for Representation and Exchange of Biochemical Network Models, *Bioinformatics* ,19,pp. 524, 2003.

[67] A. Finney and M. Hucka, Systems Biology Markup Language: Level 2 and Beyond, *Biochemical Society Transactions* ,31,pp. 1472, 2003.

[68] T. Pfeiffer, I. Sanchez Valdenebro, J.C. Nuno, F. Montero and S. Schuster, METATOOL: for studying metabolic networks, *Bioinformatics*, pp. 251-257, 1999.

[69] J.H.G.M. van Beek, A.C. Hauschild, H. Hettling and T.W. Binsl, Robust modelling, measurement and analysis of human and animal metabolic systems, philosophical

transactions, *Series A, Mathematical, Physical, and Engineering Sciences*,pp. 1971-1992, 2009.

[70] D. Gonze and M. Kaufman, Lecture notes: Chemical and enzyme kinetics, *Master en Bioinformatique et Modelisation*, , 2009-10 .

[71] L. Michaelis and M. Menten, Die Kinetik der Invertinwirkung, *Biochem. Z.*, 49,pp. 333-69, 1913.

[72] G.E. Briggs and J.B.S. Haldane, A note on the kinetics of enzyme action, *Biochem. J.*, 19,pp. 338-39, 1925.

[73] E.O. Voit and J. Almeida, Decoupling dynamical systems for pathway identification from metabolic profiles, *Bioinformatics*, 20,pp. 1670-81, 2004.

[74] G. Goel, I.C. Chou and E.O. Voit, Biological systems modeling and analysis: A biomolecular technique of the twenty-first century, *J. Biomol. Tech.*, 17,pp. 252-69, 2006.

[75] F. Mao, H. Wu, P. Dam, I.C. Chou, E.O. Voit and Y. Xu, Prediction of biological pathways through data mining and information fusion. Computational Methods for Understanding Bacterial and Archaeal Genomes, *Imperial College Press*, 151,pp. 553-77, 2008.

[76] H.K. Khalil, Nonlinear Systems, Third edition, *Prentice hall*, ISBN 0130673897, 2002.

[77] M.R Roussel, Lecture notes: Stability analysis for ODEs, *University of Lethbrige, Canada*, , 2005.

[78] J.D. Murry, Mathematical Biology, Second edition, *Bioinformatics texts, Springer*, , 1993.

[79] D. Kondepundi and I. Prigogine, Modern thermodynamics, *Wiley, New York.*, , 1998.

[80] J.B. Fraleigh and R.A. Beaurgrad, Linnear Algebra *Publisher: Addison-Wesley*, ISBN 13: 9780201526752, 1995.

[81] D. Morvan, A. Demidem, J. Papon, M. De Latour and J.C. Madelmont, Melanoma tumors acquire a new phospholipid metabolism phenotype under cystemustine as revealed by high-resolution magic angle spinning proton nuclear magnetic resonance spectroscopy of intact tumor samples, *Cancer research*, 62,pp. 1890-7, 2002.

[82] E. Hernando, J. Sarmentero-Estrada, T. Koppie, C. Belda-Iniesta et al., A critical role for choline kinase-alpha in the aggressiveness of bladder carcinomas, *J. Onco. gene.*, 28,pp. 2425-35, 2009.

[83] M. Bayet-Robert, D. Loiseau, P. Roi, A. Demidem, C. Barthomeuf, G. Stepien and D. Morvan, Quantitative two-dimensional HRMAS 1H-NMR spectroscopy-based metabolite profiling of human cancer cell lines and response to chemotherapy, *Magnetic Resonance in Medicine J.*, 63,pp. 1172-83, 2010.

[84] D. Drnevich and T.C. Vary, Analysis of physiological amino acids using dabsyl derivatization and reversed-phase liquid chromatography, *J Chromatogr*, 613,pp. 137-44, 1993.

[85] J.Y. Chang, R. Knecht and D.G. Braun, Amino acid analysis in the picomole range by precolumn derivatization and high-performance liquid chromatography, *Methods Enzymol*, 91,pp. 41-8, 1983.

[86] N.D. Ridgway and D.E. Vance, Specificity of rat hepatic phosphatidylethanolamine N-methyltransferase for molecular species of diacyl phosphatidylethanolamine, *J Biol Chem*, 263,pp. 16856-63, 1988.

[87] L. Tessitore, I. Dianzani, Z. Cui and D.E. Vance, Diminished expression of phosphatidylethanolamine N-methyltransferase 2 during hepatocarcinogenesis, *Biochem J Pt 1*, 337,pp. 23-7, 1999.

[88] I. Baburina and S. Jackowski, Cellular responses to excess phospholipid, *J Biol Chem*, 274,pp. 9400-8, 1999.

[89] M. Houweling, Z. Cui, L. Tessitore and D.E. Vance, Induction of hepatocyte proliferation after partial hepatectomy is accompanied by a markedly reduced expression of phosphatidylethanolamine N-methyltransferase-2, *Biochim Biophys Acta*,1346,pp. 1-9, 1997.

[90] C.J. Walkey, L. Yu, L.B. Agellon and D.E. Vance, Biochemical and evolutionary significance of phospholipid methylation, *J Biol Chem*, 273,pp. 27043-6, 1998.

[91] N. Detich, S. Hamm, G. Just, J.D. Knox and M. Szyf, The methyl donor SAdenosylmethionine inhibits active demethylation of DNA: a candidate novel mechanism for the pharmacological effects of S-Adenosylmethionine, *J Biol Chem*,278,pp. 20812-20, 2003.

[92] D. Morvan, A. Demidem, J. Papon and J.C. Madelmont, Quantitative HRMAS proton total correlation spectroscopy applied to cultured melanoma cells treated by chloroethyl nitrosourea: demonstration of phospholipid metabolism alterations, *Magn Reson Med*, 49,pp. 241-8, 2003.

[93] D. Morvan and A. Demidem, Metabolomics by proton nuclear magnetic resonance spectroscopy of the response to chloroethylnitrosourea reveals drug efficacy and tumor adaptive metabolic pathways, *Cancer Res*, 67,pp. 2150-9, 2007.

[94] R.A. Leach and M.T. Tuck, Methionine depletion induces transcription of the mRNA (N6-adenosine) methyltransferase, *Int J Biochem Cell Biol*, 33,pp. 1116-28, 2007.

[95] D.M. Kokkinakis, A.G. Brickner, J.M. Kirkwood, X. Liu, J.E. Goldwasser, A. Kastrama, C. Sander, D. Bocangel and S. Chada, Mitotic arrest, apoptosis, and sensitization to chemotherapy of melanomas by methionine deprivation stress, *Mol Cancer Res*, 4,pp. 575-89, 2006.

[96] V. Janssens and J. Goris, Protein phosphatase 2A: a highly regulated family of serine/threonine phosphatases implicated in cell growth and signalling, *Biochem J*, 353,pp. 417-39, 2001.

[97] S. Guenin, L. Schwartz, D. Morvan, J.M. Steyaert, A. Poignet, J.C. Madelmont and A. Demidem, PP2A activity is controlled by methylation and regulates oncoprotein expression in melanoma cells: A mechanism which participates in growth inhibition induced by chloroethylnitrosourea treatment, *Int J Oncol*, 32,pp. 49-57, 2008.

[98] P.P. Ruvolo, Intracellular signal transduction pathways activated by ceramide and its metabolites, *Pharmacol Res*, 47,pp. 383-92, 2003.

List of Figures

2.1 **Multi-enzyme reaction**: metabolic pathway where multiple biotransformations take place. The substrate of each reaction is the product of the previous reaction.(See [**23**]) 28

2.2 **Cell membrane structure:** proteins and phospholipids are major components of biological membranes. (Image source: http://commons.wikimedia.org/wiki/File:Cell membrane detailed diagram 30

2.3 Glycerophospholipid metabolism ; supplied from KEGG database. 32

2.4 **Schematic representation of the model.** Arrows with VM_i and KM_i parameters refer to enzymatic reactions while the others represent simple reactions. Blue and green arrows represent Choline cycle and Ethanolamine cycle repectively and Pink arrows correspond to reactions which connect these two sub-cycles. **Reactants:** Cho (Choline), PC (Phospho-Choline), PtdCho (Phosphatidyle-Choline), GPC (Glycero-PhosphoCholine), Eth (Ethanolamine), PE (Phospho-Ethanolamine), PtdEth (Phosphatidyle-Ethanolamine), GPE (Glycero-PhosphoEthanolamine). **Enzymes:** CK (Choline-Kinase), EK (Ethanolamine-Kinase), CCT/CPT (PhosphoCholine-Cytidyl-Transferase), ECT/EPT (PhosphoEthanolamine-Cytidyl-Transferase), PEMT (PhosphatidyleEthanolamine-N-methyl-Transferase), PlpA2 (PhosphoLipase A2), PlpC (PhosphoLipase C), PlpD (PhosphoLipase D). **Parameters:** VM (Michaelis maximum reaction rate), KM (Michaelis concentration constant), k_i(Rate constants for external reactions). 33

2.5 **Chemical structures of metabolites.** 34

4.1 The relationship between cyclin and cdc2 in the cell cycle (proposed by J. Tyson in [**50**]). 51

4.2 result of stability analysis for steady state point associated to values correspond to $0 < k_4 < 500$ and $0 < k_6 < 5$. Black color shows the stable regions. 52

5.1 **Changes in initial concentrations** [**A**] Changes of initial concentration of PhosphatidylCholine. [**B**] Phase space for Choline and PhosphoCholine. [**C**] An Example of different initial concentrations evoluing into steady state. In **A** and **B** the color change from red to blue refers to approaching the steady-state. In **C** each color associates to the concentration of one of the reactants. Concentrations values are given in $\mu mol.g^{-1}$. 57

5.2 **Steady State Concentration vs. Enzyme Concentration** [**A**] Change of steady state point for the reaction of PtdEth and GPE. On each of these diagrams, each point (VM, $\tilde{X}i$) corresponds to a concentration of the reactant X_i at the steady state. [**B**] Change of steady state point for the reaction of PtdEth and PtdCho. The red point in each of these diagrams is associated to the concentration at the steady state of the experimental values. Concentration values are given in $\mu mol.g^{-1}$. 60

5.3 Rate vs. Concentration A: Rate vs. Concentration for PhtdEth: Each experiment is shown by a different colour in this diagram. The steady state is obtained when the concentration of PtdEth is around 11 $\mu mol.g^{-1}$. B: Rate vs. Concentration: Each diagram corresponds to the change in concentration of one reactant vs. its reaction rate. We define the slope (k) as 'rate coefficient' which is used as a parameter in analysis concerning the speed of reaching the steady state. Values are given in $\mu mol.g^{-1}$ for Concentrations and in $\mu mol.g^{-1}.s^{-1}$ for Rates . 62

5.4 **Speed Analysis** -k (Rate Coefficients) vs. Concentration of enzyme PEMT(real values). The red point on each diagram is associated to rate coefficient at the steady state of the experimental values. Concentrations values are given in $\mu mol.g^{-1}$. 63

6.1 **Treatment Phases** Growth curves of untreated (white circles) and CENU-treated tumors during the growth inhibition phase to treatment (black circles) and the growth recovery phase (gray circles). CENU was given intratumorally at days 11, 14, and 18. Bars, SD. 68

6.2 **Schematic representation of active pathways of the model of phospholipids of B16 melanoma under CENU treatment. Reactants:** Cho(Choline), PC(Phospho-Choline), PtdCho(Phosphatidyle-Choline), PE(Phospho-Ethanolamine),

PtdEth(Phosphatidyle-Ethanolamine). **Parameters:** VM (Michaelis maximum reaction rate). The Memory effect group's parameters and the related pathway are shown by blue color. The Definitively changed group's parameters and the related pathway are shown by red color. The Finally changed group's parameters and the related pathway are shown by green color. 74

6.3 **Schematic representation of active pathways of the model of phospholipids of 3LL carcinoma under CENU treatment. Reactants:** Cho(Choline), PC(Phospho-Choline), PtdCho(Phosphatidyle-Choline), PE(Phospho-Ethanolamine), PtdEth(Phosphatidyle-Ethanolamine). **Parameters:** VM (Michaelis maximum reaction rate). The Memory effect group's parameters and the related pathway are shown by blue color. The Definitively changed group's parameters and the related pathway are shown by red color. 75

7.1 **Schematic representation of the model of interrelation of Methionine synthesis with Phosphatidylcholine synthesis.** VM_i and KM_i parameters refer to enzymatic reactions while the others represent simple reactions. Input and output arrows indicate external reactions in which the reactant has the role of substrate or product. **Reactants**: Cho(Choline), PC(Phospho-Choline), PtdCho(Phosphatidyle-Choline), GPC(Glycero-PhosphoCholine), Eth(Ethanolamine), PE(Phospho-Ethanolamine), PtdEth(Phosphatidyle-Ethanolamine), GPE(Glycero-PhosphoEthanolamine). **Enzymes:** CK(Choline-Kinase), EK(Ethanolamine-Kinase), CCT/CTP(PhosphoCholine-Cytidyl-Transferase), ECT/EPT(PhosphoEthanolamine-Cytidyl-Transferase), PEMT(PhosphatidyleEthanolamine-N-methyl-Transferase), PlpA2 (PhosphoLipase A2), PlpC(PhosphoLipase C), PlpD(PhosphoLipase D). **Parameters:** VM (Michaelis maximum reaction rate), KM (Michaelis concentration constant), k1-k12 (Rate constants for external reactions). Interrelation in presented in **four steps:** 1)Reaction catalyzed by betaine homocysteine methyltransferas; 2)Reaction catalyzed by methionine adenosyltransferas; 3)Transethylations; 4)Phosphatidylethanolamine-N-methyltransferase (PEMT). 79

7.2 **A:** ^{1}H-NMR metabolic profiling of the effects of MDS. Typical 1D spectra of: Std spectrum, MDS spectrum at day 4 and post-MDS spectrum after 6 days of reinfusion in Std medium. Chemical shifts are given in ppm; the hyphenated numbers are the chemical shifts of protons to which this proton is scalar coupled: Cho (3.20, 3.55-4.07), PC (3.23, 3.62-4.18),

PtdCho (3.23, 3.68-4.39), GPC (3.23, 3.68-4.34), Eth (3.15-3.80), PE (3.22-3.99), PtdEth (3.30-4.20), GPE (3.30-4.12). Identified metabolites were the following: 1, PE; 2, PC; 3, GPE; 4, GPC+PC. Cell culture and ^{1}H-NMR spectroscopy analysis were performed as described under Materials and Methods section. Spectra are representative of three experiments delivering comparable results. **B:** Average concentrations of B16 (in vitro). Phases; Std: untreated cells in Std medium; MDS: cell growth inhibition in MDS group; post-MDS: cell growth recovery after MDS. These concentrations are derived from 1D and 2D spectra. 80

7.3 **Schematic representation of active pathways of the model in each phase. Reactants:** Cho(Choline), PC(Phospho-Choline), PtdCho(Phosphatidyle-Choline), PE(Phospho-Ethanolamine), PtdEth(Phosphatidyle-Ethanolamine). **Parameters:** VM (Michaelis maximum reaction rate). The Memory effect group's parameters and the related pathway are shown in blue color. The Definitively changed group's parameters and the related pathway are shown in red color. 82

7.4 **Dynamic simulations based on estimated parameters.** (evolution of concentration of each of reactants of the model in time). Models 1) **Std**: model of untreated cells in Std medium (shown by bleu color); 2) **post-MDS**: model of cell growth recovery after MDS. **M-Std**: proposed model for Std in which the explicative parameters are modified. All the initial concentrations are fixed to 1 $\mu mol.g^{-1}$. in order to obtain a general comparison view of the three sets of simulations. 85

A.1 **Time evolution of the concentration of the substrate and product.** 98

A.2 **Activation Energy:** diagram of a catalytic reaction showing difference in activation energy in uncatalysed and catalysed reaction (taken from Wikipedia: Mechanisms of catalysis) 102

A.3 **Conversion of sucrose to glucose.** 1: The substrate, sucrose, consists of glucose and fructose bonded together. 2: The substrate binds to the enzyme, forming an enzyme-substrate complex. 3: The binding of the substrate and enzyme places stress on the glucose fructose bond and the bond breaks. 4: Products are released and the enzyme is free to bind other substrates. 103

A.4 **Michaelis-Menten mechanism** for the enzyme-catalysed reactions to explain this saturation in speed. S(Substrate), P(Product), E(Enzyme), C(enzyme-substrate Complex) (see [**71**]) 103

A.5 **Maud Menten and Leonor Michaelis**, who together pioneered the development of enzyme kinetics by formulating the Michaelis-Menten equation to describe the steady state action of enzymes. 104

A.6 **Evolution of the concentration in an enzyme-catalyzed reaction.** E: Enzyme, S: Substrate, ES: enzyme-substrate complex, P: Product. ([**70, 72**]) 105

A.7 **Michalis-Menten kinetic.** v: reaction rate, V_{Max}: maximum reaction rate, K_M: inverse of enzyme affinity, S: substrate's concentration. (see [**71**]) 107

C.1 Classification of planar systems based on their eigenvalues 117

E.1 **MDS inhibitory effect on B16 melanoma cells proliferation.** The first group (Std) was cultivated in Std medium. The second group (MDS) was cultivated in MDS medium for 4 days and replaced in Std medium. Then cells were cultivated in Std medium. Results are the mean of three independent experiments. **; p ¡ 0.01, MDS *vs* Std. 123

E.2 **Effect of MDS and its association with chemotherapy on phosphatidylethanolamine-N-methyltrasferase activity.** PEMT activity was assessed *in vitro* and the incorporation of [$^{14}CH_3$]-methyl groups in phosphatidylethanolamine was determined. One Unit represents 1 pmole methyl residue transferred/min/mg protein. *; $p < 0.05$, when compared to UN Std; **; $p < 0.01$, when compared to UN Std; Mann-Whitney test. Results are the mean of three independent experiments 124

F.1 A general schema of the first version of MPAS. 128

F.2 An example of MPAS application to model phospholipid biosynthesis. 131

List of Tables

1 List of the reactions of the phospholipids system 40

2 An example of the different rate laws used in the model of the phospholipids 41

1 Parameter values used in the numerical solution of the model equations (proposed by J. Tyson in [**50**]). 51

1 **Concentrations of rat's liver metabolites** 58

2 **Estimated parameter values for rat's liver metabolites** 58

1 **Average concentrations of B16 melanoma tumor model metabolites** 68

2 **Average concentrations of 3LL carcinoma tumor metabolites** 69

3 **Estimated parameter values for mouse B16 melanoma metabolites** 70

4 **Estimated parameter values for 3LL carcinoma metabolites** 71

5 Comparative analysis for rate parameters of B16 melanoma. 72

6 Comparative analysis for rate parameters of 3LL carcinoma. 73

1 **Average concentrations of B16 (in vitro).** 78

2 Estimated parameter values for B16 in vitro. 87

3 Comparative analysis for rate parameters. 88

4 The results of Sensitivity analysis for Std , MDS and post-MDS phases. 89

1 Example: System of chemical reactions. 101

Index

π-calcul, 23
^{13}C NMR spectroscopy, 31
^{1}H-NMR spectroscopy, 119
^{31}P NMR spectra, 55
3LL carcinoma, 67, 119

Activation energy, 103
Artificial Biochemistry, 23

B16 melanoma , 67, 119
BiGG, 29, 46, 128
Biomolecular, 97
Biotransformation, 28
Bottom-up modeling, 109
BRENDA, 29
Briggs-Haldane, 102
Briggs-Haldane equation, 105

Cancer, 22
Cell division cycle, 50
Cell metabolism , 27
CENU, 67, 77, 119
Chemical Reactions, 97
Chloroethyl Nitrosourea, 67, 119
Choline cycle, 32
Combined therapy, 125
Comparative analyses, 78
Comparative analysis, 69
Complex eigenvalue, 116
Complexity, 64
Computational biology, 19
Concentrations, 55
Continuous model, 38

Degradation, 99
Deterministic model, 38
Differential equations, 39
Diffusion Phenomena, 46
Diffusion phenomena, 41
Discrete model, 38
Dynamic model, 38, 111

Eigenvalue, 111
Eigenvector, 111
Enzyme, 101
Enzyme concentration, 59
Enzyme kinetic, 101
Equilibrium hypothesis , 106
Equilibrium point, 98
Ethanolamine cycle, 33
Evolution equation, 101, 103
External reactions, 34

Focus, 116
Forward modeling, 109

Glycerophosphoipid, 27
Glycerophospholipid, 22
Glycerophospholipid metabolism, 31
Graph construction, 130

Homeostasis, 34
Homogeneous model, 38
HPLC, 110
Human disease, 27

in silico, 29
in vitro, 46
In vivo, 119
in vivo, 46
Inverse modeling, 110
Irreversible reaction, 98
Irriversible chemical reaction, 98

Jacobian matrix, 116

Karuch-Kuhn-Tucker theorem, 49
KEGG, 29, 46, 128
Kennedy pathway, 30
Kinetic data, 21
Kinetic modeling, 21
KKT, 49
knowledge discovery, 20

Linear stability analysis, 112
Lyapunov's criterion, 112

Mass action law, 97, 99
Mathematical modeling, 37
Membrane, 27, 30
Metabolic pathway, 28
Metabolism, 27, 28
Metabolomics, 128
Metatool, 134
Methionine, 77, 121
Methionine deprivation, 77, 121
Methylation pathway, 30
Michaelis-Menten, 102
Michaelis-Menten equation, 102
Michaelis-Menten kinetic, 97
Michalis-Menten constant, 106, 107
Model, 20
Modeling process, 39
Monomolecular, 97
MPAS software, 127
MS, 110
Multi-substrate reaction, 130

Network structure, 39
NMR, 31, 110
NMR spectroscopy, 55
Nonlinear algebric problem , 47

ODE, 23, 39
ODE-based model, 46
Open chemical system, 97

Parameter estimation, 45, 47, 55
PEMT, 55
Petri, 134
Phase spaces, 56
Phospholipids, 29
Product, 28
Promotology, 128
Proof of stability, 64
Proteomics, 128

Quasi-steady state approximation, 106

Rate law, 39
Reactant, 97
Reaction rate, 99
Real eigenvalue, 116

SBML, 129
Sensitivity analysis, 81
Simulation, 20, 45, 49
simulation based methods, 20
Software, 127
Spatial model, 38
Speed analysis, 61
Stability analyses, 63
Stability criterion, 116
Static model, 38
Steady state, 109
Steady state oncentration, 59
Steady state point, 61
Stochastic model, 38
Stoechiometric coefficient, 100
Stoichiometric matrix, 39, 41
Stoichiometry, 39
Substrate, 28
Synthesis, 99
System of chemical reactions, 100
Systems biology, 19, 20

Top-down modeling, 110
Transcriptomics, 128
Treatment protocol, 119
Trimolecular, 97

Zero-order kinetic, 107